Title
Air Quality Responses to Changes in Black Carbon and Nitrogen Oxide Emissions

Author
Millstein, Dev

Publication Date
2009

Peer reviewed|Thesis/dissertation

Air Quality Responses to Changes in Black Carbon and Nitrogen Oxide Emissions

by

Dev Ethan Millstein

A dissertation submitted in partial satisfaction of the

requirements for the degree of

Doctor of Philosophy

in

Engineering-Civil and Environmental Engineering

in the

Graduate Division

of the

University of California, Berkeley

Committee in charge:

Professor Robert A. Harley, Chair
Professor William W Nazaroff
Professor Ronald C. Cohen

Fall 2009

Air Quality Responses to Changes in Black Carbon and Nitrogen Oxide Emissions

by Dev Ethan Millstein

The dissertation of Dev Ethan Millstein, titled Air Quality Responses to Changes in Black Carbon and Nitrogen Oxide Emissions, is approved:

Chair _____ Date _____

_____ Date _____

_____ Date _____

University of California, Berkeley

Abstract

Air Quality Responses to Changes in Black Carbon and Nitrogen Oxide Emissions

by

Dev Ethan Millstein

Doctor of Philosophy in Engineering – Civil and Environmental Engineering

University of California, Berkeley

Professor Robert A. Harley, Chair

Fine particulate matter (PM) affects public health, visibility, climate, and influences ecosystem productivity and species diversity. Diesel engines are an important source of air pollution and will face a variety of new regulations, so emissions from these vehicles are expected to undergo changes over the next decade that will have important effects on primary PM emissions, especially black carbon (BC) emissions, as well as nitrogen oxide (NO_x) emissions and therefore secondary pollutants such as ozone and PM nitrate. Analysis of observed and modeled air quality responses to changes in diesel engine emissions provides insights into the relative importance of diesel emissions and the effects of future emission controls.

Yearlong records of online measurements of black/elemental carbon at Fresno, St. Louis, and Pittsburgh were analyzed as part of this research. Diesel truck activity decreases substantially on weekends, and the pollutant time series were analyzed to look for corresponding reductions in ambient BC concentrations. Significant weekend BC reductions of 22±6 and 25±5% were found at Fresno and St. Louis, respectively. Smaller reductions were observed at Pittsburgh. Continuous measured records of fine particulate nitrate were also analyzed over yearlong periods at the three locations mentioned above and at Claremont, CA, an inland location within the Los Angeles basin. Reductions in PM nitrate were observed on Sundays and Mondays, indicating a delayed response to NO_x emission reductions that occur on Saturdays and Sundays. Nitrate reductions of 23±12, 29±23, and 16±9% were observed on Mondays at Fresno, Claremont, and St. Louis, respectively, relative to 7-day moving averages.

Exhaust emissions from diesel-powered construction equipment are typically estimated using statistical models. Both the emission estimates and the underlying engine activity estimates are subject to large uncertainties that are not routinely quantified. A fuel-based inventory of construction equipment emissions for California was developed and showed NO_x and exhaust PM emissions to be 4.5 and 3.1 times smaller, respectively, than official emission inventory estimates developed by California Air Resources Board staff. Also, a revised description of the spatial distribution of diesel engine activity based on construction permit data showed

construction activities had moved on from older housing development projects along the coast to new locations further inland in Southern California. Updating the construction inventory had significant effects on air quality model predictions for NO_x, BC, and ozone.

A gridded Eulerian model was used to assess weekend effects on particulate matter and compare model predictions weekly nitrate cycles to the observational analysis described above. The model incorporated the new construction inventories described above. This model was further employed to analyze the air quality effects of new regulations on in-use diesel trucks.

The model was run over two seasons, and a baseline scenario was compared to a scenario including weekday emissions substituted for weekend emissions. The model analysis showed similar weekend reductions of BC to changes at ground-based observation sites in southern California. Unlike BC, particulate nitrate is a secondary pollutant with non-linear and non-intuitive dependence on precursor emissions. Analysis of particulate nitrate effects was also challenging because observed weekend effects were smaller than for BC, and meteorological variability made the signal harder to discern. Both modeled and observed reductions in nitrate were found on summer Mondays at Claremont (inland site). Process analysis showed that in some locations weekend NO_x reductions could lead to higher nitric acid production and higher nitrate levels, as there are factors that offset the effect of lower weekend NO_x on the rates of both daytime ($OH+NO_2$) and nighttime (via N_2O_5) pathways to nitric acid formation. An important difference between modeled nitrate and observed nitrate was found during the fall season: modeled nitrate increased on Monday.

The effects on future air quality of new regulations requiring the retrofit of in-use heavy-duty diesel trucks and buses to meet stringent PM emission requirements were evaluated. By 2014, the in-use retrofit rule is predicted to reduce average ambient BC concentrations in southern California by 12±2 and 14±2% during the summer and fall, respectively, relative to a baseline scenario that included emission decreases due to fleet turnover effects but no retrofits. Primary NO_2 emissions are predicted to increase with greater use of oxidative particle filters, however, ambient NO_2 concentrations are not predicted to increase as parallel, but less stringent, retrofit requirements reduce total NO_x emissions. Increases in ambient ozone and particulate nitrate concentrations were predicted to occur within the Los Angeles basin, especially during the fall season, due to an increase in the NO_2/NO_x emission fraction and reduced total NO_x emissions.

To Rachel and our son Rani,

To my parents, and to my brothers.

Contents

Acknowledgements

Thanks to Professor Rob Harley, my research advisor. His support and guidance over these years have been invaluable. I thank him for inspiring me and for introducing air quality engineering to me, although now when a diesel truck passes I am forced to hold my breath. Thanks to Professor Bill Nazaroff for the illuminating classes and the insightful discussions about my research and the broader field. Also thanks to Professors Harley and Nazaroff for organizing our research group, the "Airheads." Thanks to Professor Ronald Cohen for his helpful thoughts about my research as well as serving on my dissertation committee.

Thanks to Susanne Hering of Aerosol Dynamics, especially for her help with the nitrate measurements in Chapter 3. Thanks to Philip Fine, Peter Jaques, and Costas Sioutas of the University of Southern California; Judy Chow and John Watson of the Desert Research Institute; Cliff Davidson, Andrey Khlystov, Spyros Pandis, Allen Robinson, and Ann Wittig of Carnegie Mellon University; Catherine Reid and Jay Turner of Washington University in St. Louis.

Thanks to Bruce Jackson of the California Air Resources Board who was especially helpful working with emission inventories. Thanks also to Klaus Scott and Todd Sax also of the California Air Resources Board. Thanks to Bong Kim, Satoru Mitsutomi, and Jean Ospital of the South Coast Air Quality Management District. And thanks to Ben Bartolotto of the Construction Industry Research Board.

I am grateful for the financial support from the California Air Resource Board, the Coordinating Research Council and the University of California Transportation Center.

Thanks to Airheads! Thanks to Sharon Shearer, Seema Bhangar, Arman Shehabi, Bev Coleman, George Ban-Weiss, Ling Jin, Nasim Mullen, Drew Gentner, Tim Dallmann, and Brian McDonald for creating such a great work environment and for the support and close friendship.

Thanks to my friends and family. Thanks to Sara and Neil, and Al and Isabel for lending a hand. My parents have been immensely supportive, especially helpful and wonderful with Rani. Thanks to my brothers, Aram and Brenden, for their support, love, and for always brightening the day. And special thanks to Brenden for the formatting help. I love all of you.

Lastly, I am grateful to Rachel, whose support and love I cherish.

Chapter 1

INTRODUCTION

1.1 Air Pollution Problems

Airborne fine particulate matter or $PM_{2.5}$ is a widespread air pollution problem. $PM_{2.5}$ refers to particles with aerodynamic diameter $D_P < 2.5$ μm. In the U.S., annual average $PM_{2.5}$ levels that exceed the national air quality standard of 15 μg m^{-3} are observed in California and in numerous states east of the Mississippi River (Blanchard, 2004). Though current air quality standards are defined in terms of total particle mass concentration, to understand $PM_{2.5}$ problems it is helpful to know contributions to the total from key constituents such as carbon, ammonium, nitrate, and sulfate. In the eastern U.S., ammonium sulfate accounts for one quarter to over half of annual average $PM_{2.5}$ mass concentration; sulfate levels are highest in summer months. Carbonaceous particles are also important contributors to $PM_{2.5}$, whereas nitrate levels are relatively low. California, in contrast, typically experiences peak $PM_{2.5}$ concentrations during winter months, with nitrate and carbon (including both organic carbon and soot or elemental carbon, EC) dominating fine particle mass concentration (Blanchard, 2004).

In the US, and especially California, diesel combustion is a particularly important source of elemental carbon (Watson and Chow, 2002b). Diesel vehicles are also an important and growing source of total nitrogen oxides (NO_x) emissions because diesel fuel use has increased faster than use of gasoline, and the NO_x emission factor for gasoline engines decreased faster than that for diesel engines (Harley et al., 2005; Ban-Weiss et al., 2008b). NO_x is a precursor to particulate nitrate.

Health and environmental effects have been attributed to PM, NO_x, and products from atmospheric reactions involving NO_x. Pope and Dockery (2006) describe evidence of a correlation between short-term and long-term exposure to elevated ambient PM and higher morbidity and mortality rates over varying time frames and across locations. Nitrogen dioxide measured indoors has been associated with increased asthma symptoms in young children

(Hansel et al., 2008). Recently, the US EPA has proposed strengthening the ambient air quality standards for NO_2 and proposed adding a monitoring network focus on near road-way exposure as opposed to only community-wide ambient exposure (EPA, 2009).

Through the primary photolytic cycle, NO_x emissions play an important role influencing ozone levels. High ozone levels have been found to correlate with acute health effects, such as increased daily mortality (Ito et al., 2005), and a worsening of conditions for asthmatics (Gent et al., 2003). The Children's Health Study (Peters et al., 1999) analyzed the correlations of ambient air pollutants with health outcomes for children throughout different communities in and around Los Angeles. The Children's Health Study found a correlation between some pollutants, such as O_3, HNO_3, and acetic acid, and increased use of asthma medication. It was found that medication use was more prevalent for children who spent more time outdoors (Millstein et al., 2004).

Additional environmental concerns related to particulate matter and NO_x emissions include visibility reduction, nutrient cycling (from nitrogen deposition) and related ecological effects, including a loss of species diversity and increased fire frequency (Clark and Tilman, 2008; Fenn et al., 2003), and atmospheric warming due to increased concentrations of tropospheric ozone and black carbon (see for example: Kim and Ramanathan 2008).

These health and environmental effects provide motivation for more stringent regulations on new diesel engines. The combination of stronger regulations and improved emissions control technologies is expected to result in large changes to diesel engine emissions. A mandated switch to lower sulfur diesel fuel facilitates the use of post-combustion treatment technologies, such as diesel particle filters (DPF). Regulations requiring the use of DPFs are expected to contribute to progress in controlling diesel engine emissions of $PM_{2.5}$ (Durbin et al., 2003).

Research into the effects of air quality regulations must take into account the complicated and non-linear response of ambient pollutant concentrations to emission changes. One method used to investigate these dynamic relationships is to study pollutant levels during a period that includes specific emission changes, for example Harley et al. (2006) studied the effects of fuel reformulation by comparing time series of direct benzene emissions to ambient concentrations. Air quality modeling complements the observational record as emission perturbations can be tested under new, or expected future conditions, and across locations and times without a continuous observational record. For example, Millstein and Harley (2009b) and Steiner et al. (2006) examine the effects of increasing temperature on future air quality in California.

Variation between weekends and weekdays of residential, commercial, and industrial activity patterns affect anthropogenic emissions of ozone precursors, primary PM and PM precursors. Diesel activity decreases substantially on weekends (Harley et al., 2005; Yarwood et al., 2008; Chinkin et al., 2003), offering a natural experiment that may permit direct observation of the effects of changes in emissions on air quality. Finding weekly signals in observed air pollution time series requires long records of pollutant concentrations to control for meteorological factors and other sources of variability so as to isolate variation due to weekend emission changes.

Analysis of weekend effects on ozone has been ongoing for over 30 years (Cleveland et al., 1974; Marr and Harley, 2002b; Murphy et al., 2007). Weekly cycles in black carbon have also

been identified in previous studies (Allen et al., 1999; Hies et al., 2000; Motallebi et al., 2003; Kirchstetter et al., 2008). These studies have shown that in certain locations secondary pollutants like ozone may increase on the weekend as opposed to black carbon, which tends to be reduced on weekends. The information that ozone responds differently to emission reductions depending on local conditions is important to take into account when predicting the effects of regulatory policies. But there is a need to understand the response to emission changes of other secondary pollutants, such as particle nitrate. While the past studies mentioned here analyze weekly cycles in one location or one U.S. state, comparing results across multiple regions is useful to analyze what weekly effects will happen where, and what aspects of each region leads to different responses.

Unlike ozone and black carbon, evidence of a weekly cycle in fine particulate nitrate concentrations is less clear, though the need to control nitrate in the particle phase is sometimes cited as a justification for control of NO_x emissions. Many filter-based measurement campaigns collect samples only once every 3-6 days, and are not intensive enough to isolate effects of lower weekend NO_x emissions. Blanchard and Tanenbaum (2003) and Harley et al. (2005) found no weekly cycle in particulate nitrate. Motallebi et al. (2003) reported average 6% weekend reductions in fine particulate nitrate levels in southern California.

This dissertation adds to the current state of knowledge in a number of ways. The research here describes weekly cycles in particle nitrate, and expands the study of weekend response in black carbon to new locations. Chapter 5 presents a new evaluation of the mechanism for varying weekly patterns in nitrate through the use of an air quality model. New analysis of construction emission inventories is used in the air quality modeling, and may help to better define emission inventories in other locations. Finally, the modeling framework built throughout this dissertation is used to evaluate a recently adopted diesel trucking emission regulation in California.

1.2 Research Objectives

This research aims to improve the understanding of the response of fine particulate matter, O_3 and NO_x concentrations to changes in emissions from diesel sources. Analyses of observed pollutant time series and analyses of air quality model outputs will be used to evaluate pollutant response to changing emissions. Air quality modeling is also used to evaluate the benefits and potential adverse effects of newly adopted diesel engine emission controls. Specific objectives are to:

1) Quantify weekly patterns in observed 24-h average and diurnally varying concentrations of fine particulate black carbon and nitrate. Compare results across multiple urban locations in different regions of the United States. The characterization of weekly cycles in particle nitrate will provide new insight into the response of nitrate to weekly NO_x reductions and the potential effects of NO_x emission control on nitrate concentrations. Comparisons across locations of weekly cycles in both black carbon and nitrate will provide new insight into the effectiveness of regulating diesel emissions at each location.

2) Develop, evaluate, and improve emission inventories for diesel-powered off-road construction equipment. Total mass emissions of NO_x and exhaust PM, as well as the spatial distribution of these emissions to the county and city levels will be considered. Improving emission inventories

will limit sources of air quality modeling error and allow more accurate evaluation of the effects of various regulatory options.

3) Evaluate air quality model accuracy in reproducing observed temporal patterns in fine particulate nitrate and black carbon. Current air quality modeling efforts that investigate weekly cycles focus on ozone air quality, an objective here is to expand the model analysis to focus on weekly cycles in elemental carbon and nitrate. An additional goal is to use the air quality model to gain insight into the processes that affect nitrate response to weekend NO_x emission reductions. Understanding the processes that govern the nitrate response to NO_x emissions reductions will allow for better evaluation of the effects of NO_x controls on nitrate concentrations.

4) Evaluate the effects, both positive and negative, of a new emission control rule in California that will accelerate dramatically the retrofitting or replacement of in-use heavy-duty diesel engines to meet current heavy-duty engine exhaust emission standards.

1.3 Outline

Chapter 2 applies spectral analysis methods to time series of black carbon measurements in 3 urban areas: Fresno, CA, St. Louis, MO, and Pittsburgh, PA. The measured data are from the EPA PM supersites research program, and feature new and unusually long records of high time resolution data, which permit more in-depth analysis than has been reported previously.

Chapter 3 presents an analysis of long records of continuous fine particulate nitrate concentration measurements at the 3 sites listed above, plus Claremont in southern California. Yearlong records of data from a new semi-continuous impactor/thermal desorption sampling system are used in these analyses. Past work has focused on analysis of multiple pollutants at a single location; here I consider patterns across 4 research-grade field measurement sites. The potential for interactive effects between changes in sulfate and nitrate (via differences in ammonia availability) are also assessed using extensive, simultaneous measurements of these pollutants at Pittsburgh, where the influence of coal-fired power plant emissions is high.

Chapter 4 demonstrates that large emission inventory uncertainties persist for important source categories, as illustrated here for the case of diesel-powered off-road construction equipment. Various methods for estimating total emissions of NO_x and exhaust PM, and the spatial distribution of these emissions are evaluated. The effects of emission inventory updates on air quality are examined using an Eulerian photochemical air quality model.

Chapter 5 examines the modeled responses of fine particulate elemental carbon and nitrate concentrations in southern California to weekday/weekend changes in emissions across different seasons. Through use of integrated reaction rate (process) analysis as a model probing tool, and by considering a hypothetical alternate emission scenario with weekday emissions everyday, predicted changes in fine particulate matter on weekends are evaluated and compared against observations.

Chapter 6 evaluates the air quality effects of recently adopted regulations requiring the replacement or retrofitting of all older (pre-2007) on-road heavy-duty diesel engines in

California by 2014. This measure will reduce exhaust PM emissions, but there are concerns about short-term adverse effects from an increased NO_2/NO_x ratio in primary diesel exhaust emissions. In the past, diesel NO_x emissions consisted almost entirely of nitric oxide (NO). The analysis considers effects of diesel engine retrofits on fine particulate mass, EC, and nitrate, as well as NO_2 and ozone in the gas phase.

Chapter 7 summarizes major research findings and provides recommendations for further research.

Chapter 2

ANALYSIS OF BLACK CARBON TIME SERIES

2.1 Introduction

The main objective of the research reported in this chapter is to analyze time series of measured particle-phase pollutant concentrations to determine if weekly cycles are present in the data from 3 locations, Fresno, St. Louis, and Pittsburgh. In contrast to past studies that analyzed filter-based PM data, we use data from online measurement methods that provide high time resolution. Our focus is specifically on the black/elemental fraction of carbon particles. These pollutants are linked in part to diesel engine emissions, which are known to decrease substantially on weekends (Dreher and Harley, 1998; Chinkin et al., 2003; Harley et al., 2005). Improved understanding of atmospheric responses to emission changes on weekends could help strengthen the technical basis for policy decisions that will reduce emissions on all days of the week in the future.

Major emission sources of black carbon (BC), also known as soot, include fossil fuel combustion and biomass burning, and in many locations, residential combustion of biomass and coal for heat or cooking (Streets et al., 2001; Novakov et al., 2003; Bond et al., 2004). High soot emission rates are observed from combustion sources where air and fuel are not well mixed, or where the supply of air is inadequate (e.g., diesel engines, residential use of wood or coal for space heating).

Particulate carbon is typically measured by thermal-optical analysis of samples collected using quartz filters. Total particulate carbon is divided into elemental carbon (EC, refractory) and

organic carbon (OC, volatile) fractions. This split is defined operationally as part of thermal/optical analysis procedures (Chow et al., 1993; Birch and Cary, 1996). There are also semi-continuous techniques for measuring BC (Hansen et al., 1984; Adams et al., 1989; Turpin et al., 1990), and visible light absorption by aerosols (Bond et al., 1999).

The size distribution of fresh soot emissions in motor vehicle exhaust is unimodal with a peak around 0.1 μm (Venkataraman et al., 1994). Atmospheric aerosols exhibit a more complex distribution of soot mass, including a predominant mode in the upper submicron size range, in addition to ~0.1 μm and coarse modes (Venkataraman and Friedlander, 1994; Berner et al., 1996).

Various investigators (Allen et al., 1999; Harley et al., 2005; Hies et al., 2000; Motallebi et al., 2003) have reported weekly cycles in BC/EC, with minima observed on Sundays. While this response to a change in primary pollutant emissions is expected, there is uncertainty about the relative importance of diesel exhaust vs. other sources of BC emissions. Further study of weekly cycles in carbon particle concentrations may help to advance understanding of source contributions from diesel vs. gasoline engines, wood burning, etc. This chapter demonstrates that spectral analysis can be applied to a primary PM constituent, such as BC, to determine the relative influence of different time periods on the variation concentration levels. Spectral analysis had previously been used to analyze O_3 time series. Additional information is gained by comparing trends in BC across locations and the analysis of a BC, a primary pollutant, provides context for the discussion of trends in secondary nitrate particle trends in chapters 3, 5, and 6.

A strong weekly BC cycle is expected if diesel exhaust is the dominant source of this pollutant (Harley et al., 2005); seasonal variations in the amplitude of the weekly cycle may reflect ambient temperature effects on cold start emissions from gasoline engines (Mulawa et al., 1997), or variations in the amount of wood-burning.

Weekly cycles in atmospheric BC levels may affect photolysis rates and ozone formation through changes in aerosol optical depth and single scattering albedo, which defines the relative amount of light scattering vs. absorption by aerosols (Dickerson et al., 1997; Dreher and Harley, 1998). The effect on ozone of decreasing aerosol optical depth on weekends was found to be small in southern California (Yarwood et al., 2003), as BC does not constitute a large fraction of $PM_{2.5}$ mass. Christoforou et al. (2000) note that between 1982 and 1993 in the Los Angeles area, decreased concentrations of EC and sulfate and accounted for much of the reduction in $PM_{2.5}$ mass that occurred over that time period. Radiative effects of soot should therefore be decreasing over time, whereas weekday-weekend differences in ozone were observed to be spreading to more locations over the same time period. Increased occurrences of the ozone weekend effect is probably due to an increase of regions where ozone production is VOC limited (Marr and Harley, 2002a; Fujita et al., 2003).

Between 1990 and 2000, there was progress in controlling U.S. motor vehicle emissions, despite growth in the number of vehicles and the amount of driving. Reasons for the emission reductions include fuel reformulation, advances in engine design, and improvements in catalytic converters and other control technologies. For gasoline engines, VOC and CO emissions have been controlled more effectively than NO_x, though emissions of all of these pollutants have been

reduced (Kean et al., 2002; Parrish et al., 2002). For diesel engines, particulate matter emissions were reduced, but there was little if any change in NO_x emission rates (Yanowitz et al., 2000a). Also between 1990 and 2000, on-road use of diesel fuel grew at a rate that was 3 times faster than gasoline (Harley et al., 2005).

In this chapter, seasonal, weekly and diurnal patterns of BC concentrations are reported and analyzed across three urban areas in the United States. Comparisons across the different locations help provide insight into the regional differences in emissions and meteorology that cause different trends in each location. Spectral analysis is used to define the relative importance of seasonal, weekly and diurnal patterns on BC concentrations. In addition, concentrations over each specific weekday are averaged and compared to define the magnitude of weekly cycles. Results from this analysis provide a general description of BC trends at different locations and can provide a context for thinking about emission control strategies across many different regions.

2.2 Methods

Concentrations of particle-phase pollutants vary on many time scales. Here we study diurnal, weekly, and seasonal patterns in measured concentrations of BC. The sections that follow describe four PM supersites where speciated $PM_{2.5}$ data were acquired, the measurement methods used at these sites, and time series analysis methods applied to the data as part of this research.

Field Measurement Sites

Fresno. The city of Fresno, CA, is situated near the center of California's San Joaquin Valley. The Valley encompasses nearly 64,000 km^2, and is bordered by the Coastal Mountains to the west, by the Sierra Nevada Range along the east, and by the Tehachapi Mountains to the south. The metropolitan area of Fresno, with approximately 500,000 inhabitants, is the largest population center within 150 km. Much of the surrounding area is farmland. A major state freeway passes through the western half of the city.

Measurements are taken from the Fresno EPA Super-Site, which shares facilities with a California Air Resources Board monitoring station at 3425 First Street, in the city of Fresno. The station is 5.5 km north-northeast of the downtown commercial district, and is surrounded by commercial establishments, office buildings, churches, schools and single-family homes. Sampling inlets are located on the rooftop of a two-story office building, 10 m above ground level, and 30 m from the street. Measurements of nitrate and BC were taken from 9/1999-10/2000 and 12/1999-7/2002, respectively. Details are given by Watson et al. (2000).

Pittsburgh. The Pittsburgh, PA, metropolitan area, with two million inhabitants, is situated in between the Midwest, with its coal-fired electric power generation utilities and agricultural sources, the Eastern Seaboard, with its heavily populated urban centers.

Data used here are taken from the Pittsburgh Air Quality Study central monitoring site (Wittig et al., 2004a) located at Schenley Park, a 456 acre wooded park in the city of Pittsburgh, near the campus of Carnegie Mellon University. The site is approximately 6 km from downtown and 500 m from the nearest heavily traveled street. Monitoring was conducted from a trailer designed

expressly for the study. Inlets were positioned 2 m above the rooftop, or approximately 6 m above the ground. Measurements were made from July 2001 through August 2002.

St. Louis. The city of St. Louis, MO, is situated along the Mississippi River. The greater St. Louis metropolitan area has a population of approximately 2.7 million. The largest local industry is the manufacture of military aircraft. Data are taken from the core monitoring site of the St. Louis - Midwest Supersite, located across the Mississippi River from St. Louis, in the town of East St. Louis, Illinois. For the dominant meteorological conditions the site is downwind of the urban area of St. Louis and numerous industrial sources. St. Louis' central business district is 3 km to the west of the site. Other significant point sources are a steel mill situated 10 km to the north, copper products and zinc processing plants 3 – 4 km SSW of the site, and a lead smelter 40 km to the SSW. Source apportionment analysis shows the influences of these sources, as well as those from gasoline vehicles, diesel trucks, and railroads (Lee et al., 2006).

The core monitoring site measurements were made from two trailers located immediately adjacent to the Illinois EPA compliance monitoring station at S. 13th Street and Tudor Avenue. Inlets were placed 2 m above the trailer roofs. The immediate neighborhood of the site is relatively low density, mixed use residential and light commercial. Monitoring was conducted from April 2001 through June 2003, with a subset of the measurements continuing until June 2005. Turner and coworkers at Washington University led these measurements efforts (Reid et al., 2005).

Measurement Methods

Black Carbon. BC data for Fresno and St. Louis were measured using an aethalometer (Magee Scientific AE14U, Berkeley, CA). As described by Hansen et al. (1984), this instrument measures the change in filter opacity with particle loading by comparison of the light transmittance at 880 nm between the particle deposit on a quartz filter tape to a clean portion of the same tape. Both light scattering and "shadowing" can affect the concentrations reported by the aethalometer as the aerosol load increases and methods exists to correct for these issues (Weingartner et al., 2003). The instrument incorporates an automated system to advance the filter tape when the filter darkness passes a preset threshold, thus keeping the measurements within a linear response range. In urban atmospheres, BC is the dominant light absorbing species, and the aethalometer attributes all of the observed light absorption to BC.

Over the years there have been numerous comparisons of the aethalometer signal to EC or BC as determined by thermal-optical analysis of integrated aerosol samples. Allen et al. (1999) present comparisons to integrated quartz filter samples analyzed by thermal-optical reflectance in Uniontown, PA. Babich et al. (2000) present a similar comparison across seven different US cities. These studies found correlation of the order of $R^2 \sim 0.95$, with slope varying from 0.6 to 0.9. Hansen and McMurry (1990) compared the aethalometer and MOUDI impactor, wherein EC was from the impactor was determined by thermal evolution from aluminum substrates. This study found correlation of the order of $R^2 \sim 0.95$, with slope varying from 0.6 to 1.0.

Table 2.1 shows the comparison to parallel filter measurements for the data used here. At Fresno, sampling every sixth day on quartz filters was done using the IMPROVE protocol for the thermal optical reflectance method of Chow et al. (1993). Observed concentrations varied from

0.2 to 10 $\mu g/m^3$ for 24-hr averaging periods. Regression of the aethalometer against the EC from the Federal Reference Method (FRM) sampler operated with a quartz filter, gives a slope of 0.79±0.03 and R^2=0.94, as reported by Watson and Chow (2002a). The ratio of mean values is the same as the slope. At St. Louis, the dynamic range in BC concentrations is small, with values of 0.2 to 2 $\mu g/m^3$, and the correlation between the aethalometer and filter is correspondingly lower. The regression slope and the ratio of mean values for comparisons to filters analyzed by the IMPROVE protocol are somewhat lower (0.6) than observed at Fresno.

At St. Louis, comparisons of aethalometer data was made to EC concentrations determined by both the NIOSH and IMPROVE protocols. These protocols differ in the temperature ramp and manner in which the pyrolysis correction is done. As described by Chow et al. (2001; 2004a), the methods agree on the value for total carbon concentration, but differ on the split between organic and elemental. At St. Louis, the aethalometer data correlated best with the filters analyzed by the IMPROVE protocol, with R^2=0.8. On average, the aethalometer BC values are intermediate between the EC reported by the two filter methods.

Elemental Carbon. At the Pittsburgh site, time-resolved measurements for organic and EC were obtained with the Sunset Laboratories aerosol carbon analysis field instrument, an instrument based on the in-situ carbon analyzer of Turpin et al. (1990). With this instrument, particles are collected on a quartz filter for a period of 100 to 220 minutes, followed by immediate thermal analysis, as described by Lim and Turpin (2002) and Cabada et al. (2004). The analysis is essentially a two-step process in which the filter is incrementally heated to 870°C in a pure helium atmosphere, rapidly cooled to 575°C, and then heated to 910°C in He mixed with 2% O_2. The amount of evolved carbon dioxide is determined by reduction to methane and flame ionization detection. The darkness of the filter is monitored throughout the analysis using a small laser beam at a wavelength of 633 nm to measure the light transmittance through the filter. The filter darkness is observed to first darken while being heated in the pure He atmosphere, and then lighten when heated in the presence of oxygen. The organic carbon signal is defined as that which evolves in the pure He atmosphere, plus that which must be removed during the heating step with O_2 to return the filter to its original darkness. EC is defined as the difference between the total and organic carbon. At Pittsburgh, all values were corrected for dynamic blanks generated by sampling with a Teflon filter upstream of the filter collectors.

Table 2.1: Comparison of Aethalometer to Collocated Filter Measurements

Site	Dates	Filter Method	Slope/Intercept[d]	R^2	Ratio of Means	Notes
Fresno	1/00 – 12/00	IMPROVE EC	0.79 / -0.02	0.94	0.79	a
St. Louis	01/03-05/03	IMPROVE EC	0.59 / -0.02	0.77	0.58	b
	01/03-05/03	NIOSH EC		0.61	1.15	b
	01/03-12/03	NIOSH EC			1.04	c
	01/04-12/04	NIOSH EC			1.26	c

[a] approximately every 6th-day sampling, N=50 data pairs, (Chow et al., 2004a)
[b] for every-day sampling, N=141 data pairs, results from J. R. Turner, private communication
[c] for 1 in 6 day sampling, N=58 data pairs for 2003, N=53 for 2004, from J.R. Turner
[d] intercept is in units of $\mu g/m^3$

2.3 Data Analysis

Variations in particulate matter concentrations were studied in both the time and frequency domains. In the time domain, we divided and analyzed the data by season: winter (Jan through Mar), spring (Apr through Jun), summer (Jul through Sep) and fall (Oct through Dec). The assessment of weekly cycles in the data considered both 24-h average values and diurnally varying concentration profiles at 1-h time resolution. Daily values were compared by ratio to a moving 7-day average; a pollutant with no weekly cycle would have ratios of ~1 on all days.

Spectral analysis techniques were used to study variance properties in the data as a function of frequency. A key step in this analysis is the calculation of the discrete Fourier transform, which we accomplished using the Fast Fourier Transform (FFT) algorithm included as part of MATLAB. Fourier analysis decomposes an input time series into a sum of sinusoids with different amplitudes, frequencies and phases.

As variance in the data was not stable across seasons, following Hies et al. (2000), a logarithmic transform was applied to the raw data prior to performing the Fourier analysis:

$$C_t' = \log_{10} C_t - \overline{\log_{10} C_t} \tag{2.1}$$

C_t is the measured concentration at time t; the term with an overbar indicates subtraction of the annual average of the log-transformed series, resulting in a zero mean for C_t'. For missing data, C_t was filled in by linear interpolation between the two closest recorded values. Longer data gaps present in the Fresno BC time series were filled with $C_t' = 0$.

The periodogram or power spectrum for each pollutant was constructed from the results of a discrete Fourier transform applied to C_t':

$$X(\nu_k) = \frac{1}{\sqrt{N}} \sum_{t=1}^{N} C_t' \exp\left(-2\pi i \nu_k t\right) \tag{2.2}$$

where frequency $\nu_k = k/N$ for k=0,1,…,N–1. $X(\nu_k)$ is a complex number that provides both amplitude and phase information for the specified frequency. The periodogram plots spectral power $P(\nu_k)$ versus frequency, where

$$P(\nu_k) = \left|X(\nu_k)\right|^2 \tag{2.3}$$

The periodogram does not include phase information, so it is necessary to perform time domain analyses to determine for example, on which days of the week concentrations are lowest, assuming a weekly cycle is present.

For EC at Pittsburgh, we input N=364 (52×7) daily average values in the analysis, and were particularly interested in $\nu_{52} = 52/364 = 1/7 = 0.14$ d^{-1} which indicates the weekly cycle. For Fresno and St. Louis BC data, hourly values were input with N=8736 (24×364). In this case, the periodogram can be used to identify annual, weekly, diurnal, and other cycles in the data. Note

that at least two data points are required within each cycle of the highest frequency signal being studied. It is therefore not possible to use spectral methods to study weekly cycles in most of the available historical record of filter-based particulate matter samples that typically include one 24-h average data point every 6^{th} day.

2.4 Results

BC was measured continuously using aethalometers for a period of close to two years at both Fresno and St. Louis. Online thermal optical measurements of EC were made for a period of one year at Pittsburgh. BC/EC concentration time series are presented in Figure 2.1. BC concentrations at Fresno were the highest measured, with a peak 24-hour average of ~9 $\mu g/m^3$. St. Louis and Pittsburgh both had much lower average carbon concentrations, with maxima of ~3 $\mu g/m^3$.

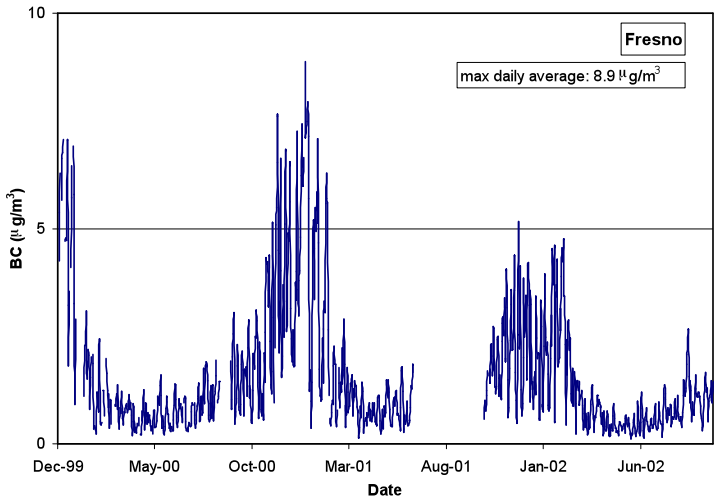

AM= 1.6
SD= 1.5
GM= 1.1
GSD= 2.3
10%= 0.4
50%= 1.0
90%= 3.6

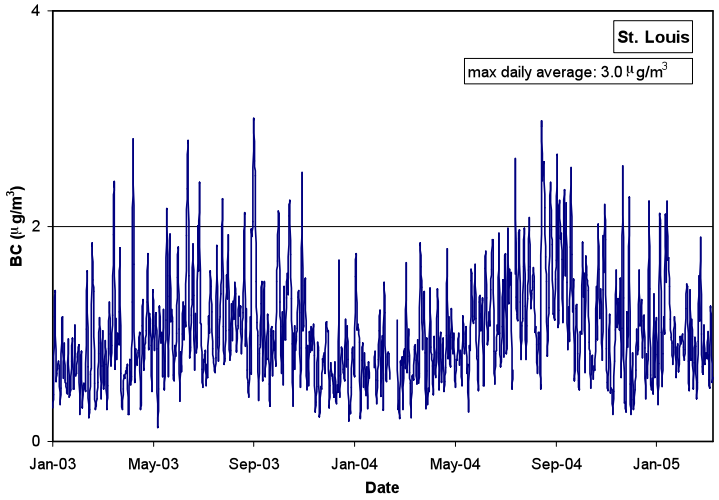

AM= 1.0
SD= 0.5
GM= 0.9
GSD= 1.7
10%= 0.5
50%= 0.9
90%= 1.7

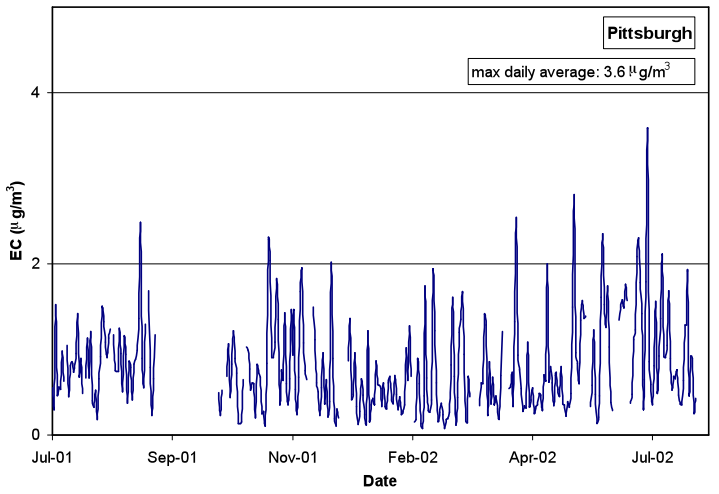

AM= 0.8
SD= 0.5
GM= 0.6
GSD= 2.0
10%= 0.2
50%= 0.7
90%= 1.5

Figure 2.1: Time series of fine black/elemental carbon concentrations (daily average values are shown here). Note different scales for each site. Arithmetic mean, standard deviation, geometric mean, geometric standard deviation, and the 10^{th}, 50^{th}, and 90^{th} percentiles are presented along with the time series for each site.

Seasonal and Diurnal Patterns. Figure 2.2 shows diurnal profiles of BC/EC concentrations by site and season. At both St. Louis and Pittsburgh, slightly higher values are seen during summer months. At Fresno, BC concentrations were higher during fall and winter months. The highest average concentration in Fresno occurs during fall and winter months from 7 PM until about midnight. These patterns could be explained by unfavorable dispersion conditions and high woodstove/fireplace emissions during fall and winter evenings. During spring and summer, Fresno BC concentrations peak in the morning hours, from 6 to 9 AM. These morning peaks can also be seen in the cooler months, but the magnitude of the morning peaks is only ~half of the evening peaks.

BC/EC concentrations at St. Louis and Pittsburgh peak during morning commute hours. At St. Louis, BC concentrations also peak in the evening, but at lower levels than the morning peaks. The evening peaks in St. Louis are unique as they are similar in magnitude to morning peaks through all seasons. At all sites, the timing of high levels of BC in the morning varies slightly with the season; warmer months show earlier morning BC peaks consistent with earlier sunrise times.

Weekly Cycles. Figure 2.3 presents BC/EC concentrations by day of week, normalized to a moving 7-day average. All three sites show weekend days that have ratios of less than one, and Tuesdays through Thursdays with ratios greater than one. St. Louis and Fresno have ratios of ~75% on Sunday, and both values are significantly less than one. In other words, Sunday BC concentrations at these two sites are ~25% less than weekly average concentrations. St. Louis also shows lower Saturday BC concentrations, with a reduction of 13±5% relative to the weekly average. The difference between reductions on Saturday and Sunday at St. Louis is not significant.

Figure 2.4 plots diurnal variations in weekday/weekend BC/EC concentrations by season. Weekly cycles are clearly evident across all sites, seasons, and most times of day. The exception is Fresno, where fall and winter weekend averages are higher at early morning hours (midnight to 6 AM) than on weekdays. This pattern points to wood-burning rather than vehicle emissions as the important source. Wood-burning was found to be an important EC source in two California studies (Chow et al., 1995; Schauer and Cass, 2000). Source apportionment using carbon isotope analysis of PM samples from Zurich, Switzerland showed significant wintertime contributions to EC from biomass burning (Szidat et al., 2006).

Variations in BC concentrations at Fresno and St. Louis by day of week are presented in Figure 2.5. St. Louis shows Sunday BC decreases from the weekly average across all seasons ranging from -38±8% to -17±13%. Fresno shows Sunday decreases across all seasons ranging from -33±9% to -13±16%. All seasons except winter have ratios significantly less than one. This analysis indicates the weekly cycle in BC is not as strong during winter in Fresno compared with the rest of the year.

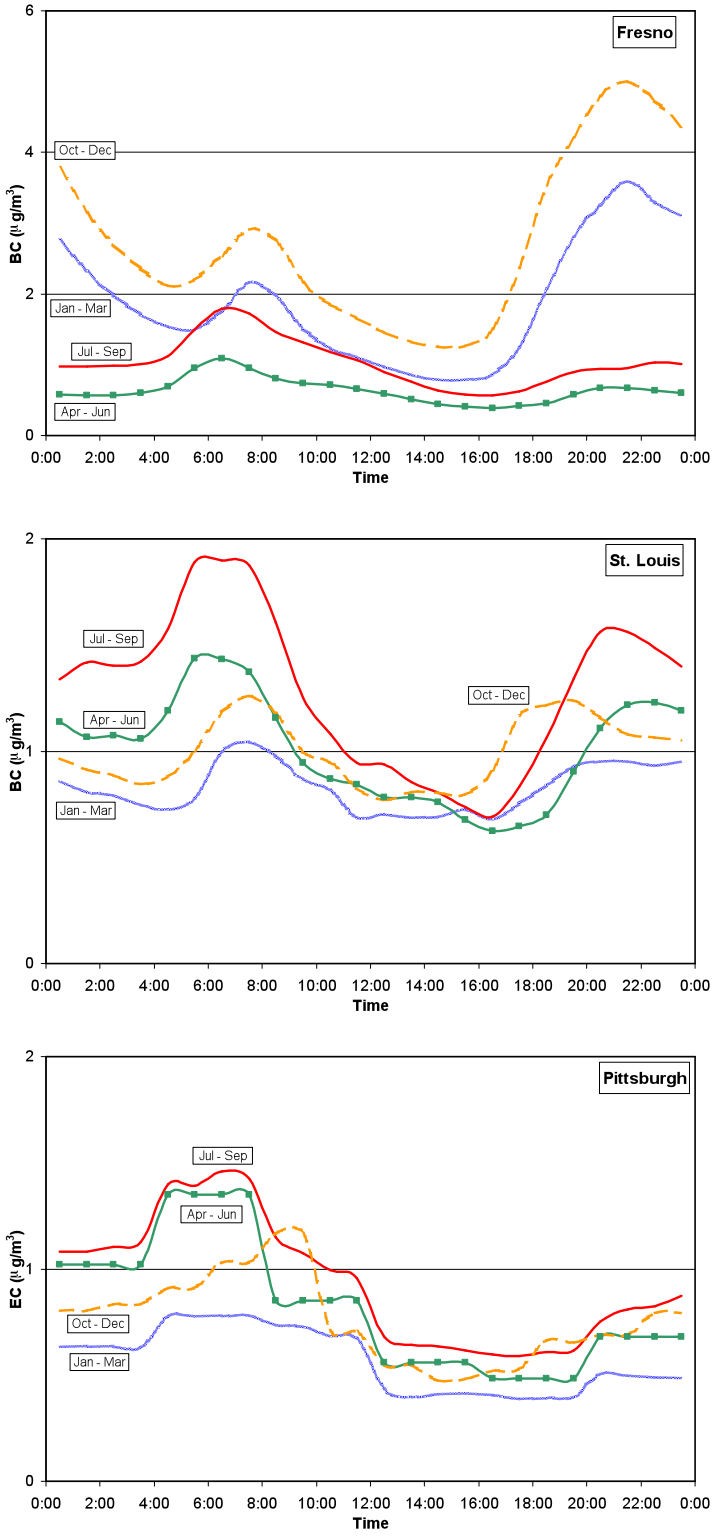

Figure 2.2: Diurnal variation in black/elemental carbon concentrations by season. Note different scales for each site. Note: Unlike continuous BC measurements at Fresno and St. Louis, EC measurements at Pittsburgh report average concentrations over 2-4 hours.

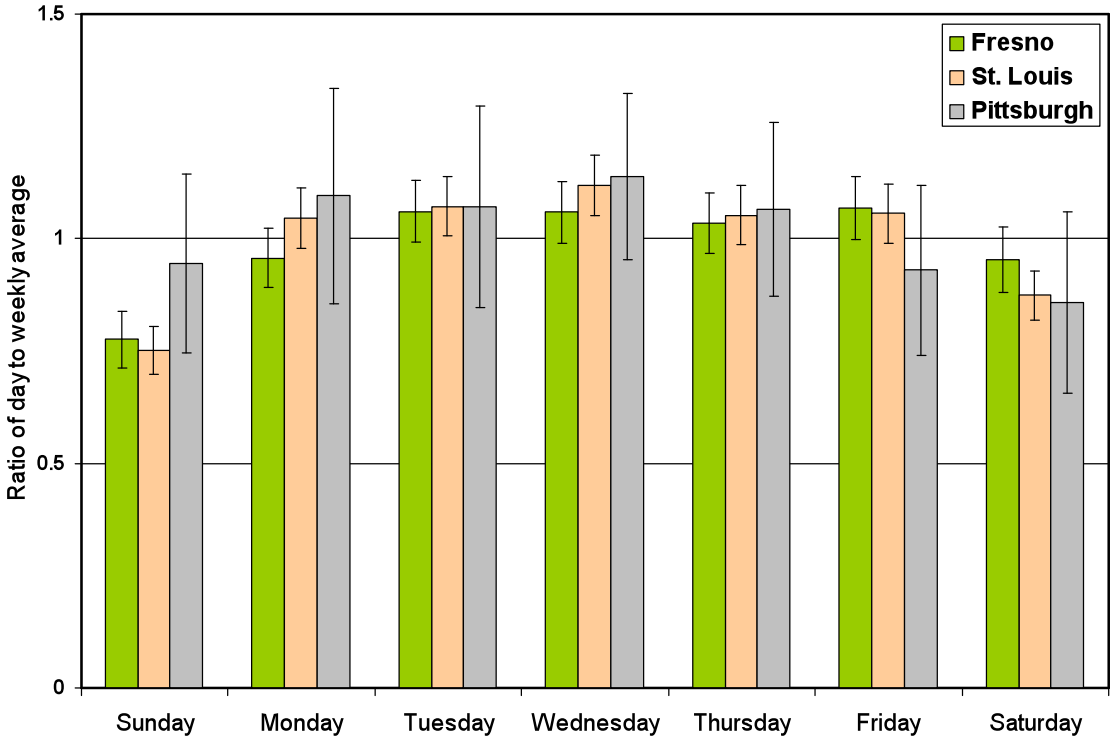

Figure 2.3: Average (±95% CI of the mean) black/elemental carbon concentrations by day of week, normalized to moving seven-day average.

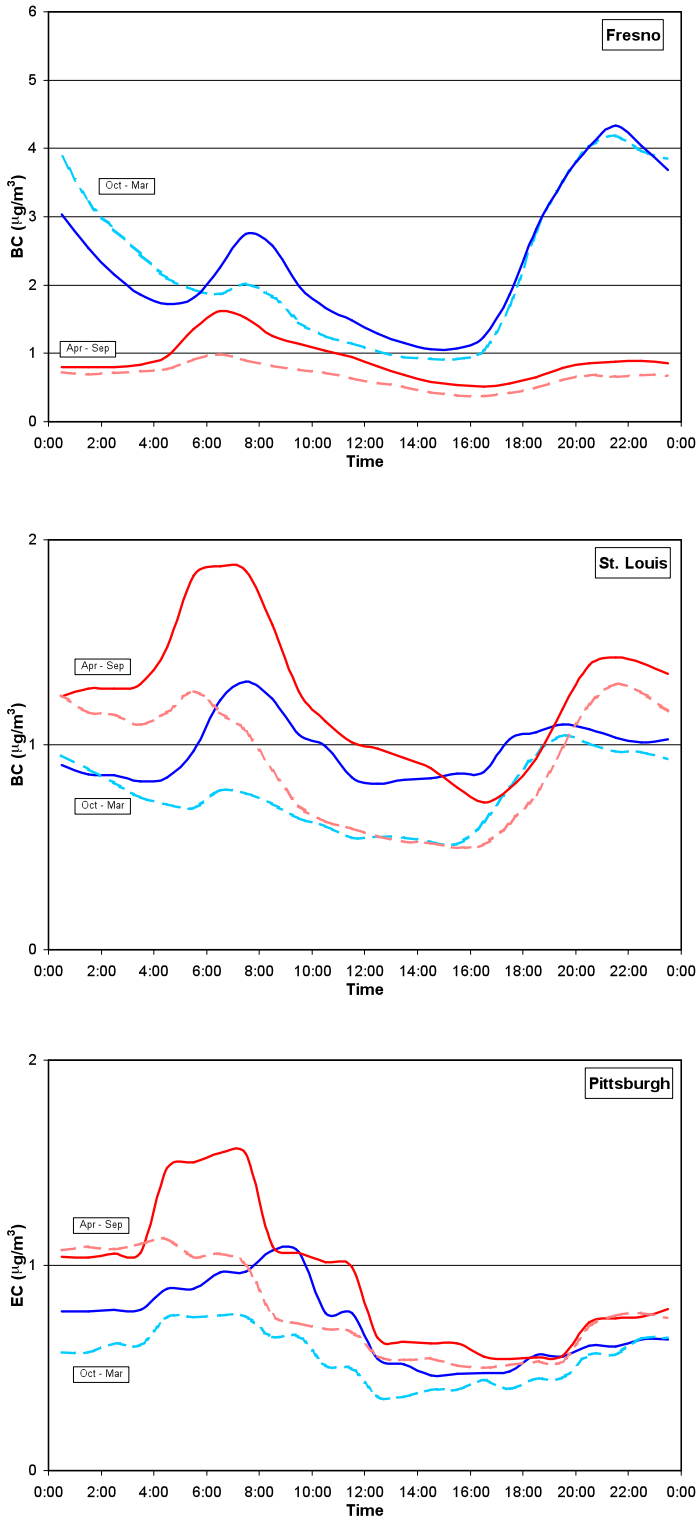

Figure 2.4: Diurnal variation in black/elemental carbon concentrations by season. Solid lines averaged over weekdays, dashed lines averaged over weekend days. Note different scales for each site.

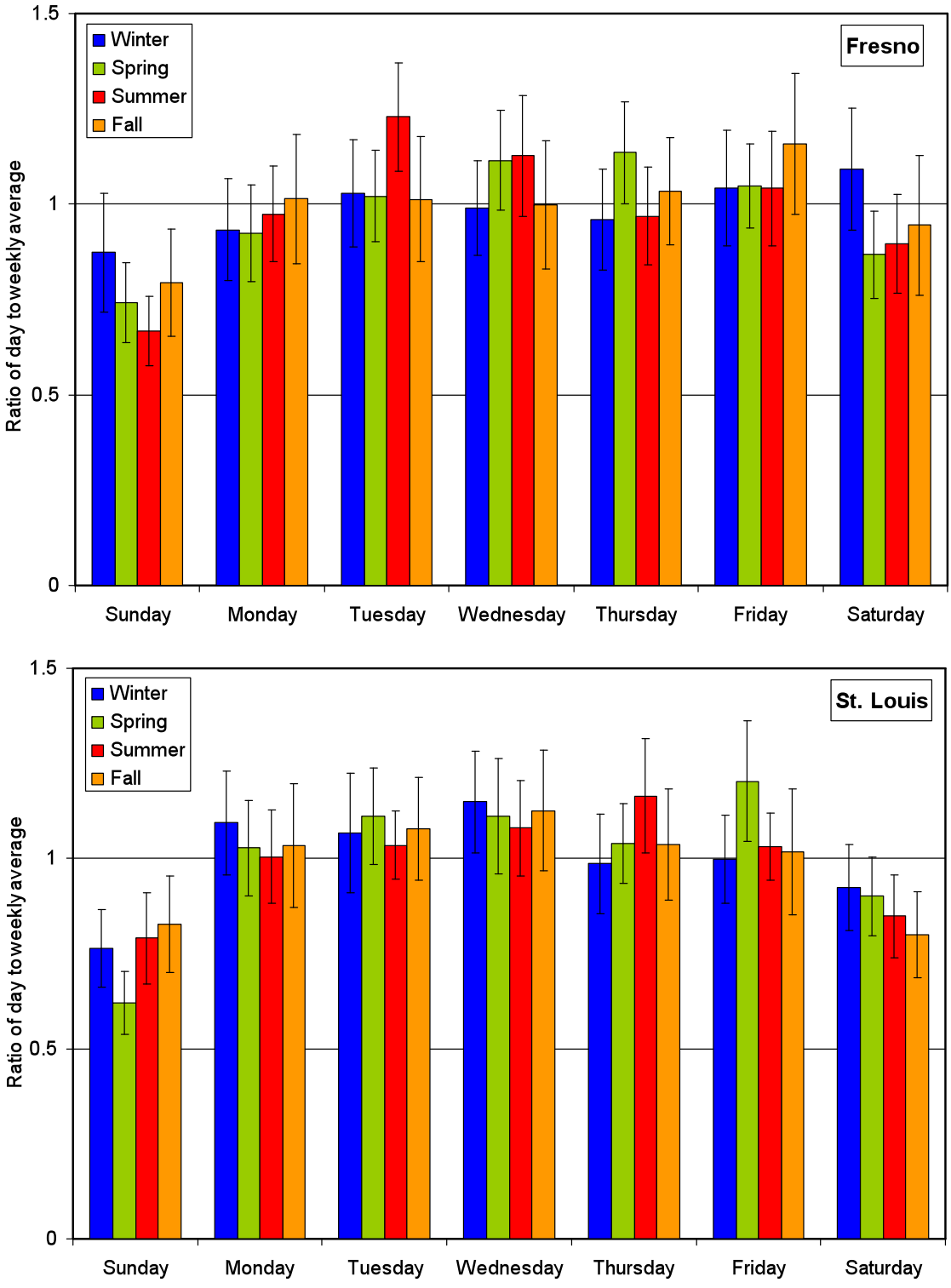

Figure 2.5: Average (±95% CI of the mean) black carbon concentrations by day of week and season, normalized to moving seven-day average.

Frequency Domain Analysis. Figure 2.6 shows periodograms for BC or EC time series at each site. For Fresno, one relatively complete year of data was available. For St. Louis, two complete years of data were available to create two periodograms, which were subsequently averaged to reduce the effects of random (white) noise in the data. The Pittsburgh EC time series had lower time resolution than either St. Louis or Fresno, so only daily average values were used to construct the periodogram for that site.

At both Fresno and St. Louis, the four strongest peaks in the periodograms are at periods (inverse of frequency) of a year, week, day, and ½ day. Smaller peaks can be seen at ½ week, 0.33 day, 0.25 day, and even 0.2 day for Fresno. Harmonics of the daily and weekly cycles are present because the signals for their time periods are not perfectly shaped sine waves. At all sites, the annual cycle is the largest source of variance in the data. At Fresno and St. Louis, the diurnal cycle combined with its first harmonic, followed by the weekly cycle combined with its first harmonic are the next two most important sources of variance in BC. At Fresno the annual cycle accounts for 35% of total variance, while diurnal and weekly cycles account for 6 and 2%, respectively. At St. Louis, however, the annual cycle accounts for only 9%, while diurnal and weekly cycles account for 4 and 3%, respectively. The low level of relative variance attributed to the weekly cycle shows their subsidiary importance relative to annual and diurnal cycles in affecting ambient BC concentrations.

In the periodogram for EC at Pittsburgh (see Figure 2.6), a peak at the period of 7 days can be seen; however, many other, seemingly randomly distributed peaks of similar magnitude can be seen nearby. The EC data from Pittsburgh are not as complete as BC data from Fresno and St. Louis; data gaps add noise to the periodogram. Similarly, in the preceding time domain analysis, Pittsburgh had much wider confidence intervals than other sites in Figure 2.3. Overall, the evidence from the time domain analyses for Pittsburgh points toward a likely weekly cycle; however, a weekly signal is not clearly evident in the periodogram.

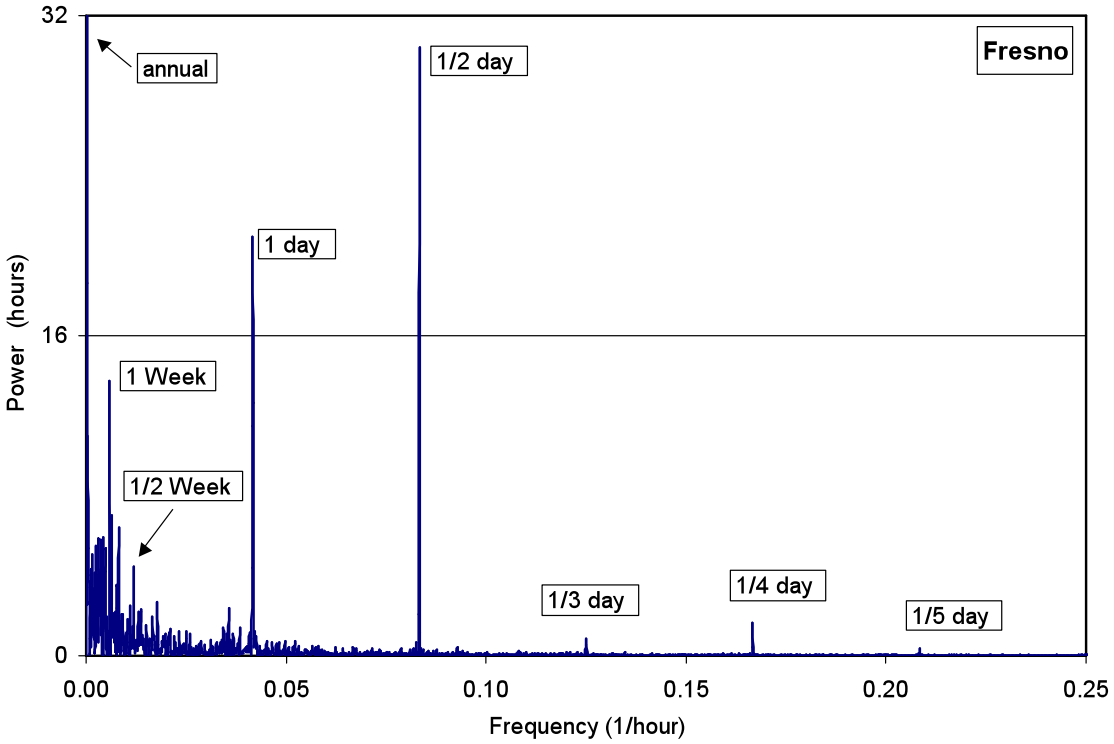
Fresno
annual
1/2 day
1 day
1 Week
1/2 Week
1/3 day
1/4 day
1/5 day
Power (hours)
32
16
0
0.00
0.05
0.10
0.15
0.20
0.25
Frequency (1/hour)

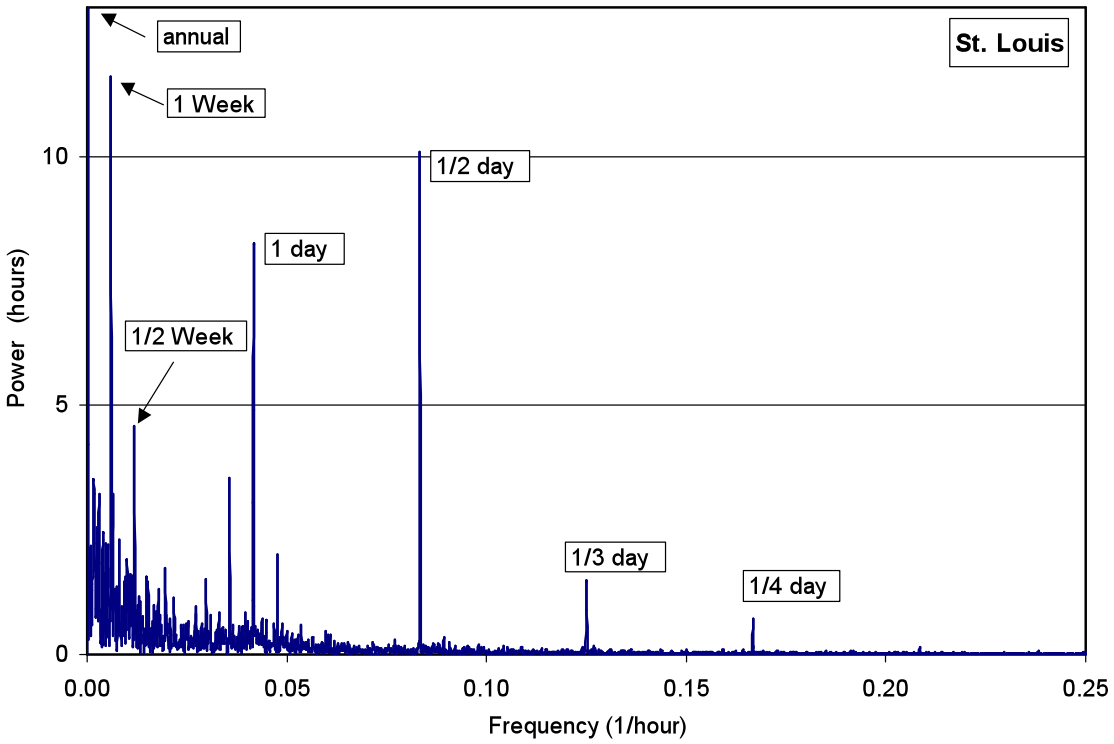
St. Louis
annual
1 Week
1/2 day
1 day
1/2 Week
1/3 day
1/4 day
Power (hours)
10
5
0
0.00
0.05
0.10
0.15
0.20
0.25
Frequency (1/hour)

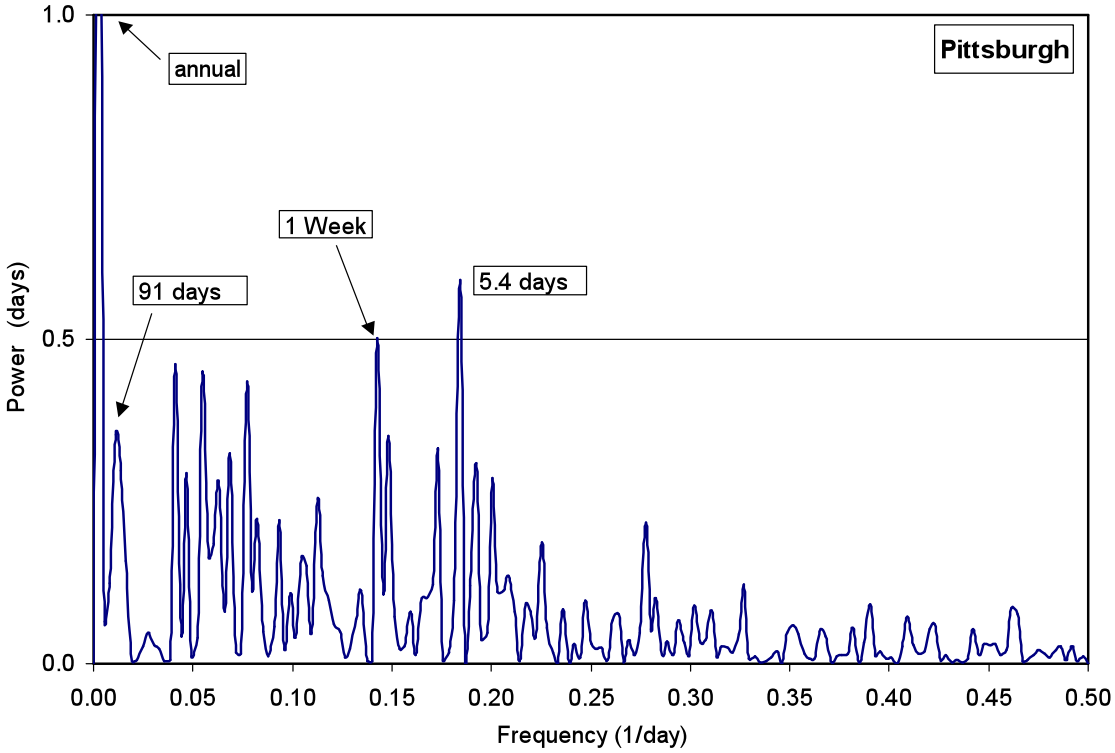

Figure 2.6: Spectral density as estimated by periodograms of daily average black/elemental carbon.

2.5 Conclusions

Weekly cycles in BC were expected and observed at St. Louis and Fresno. The relative importance of the weekly cycle at St. Louis and Fresno compared to the importance of the weekly cycle at Pittsburgh is evidence that EC levels are more sensitive to diesel vehicle emissions at St. Louis and Fresno than at Pittsburgh. Based on the relative importance of the weekly cycle controlling diesel emissions to in order to lower EC levels would be an appropriate strategy at St. Louis and Fresno, but would have limited benefits at Pittsburgh. High nighttime concentrations of BC were observed during fall and winter at Fresno. These nighttime increases were linked to smaller weekly cycles during winter. A likely nighttime source of BC is wood burning, a winter season source that could increase on weekends. Higher weekend BC concentrations were seen at Fresno during winter months between the hours of midnight and 6 AM. These overnight peaks were followed by low daytime concentrations on weekends. The contribution of residential wood combustion to wintertime $PM_{2.5}$ at Fresno has been the focus of two recent studies (Gorin et al., 2006; Chow et al., 2007). In these studies, wood smoke was found to be one of the most important sources of $PM_{2.5}$ in Fresno. This analysis demonstrates that the influence of diesel vehicle emissions on BC concentrations in urban cities across the United States is dependent on the location and season.

Chapter 3

ANALYSIS OF NITRATE TIME SERIES[1]

3.1 Introduction

Particulate nitrate is formed in the atmosphere through gas-to-particle conversion processes that start with nitrogen oxides (i.e., NO and NO_2), and proceed via formation of nitric acid as an intermediate step. An important daytime pathway involves reaction of NO_2 with the hydroxyl radical; nighttime formation pathways for nitric acid also exist (Finlayson-Pitts and Pitts, 2000). When sufficient quantities of nitric acid and ammonia are present, their reaction leads to condensation of ammonium nitrate. Conditions that favor particulate nitrate formation include abundant ammonia and nitric acid, low sulfate, low temperature, and high relative humidity (Seinfeld and Pandis, 1998). Studies of the size distribution of inorganic aerosol constituents have revealed a bimodal distribution within the accumulation mode (Hering and Friedlander, 1982; Hering et al., 1997; John et al., 1990). These modes have been linked to two particle formation mechanisms: a condensation mode at 0.2 μm related to gas-phase oxidation of SO_2 and NO_x, and a droplet mode at 0.6-0.7 μm that implies involvement of condensed phase oxidation processes.

---

[1] Reprinted in part from Millstein, D. E., Harley, R. A., and Hering, S. V.: Weekly cycles in fine particulate nitrate, *Atmospheric Environment*, 42, 632-641, Copyright 2008, with permission from Elsevier Science.

In contrast to nitrate which partitions between gas and condensed phases, sulfate formed as a result of SO_2 oxidation is found entirely in condensed phases due to the low vapor pressure of sulfuric acid (Ansari and Pandis, 1998). The most common form is ammonium sulfate, $(NH_4)_2SO_4$. If ammonia is scarce, sulfate will remain in more acidic forms such as ammonium bisulfate (NH_4HSO_4) or sulfuric acid (H_2SO_4). A potential interaction among inorganic species is that decreases in sulfate can lead to increased ammonia availability and in some cases, increased particle-phase nitrate (Ansari and Pandis, 1998).

The main objective of this research is to analyze time series of measured particle-phase nitrate concentrations, to determine if weekly cycles are present in the data. Nitrate can be linked in part to diesel engine NO_x emissions, which are known to decrease substantially on weekends (Harley et al., 2005). In reviewing ambient nitrate concentration data, different conclusions have been reached about whether significant weekly cycles in particulate nitrate are observed: Blanchard and Tanenbaum (2003) and Harley et al. (2005) found no weekday-weekend nitrate differences, whereas Motallebi et al. (2003) report small weekend decreases (6% average reduction across the sites they examined).

Previous studies of weekly cycles in PM nitrate concentrations have been constrained by sparse data (until recently PM samples were typically collected only once every 6 days; furthermore only a subset of filter samples are analyzed for chemical composition). The sparse record is due in part to reliance on labor-intensive filter-based PM measurement methods. In addition to sparse data, another concern is that standard sampling methods suffer from negative artifacts due to nitrate volatization (Hering and Cass, 1999). In recent years, a variety of online measurement methods for nitrate and other PM constituents have been developed and applied (Stolzenburg and Hering, 2000; Slanina et al., 2001; Jayne et al., 2000; Ullah et al., 2006; Weber et al., 2001). Here we use recent yearlong records of nitrate concentrations measured at 4 U.S. urban sites to study atmospheric responses to weekly cycles in anthropogenic emissions. Other investigators have reported on $PM_{2.5}$ composition and dynamics at individual sites from the EPA Supersites program (Sioutas et al., 2004). In contrast here, the study of several sites instead of one site allows for the investigation into the factors that lead to varied responses to lower weekend NO_x emissions across locations with differing geographic, meteorological, and emission regimes.

3.2 Methods

Field Measurement Sites. Nitrate measurements taken at Fresno, Pittsburgh and St. Louis were taken at the same locations as the measurements of BC and EC discussed in Chapter 2.

Claremont. As part of the Southern California Supersite, monitoring was conducted in Claremont, a city located in the east portion of the Los Angeles Basin. Claremont is routinely influenced by emissions from the Los Angeles area due to prevailing westerly winds. The sampling site was situated in a residential neighborhood, at the base of the San Gabriel Mountains along the north side of town. Measurements were made from the Supersite Aerosol Mobile Laboratory, over a period of one year beginning in September 2001, as described by Fine et al. (2004).

Measurement Methods.

Particle-phase nitrate was measured using the integrated collection and vaporization cell (ICVC) method of Stolzenburg and Hering (2000). This automated, semi-continuous method collects fine particles by impaction onto a metal surface, performs analysis in place by flash vaporization, and has a 10-minute cycle time.

At Fresno, a prototype ICVC system operated from October 1999 through July 2000. The Rupprecht and Patashnick (R&P; East Greenbush, NY) model 8400N, a commercial instrument operating on the same principle, replaced the prototype system from July through November 2000. At Pittsburgh and St. Louis, R&P model 8400N instruments were used to collect all the data. At Claremont, a custom cascaded ICVC system measured nitrate continuously in 3 size fractions (Stolzenburg et al., 2003).

The prototype ICVC system used at Fresno has a 2.5 μm cutpoint impactor to remove coarse particles, followed by an activated carbon denuder, humidifier and the collection cell. The denuder removes nitric acid and other vapor interferences. In the collection cell the humidified particles are deposited onto a bare stainless steel strip by a single-jet impactor operated at sonic flow. The aerosol sample line is contained within an aspirated sheath line, and the collection system, housed in a ventilated box, maintains the sample at near-ambient temperature. The particle deposit is heated by capacitor discharge in a nitrogen carrier gas, and the evolved nitrogen oxides are quantified using a Thermo Environmental Instruments (TEI; Waltham, MA) model 42C chemiluminescent analyzer. The typical collection period is 8 minutes followed by analysis for about 90 seconds.

R&P 8400N instruments employed at Pittsburgh and St. Louis, and for the last three months of monitoring at Fresno, utilize the same ICVC measurement approach. Particles are denuded, humidified, and collected by impaction as in the prototype unit. Differences are that a sharp-cut cyclone, rather than an impactor provides the precut. The collection is onto a nichrome rather than stainless steel strip, and evolved NO_x is measured using an Advanced Pollution Instruments (API; San Diego, CA) chemiluminscent monitor. The commercial unit provides for automatic zero and span of the NO_x monitor, a feature not included in the prototype units.

The cascaded ICVC system used at Claremont is based on the prototype system described above. Instead of a single cell, it has three cells cascaded in series to measure size-resolved nitrate concentrations (Stolzenburg et al., 2003). The three size fractions are 0.07-0.45, 0.45-1.0, and 1.0-2.5 μm; these were chosen to match size modes to different formation mechanisms (Hering et al., 1997; John et al., 1990). The sample flow passes through a 2.5 μm impactor precut, vapor denuder, a humidity conditioner, the 1 μm collection cell, the 0.45 μm collection stage, a second humidity conditioner, and the final, 0.07 μm cutpoint collection cell. Each of the three collection cells utilizes a single jet impactor collector. The final stage operates at sonic conditions and controls the sample flow rate of 0.9 L/min. The aerosol deposits from each cell are analyzed sequentially using a procedure similar to that described for the single cell ICVC. The sample train, including the preimpactor, denuder, humidifiers, and the three collection cells are enclosed and ventilated with outdoor air by an exhaust blower.

Table 3.1 compares continuous nitrate systems to integrated filter-based and impactor methods. At Fresno, comparison is made to 24-h integrated filter samples collected using the DRI

sequential sampler (Chow et al., 2005). The regression slope is closer to unity for the prototype sampler than for the R&P 8400N. Results are similar for Pittsburgh, which used 24-h integrated measurements with a denuder and Teflon-nylon filter as reference (Wittig et al., 2004b). At St. Louis, comparison is made to a HEADS sampler (Brauer et al., 1989). Here the R&P 8400N deviates from the filter measurements at higher nitrate concentrations, an effect attributed to insufficient reduction of the evolved nitrogen oxides to NO (Reid et al., 2005). A subset of the data is compared to the one-hour average nitrate concentrations obtained by the Particle in Liquid Sampler (Weber et al., 2001). For the one-hour comparison, the correlation is high, but the regression slope reflects the lower recovery at higher nitrate concentration seen with the filter measurements. At Claremont, nitrate concentrations from the cascaded ICVC are compared to denuded filter samples and to the MOUDI impactor (Fine et al., 2003). On average, the values from the cascaded ICVC were somewhat lower than the filter measurements, but higher than the impactor. The high correlations presented here indicate that day-to-day variability in nitrate concentrations at each site are well-characterized by the automated nitrate instrument, even though the mean nitrate concentrations measured by the ICVC may be lower than the filter data at some sites.

Table 3.1: Comparison of Automated Nitrate to Collocated Measurements

Site	Methods Compared	Dates	Slope/Intercept[f]	R^2	Notes
Fresno	Prototype vs Filter	12/99 – 4/00	0.90 / 0.4	0.97	a
	R&P 8400N vs Filter	8/00 – 11/00	0.84/ -0.2	0.90	a
Pittsburgh	R&P 8400N vs Filter	7/01 – 3/02	0.83 / 0.2	0.84	b
St. Louis	R&P 8400N vs Filter	2/02 – 5/03	0.62 / 0.42	--	c
	R&P 8400N vs PILS	2/02 – 4/02	0.71 / 0.40	0.89	d
Claremont	C-ICVC vs Filter	9/01 – 2/02	0.80	0.79	e
	C-ICVC vs MOUDI	9/01 – 2/02	1.12	0.53	e

[a] comparison to 24-hr denuded filter measurements, this work,
[b] comparison to 24-hr denuded filter measurements, (Wittig et al., 2004a),
[c] comparison to 24-hr denuded filters from HEADS sampler, (Reid et al., 2005)
[d] comparison to hourly nitrate from particle in liquid sampler (PILS), (Reid et al., 2005)
[e] comparison of cascaded ICVC prototype system (C-ICVC) to 24-hr denuded filters from HEADS, and size resolved measurements from the micro-orifice impactor (MOUDI). Comparison is geometric mean of measurement ratio (Fine et al., 2004).
[f] intercept is in units of $\mu g/m^3$

Supplemental Measurements at Pittsburgh. Measurements of total nitrate and ammonia were made during the Pittsburgh Air Quality Study using a steam sampler with an online ion chromatograph (Slanina et al., 2001). Particulate sulfate concentrations were measured using a flash vaporization cell coupled with a pulsed fluorescence SO_2 analyzer (Wittig et al., 2004b). This instrument follows a similar operating principle to the nitrate instrument of Hering and Stolzenburg (2000).

3.3 Results

Measured nitrate levels varied widely across sites. Average and peak concentrations are higher at Fresno and Claremont than at St. Louis and Pittsburgh (Table 3.2). The clearest seasonal changes are seen at Fresno: much higher nitrate concentrations are observed during cooler months (see Figure 3.1). Claremont experiences similar nitrate levels during winter and summer months, which is a distinctive feature among the sites studied here.

Diurnal Patterns. Diurnal variations in nitrate are shown by season in Figure 3.1. Peaks are often observed between 8 AM and noon. At all sites, spring and summer months see peak nitrate earlier in the day compared to fall and winter months. The earlier peak nitrate times are due to a combination of factors including the temperature dependence of ammonium nitrate dissociation, and the onset of convective mixing due to earlier sunrise in summer. Diurnal patterns at St. Louis and Pittsburgh are similar to those in Atlanta reported by Edgerton et al. (2006).

Weekly Cycles. Day of week variations in nitrate were examined using both hourly and daily average values. Figure 3.1 shows lower nitrate levels at most sites and seasons and at almost all hours on Sunday and Monday as compared to the rest of the week (Tuesday through Saturday). Pittsburgh does not follow the pattern of the other three sites: no weekly cycle in particulate nitrate is observed at this site. Differences are generally most apparent in Figure 3.1 at peak nitrate times. Figure 3.2 presents nitrate and NO_x concentrations by day of week, normalized to a moving 7-day average. Except for Pittsburgh, all sites show significantly lower nitrate concentrations on Mondays relative to the rest of the week. Monday nitrate decreases (±95% CI) relative to the weekly average were 23±12%, 29±23%, and 16±9% at Fresno, Claremont, and St. Louis, respectively. Fresno and St. Louis also had significantly lower nitrate levels on Sundays, with decreases of 14±12% and 21±9%. Monday nitrate reductions observed within each of the three fine particle size ranges measured at Claremont were similar to each other. Figure 3.2 suggests a pattern of a weekly minimum on Sunday or Monday, followed by a build up of nitrate through the week.

Table 3.2: Measured Seasonal Average and Peak Fine Particle Nitrate Concentrations ($\mu g/m^3$)

		Max 24-h	Mean ± Standard Deviation	
Site	Time Period	Average	Oct – Mar	Apr – Sept
Fresno	9/1999-11/2000	58.5	10.1±11.4	1.8±1.3
Claremont	9/2001-9/2002	24.6	6.1±4.3	5.8±3.7
St. Louis	3/2003-5/2005	6.2	1.8±1.2	0.8±0.7
Pittsburgh	6/2001-10/2002	6.4	1.5±1.0	0.8±0.5

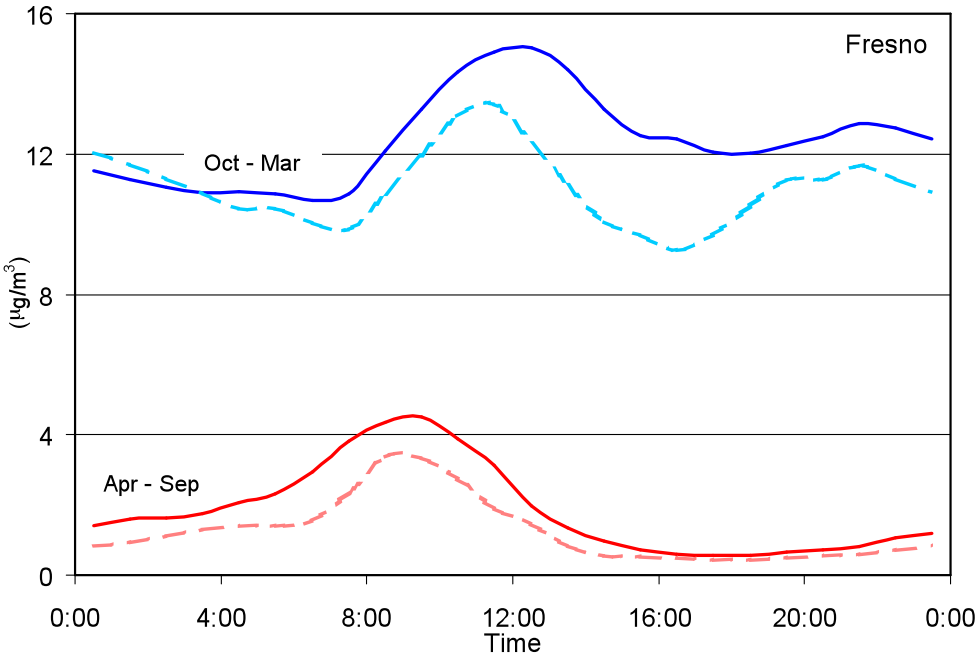
Fresno
Oct - Mar
Apr - Sep
16
12
8
4
0
(μg/m3)
0:00
4:00
8:00
12:00
16:00
20:00
0:00
Time

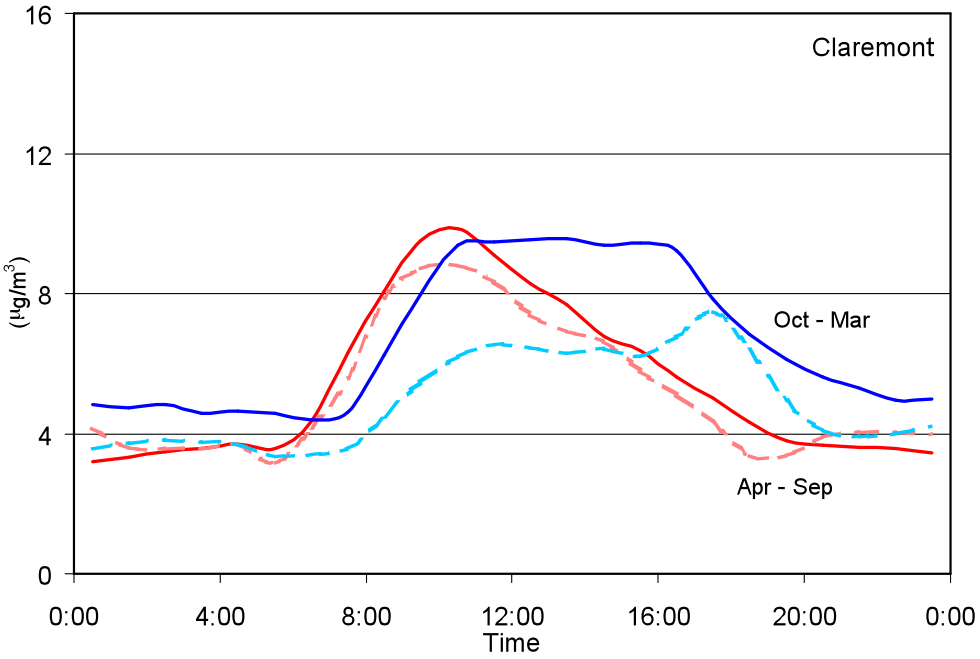
Claremont
Oct - Mar
Apr - Sep
16
12
8
4
0
(μg/m3)
0:00
4:00
8:00
12:00
16:00
20:00
0:00
Time

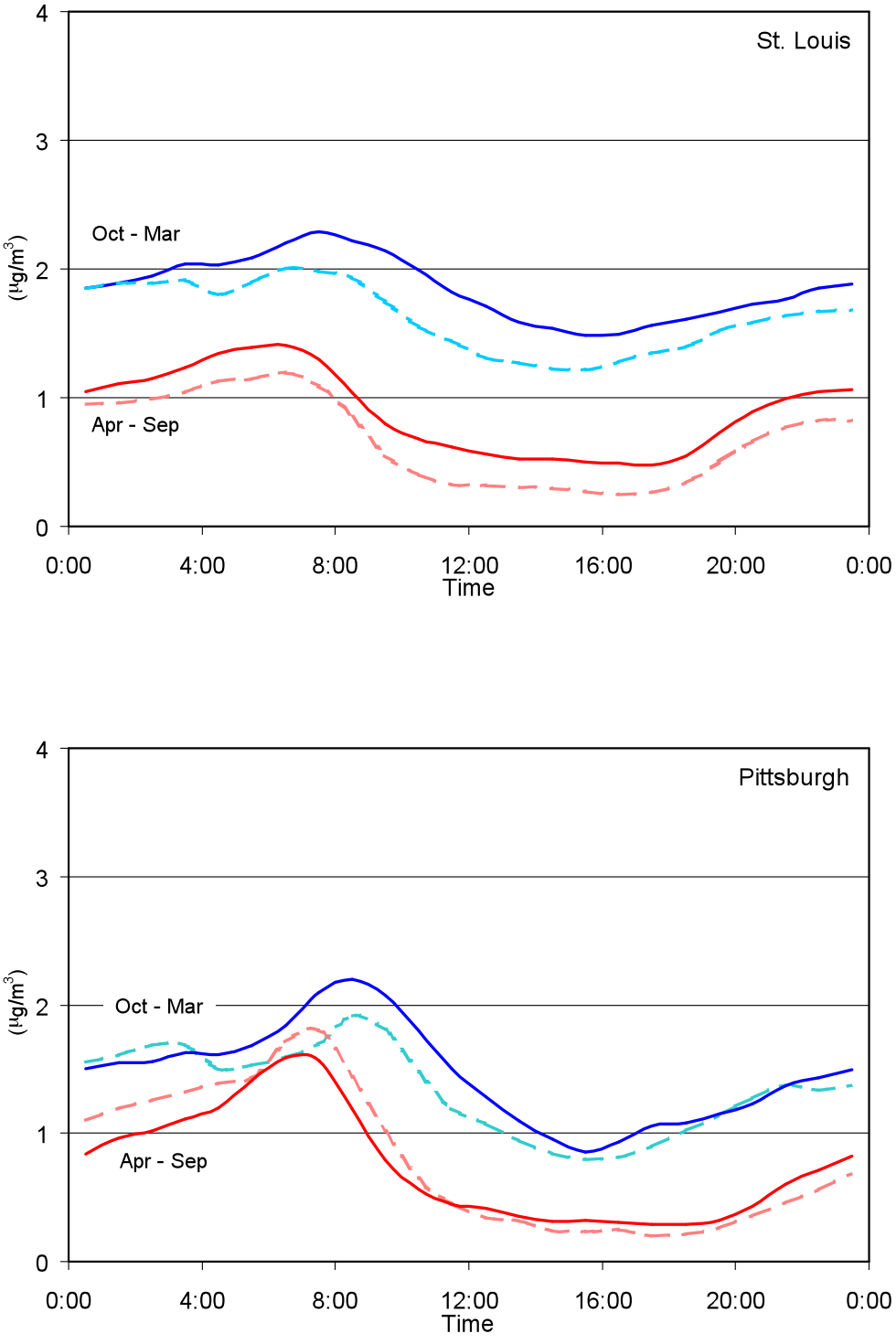

Figure 3.1: Diurnal variation in fine particle nitrate concentrations. Solid lines: Tuesday through Saturday. Dashed lines: Sunday and Monday.

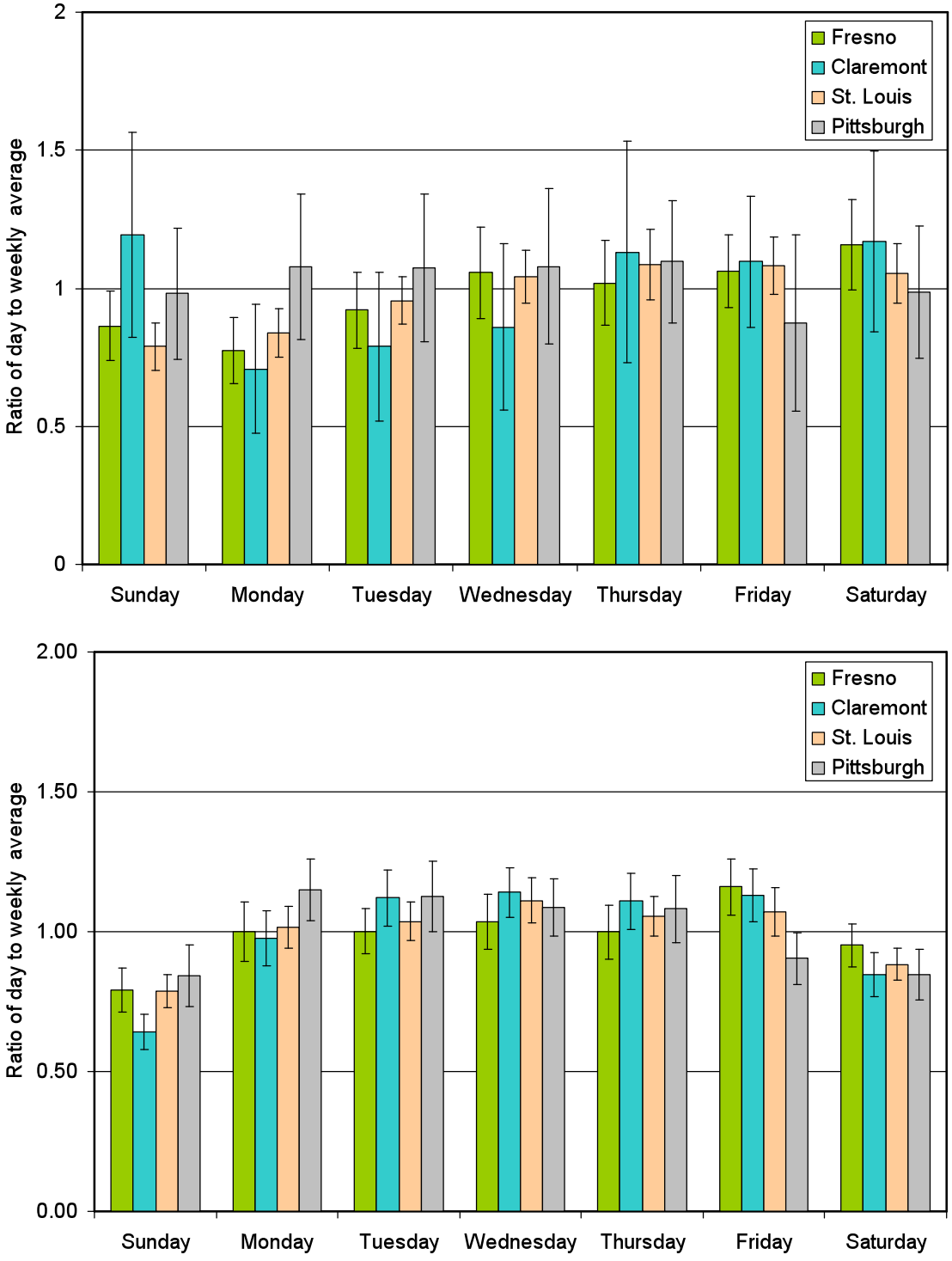

Figure 3.2: Average (± 95% CI) fine particle nitrate concentrations (top) and NO_x (bottom) by day of week, normalized to moving seven-day average.

Table 3.3: Observed Daily Changes in NO_x[a] and $PM_{2.5}$ Nitrate Relative to Moving 7-Day Averages

	Saturday		Sunday		Mondays	
Site	NO_x	Nitrate	NO_x	Nitrate	NO_x	Nitrate
Fresno[b]	–5±8%	+16±16%	–21±8%	–14±12%	0±11%	–23±12%
Claremont[c]	–15±8%	+17±33%	–36±6%	+19±37%	–2±10%	–29±23%
St. Louis	–12±6%	+6±11%	–21±6%	–21±9%	+2±7%	–16±9%
Pittsburgh	–15±9%	–3±17%	–16±11%	–6±13%	+15±11%	+4±15%

[a] NO_x was analyzed over the same period as nitrate at each location.

[b] NO_x converter externally mounted to minimize inlet losses of species such as nitric acid

[c] NO_x concentrations measured at Pomona, located ~9 km SW of Claremont site

Past studies (Blanchard and Tanenbaum, 2003; Harley et al., 2005; Motallebi et al., 2003) have found little or no evidence of weekly cycles in fine particulate nitrate. In contrast, our analysis indicates significant weekly variation in nitrate at 3 of 4 sites examined. At Claremont and Fresno, the lowest nitrate concentrations are observed on Mondays, vs. roughly equal concentrations on Sundays and Mondays at St. Louis. Observed decreases in nitrate are likely a delayed response to weekend decreases in NO_x emissions beginning on Saturday.

Co-located measurements of NO_x concentrations were made at Fresno, St. Louis, and Pittsburgh. NO_x was not measured at Claremeont, so data from a nearby air-monitoring site (Pomona) were used instead. Analysis of these data shows clear weekend NO_x reductions with Sunday minima (see Table 3.3). At Fresno, Claremont, and St. Louis nitrate reductions observed on Mondays are of similar magnitude to NO_x reductions on Sundays. However, at Fresno and St. Louis there is no statistical difference between nitrate reductions on Sunday vs. Monday. Although not statistically significant, nitrate concentrations at Claremont on Sunday were found to be larger than the weekly average. Sunday nitrate increases at Claremont may indicate that differences of meteorology or characteristic distances from major emission source locations may influence the timing of the nitrate reductions. Nitrate concentrations at Pittsburgh appear to be insensitive to weekend NO_x reductions, as discussed further below.

3.4 Discussion

Past studies of weekly cycles in nitrate levels have focused on changes observed on weekends; such analyses can miss the larger nitrate reductions observed immediately following the weekend on Mondays at some sites. At Claremont, the average normalized nitrate level remains lower than 1.0 through Wednesday, however, only the reduction on Monday is statistically significant. This study provides evidence for the existence of weekly cycles in observed nitrate concentrations associated with weekend NO_x reductions. In addition, there may be some delay in nitrate response to weekend NO_x reductions, though observational evidence is not as clear for this effect. At Fresno, Claremont, and St. Louis, mean nitrate concentrations are higher on Saturday vs. weekly average values. Although this trend is not statistically significant, it suggests carryover of higher nitrate and/or nitric acid concentrations from Friday, as there is no apparent nitrate response to lower NO_x emissions on Saturday. Similarly, lower nitrate concentrations observed on Mondays at the same sites may indicate carryover of low nitrate and/or nitric acid concentrations from the weekend. Examining seasonal patterns in nitrate response to weekend NO_x reductions (Figure 3.3) indicates the lowest nitrate day varies by season in some cases. For example, during winter months at Fresno, nitrate is lowest on Monday whereas during the summer the lowest nitrate levels are observed on Sunday. Increased carryover from the previous day during winter months may be a contributing factor to this observation. Other factors to consider include differences in prevailing air flow patterns, and smaller sample size (hence greater variability in the observations) when annual time series are divided into seasonal subsets and analyzed separately.

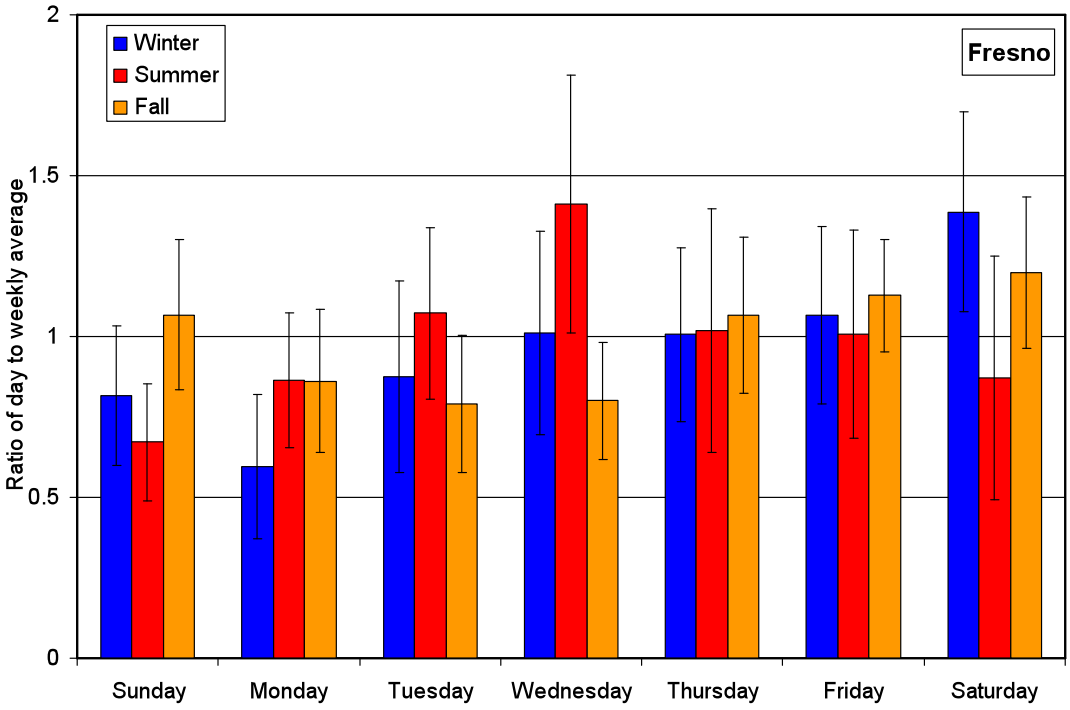
Winter
Summer
Fall
Fresno
Ratio of day to weekly average
2
1.5
1
0.5
0
Sunday
Monday
Tuesday
Wednesday
Thursday
Friday
Saturday

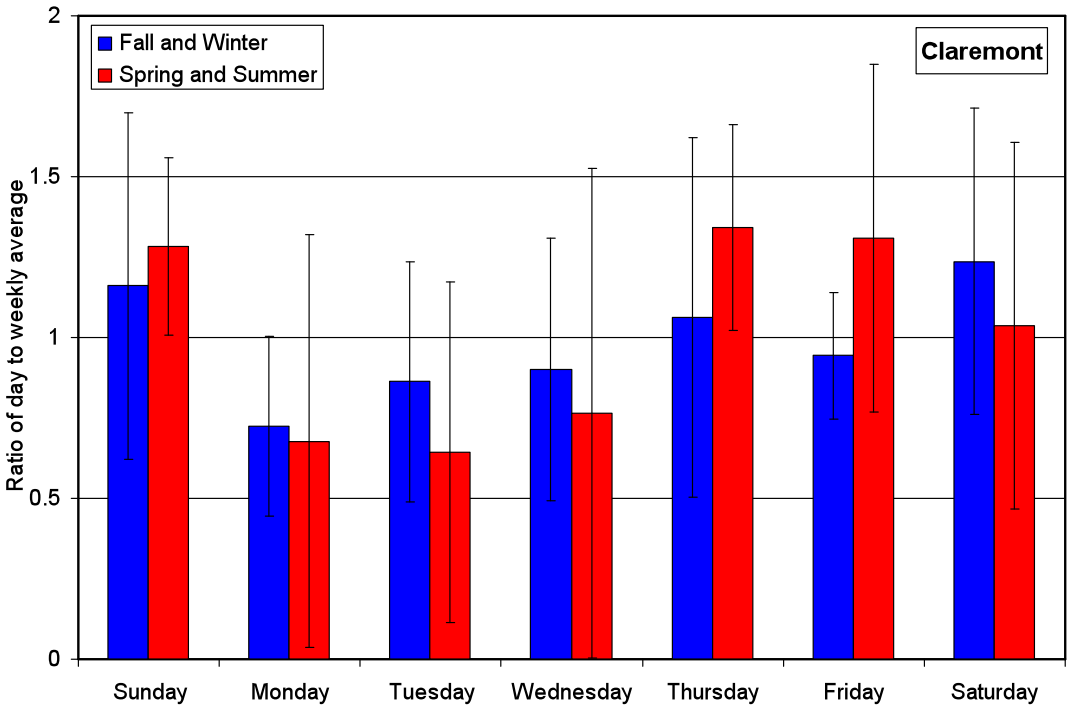
Fall and Winter
Spring and Summer
Claremont
Ratio of day to weekly average
2
1.5
1
0.5
0
Sunday
Monday
Tuesday
Wednesday
Thursday
Friday
Saturday

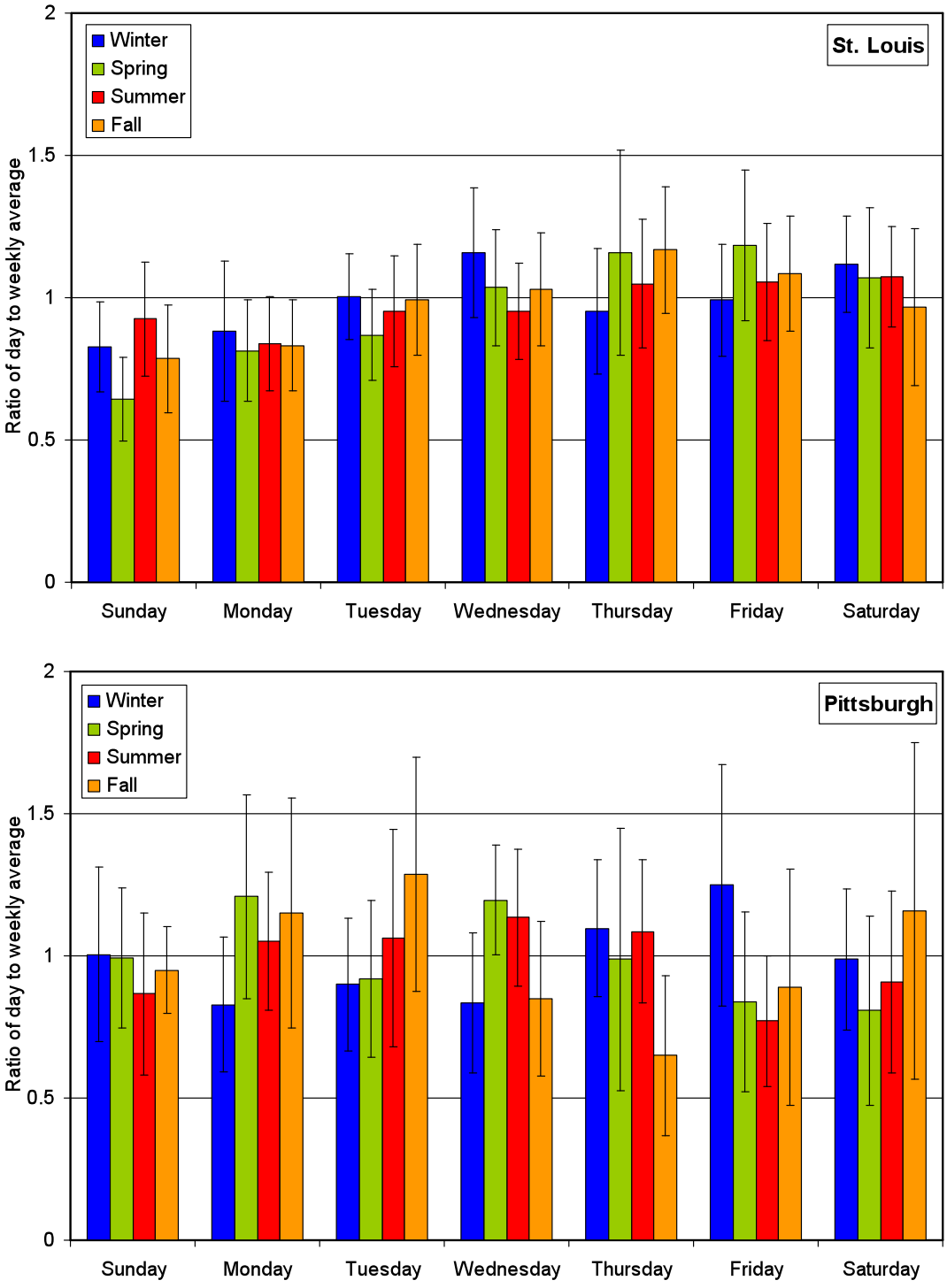

Figure 3.3: Average (± 95% CI) fine particle nitrate by day of week and season, normalized to moving seven-day average. Note: due to the instrument malfunction, Fresno spring data are not shown. Claremont fall and winter seasons and spring and summer seasons have been analyzed together due to measurement gaps during those seasons.

Pittsburgh. Significant NO_x reductions on Saturdays and Sundays (15±9% and 16±11%, respectively) do not correspond to reductions in observed nitrate levels at Pittsburgh. This lack of response is unique among the four sites examined here. Possible causes for the lack of nitrate response to lower NO_x are that (1) the magnitude of weekly NO_x reductions is too small and variable to produce an observable response in secondary products such as nitric acid and particle nitrate; (2) high sulfate concentrations limit ammonia availability for particle nitrate formation and thus nitrate concentrations are insensitive to changes in NO_x, and (3) changes in sulfate levels may obscure NO_x effects on nitrate by altering ammonia availability.

Examining the sum of gas-phase nitric acid plus particulate nitrate concentrations (Wittig et al., 2004) removes effects of gas-particle partitioning that might obscure a weekly signal in the data. Over the full annual cycle, the lowest concentrations of total nitrate (combined gas and particle phase) are observed on Sundays at Pittsburgh, see Figures 3.4 and 3.5. However, none of the days show statistically significant differences from one another or versus the moving weekly average. Relative to the other sites, weekend NO_x reductions are smaller at Pittsburgh and the associated variability is higher.

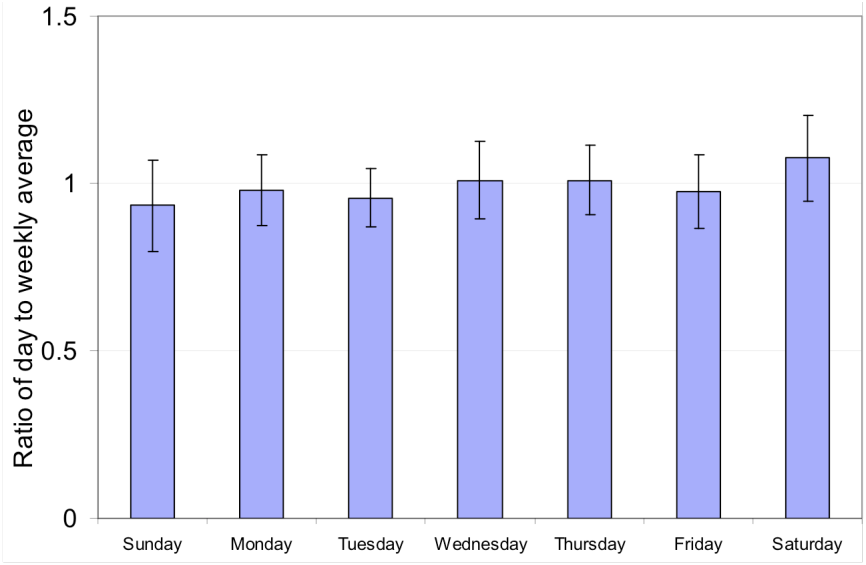

Figure 3.4: Average (±95% CI) sum of gas and particle nitrate concentrations at Pittsburgh by day of week, normalized to moving seven-day average. Shown over the full span of data (1 year).

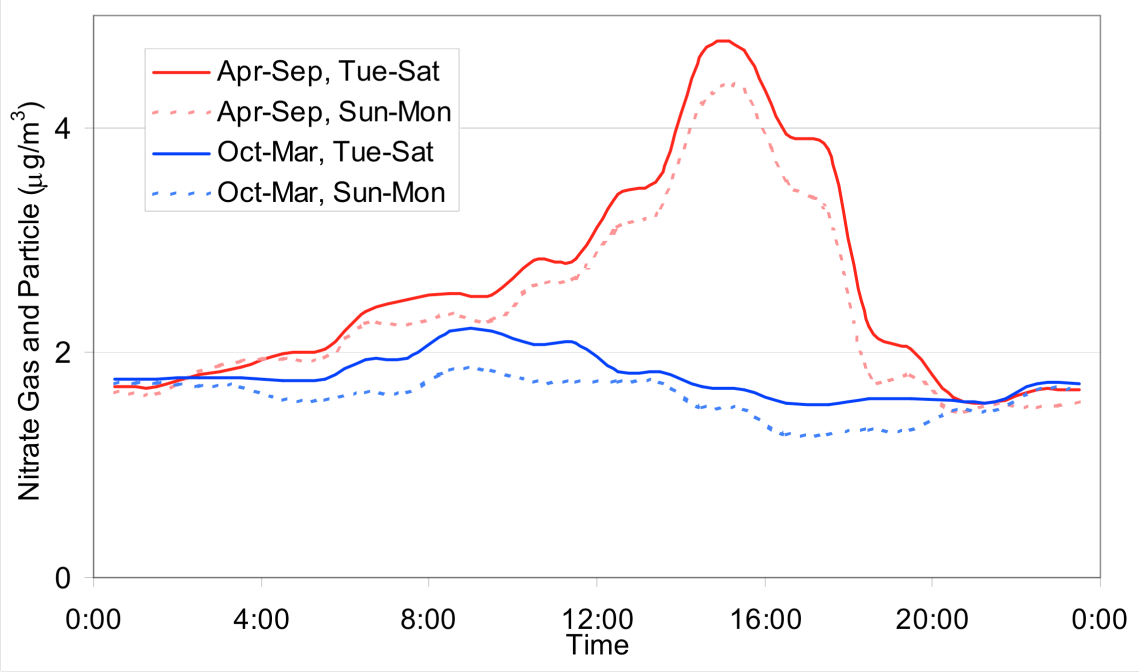

Figure 3.5: Diurnal variation of the sum of gas and particle nitrate at Pittsburgh by season and day of week.

Figure 3.6 shows diurnal variations of gas plus particle ammonium, sulfate, nitrate, and predicted ammonium in the particle phase at Pittsburgh. The ammonium prediction assumes that for each mole of nitrate and sulfate measured in the particle phase there are one and two moles of associated ammonia, respectively. At times (especially on summer afternoons); predicted NH_4^+ levels are higher than the measured sum of gas and particle ammonia. The assumption of 2 moles of NH_4^+ for each mole of sulfate particle cannot hold during these high-sulfate periods, so sulfate will be present in more acidic forms such as NH_4HSO_4 or H_2SO_4.

Sulfate can act as a sink for ammonia, making it unavailable for particle nitrate formation. The average molar ratio of sulfate to nitrate for the months of April through December is >4. During this time, there is little ammonia available to react with nitric acid as much of the ammonia is consumed by neutralizing sulfate. In this situation, weekend NO_x reductions will have little effect on particulate nitrate.

A potential for nitrate/sulfate interactions exists as sulfate reductions could lead to higher ammonia concentrations, and thus greater particle nitrate formation. At Pittsburgh, measured sulfate concentrations are lowest on Saturdays (relative to a 7-day moving average) by 26±16% and 23±21% (mean±95% CI) during spring and summer months, respectively, and on Sundays by 21±19% during winter months (see Figure 3.7). There is some indication of reductions in SO_2 and sulfate starting on Friday. Friday reductions may point toward a slow down in SO_2 emissions late in the week before the weekend. The observed sulfate reductions on Saturdays during spring and summer mirror similar changes in SO_2 (see Figure 3.7). In this case, weekend reductions in sulfate increase the ratio of fully neutralized sulfate to bisulfate, without affecting ammonia available for reaction with nitric acid. Larger decreases in sulfate are likely to cause an increase in particle nitrate concentrations as described by Takahama et al. (2004).

3.5 Conclusion

This paper shows reductions in measured concentrations of particulate nitrate associated with lower NO_x emissions on weekends. Nitrate on Monday was reduced by 23±23, 29±23, and 16±9% at Fresno, St. Louis, and Claremont respectively. Sunday NOx measurements taken during the same time periods as the nitrate measurements found reductions of 21±8, 36±6, and 21±6% at Fresno, St. Louis, and St. Louis, respectively. These observations indicate the potential to reduce $PM_{2.5}$ nitrate via NO_x control at close to a one to one relationship.

The effectiveness of NO_x as a nitrate control strategy varies by location. At Fresno, Claremont, and St. Louis reductions in nitrate were delayed vs. weekend changes in NO_x and at Pittsburgh no observable response in nitrate is seen to weekend NO_x reductions. Average nitrate concentrations at Pittsburgh were lower than average nitrate concentrations at each of the other locations and high sulfate found at Pittsburgh limited the availability of ammonia for ammonium nitrate particle formation, leading to higher HNO_3 concentrations and lower nitrate particle concentrations. These two factors, possibly combined with significantly higher Monday NOx at Pittsburgh likely helped to obscure any weekly nitrate cycles at Pittsburgh.

Further analysis at Pittsburgh examined the potential for sulfate reductions to increase nitrate concentrations. It was found that weekend sulfate reductions at Pittsburgh lead to lower the aerosol acidity, however aerosols do not reach neutrality, and thus additional ammonia does not

become available for reaction with HNO_3. Sulfate reductions of 21-26% were found on either Saturday or Sunday during the spring and summer months. This gives some indication that one need not worry about sulfate reductions leading to greater nitrate formation until reductions of greater than ~26% are realized (that is reductions relative to 2001-2002 sulfate levels in Pittsburgh).

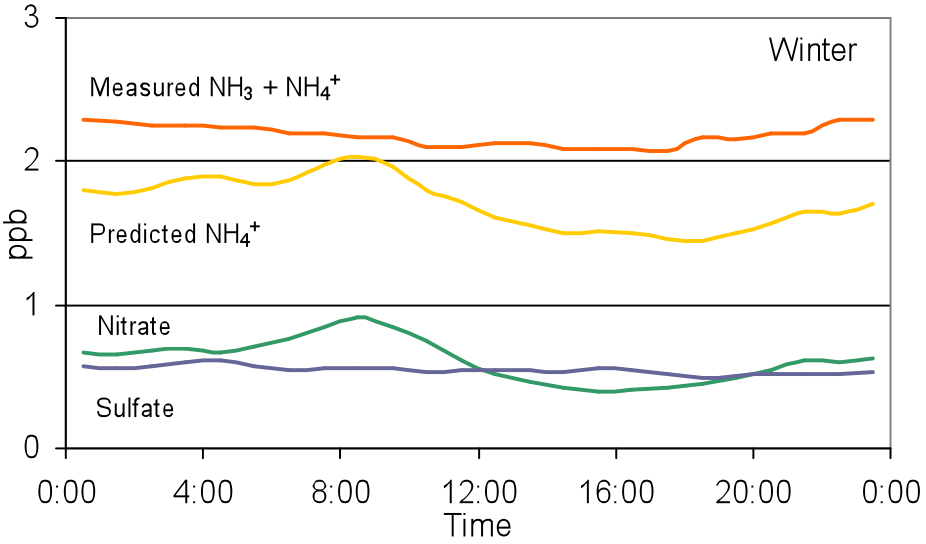
Winter
Measured NH3 + NH4+
Predicted NH4+
Nitrate
Sulfate
ppb
3
2
1
0
0:00
4:00
8:00
12:00
16:00
20:00
0:00
Time

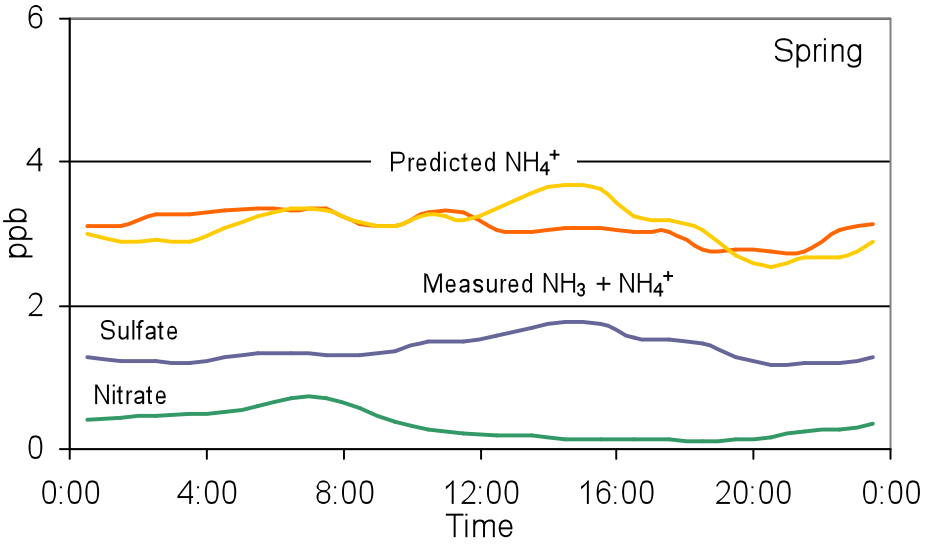
Spring
Predicted NH4+
Measured NH3 + NH4+
Sulfate
Nitrate
ppb
6
4
2
0
0:00
4:00
8:00
12:00
16:00
20:00
0:00
Time

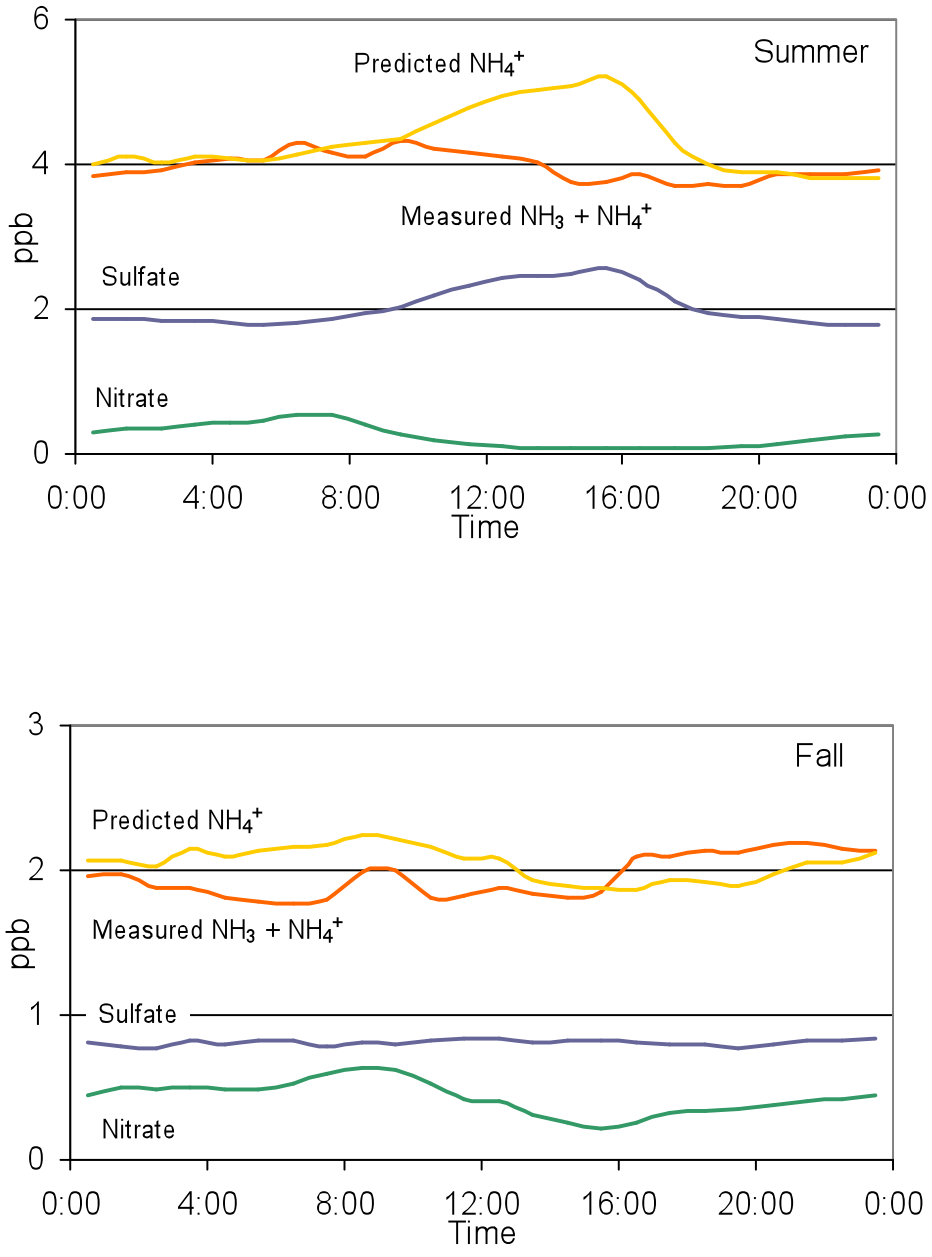

Figure 3.6: Diurnal variations in nitrate, sulfate, the measured sum of NH_4^+ and NH_3, and predicted NH_4^+ (2× sulfate + nitrate) at Pittsburgh. The unit of ppb means 10^{-9} mole of species per mole of gaseous molecules in air, and for particle species was calculated based on reported mass concentrations.

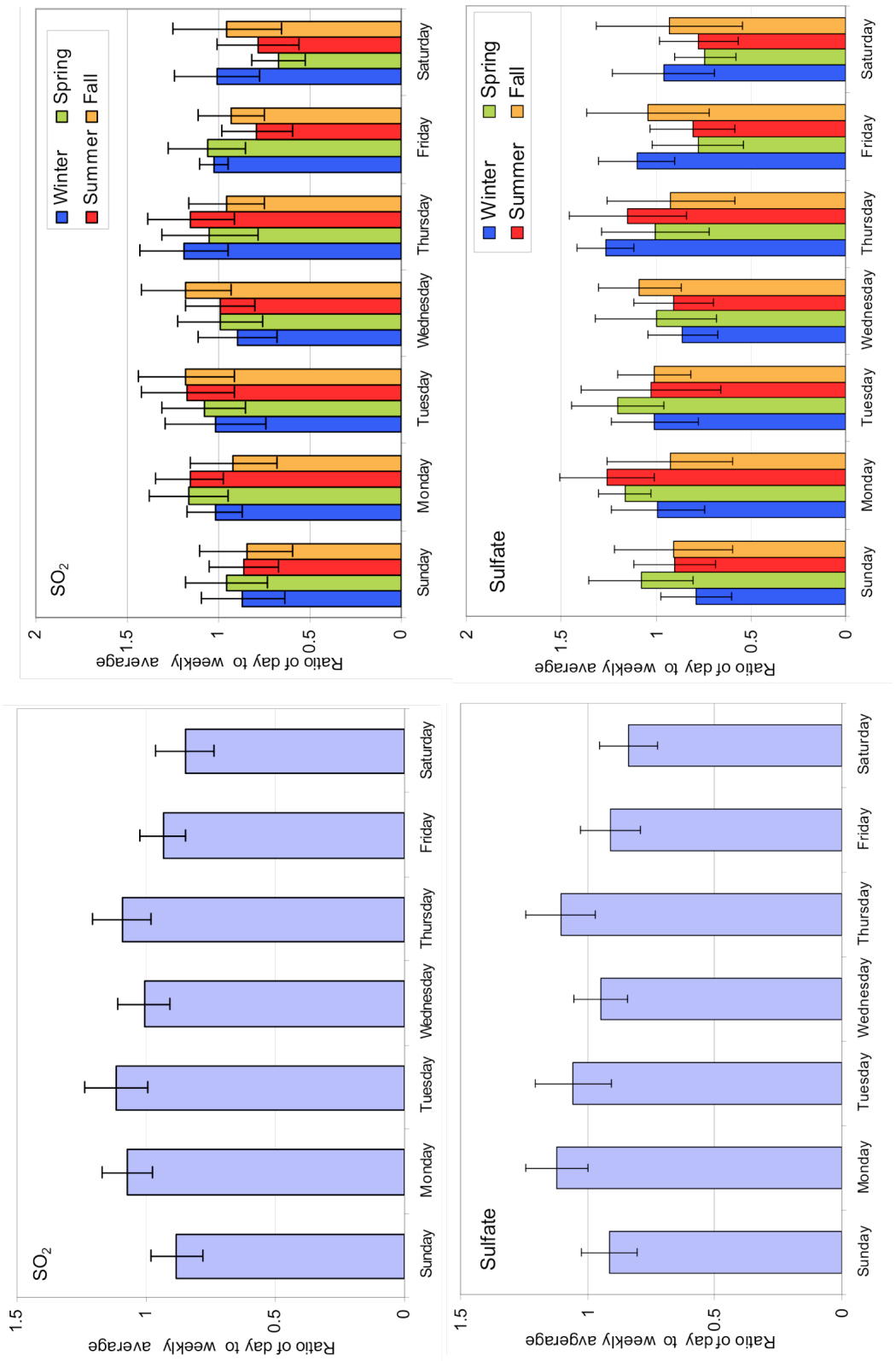

Figure 3.7: Average (±95% CI) SO_2 and sulfate concentrations at Pittsburgh by day of week, normalized to moving seven- day average. Shown over the full year and by season.

Chapter 4

EMISSIONS FROM OFF-ROAD DIESEL CONSTRUCTION EQUIPMENT[2]

4.1 Introduction

Diesel engine exhaust is a major source of emissions of nitrogen oxides (NO_x) and particulate elemental carbon (EC) or soot (Ban-Weiss et al., 2008b). As on-road engine emissions have been controlled, there has been increasing concern about the role of off-road sources of air pollution, as they were not a focus of earlier control efforts. Construction activities can include extensive use of off-road diesel-powered equipment, and are estimated to be responsible for 11 and 14% of NO_x and $PM_{2.5}$ emissions, respectively, from all mobile sources in California as of 2005 (CARB, 2009b). These construction emission estimates do not include emissions from deliveries of equipment and material to construction sites that are counted elsewhere as part of on-road motor

---

[2] Reprinted from Millstein, D. E., and Harley, R. A.: Revised estimates of construction activity and emissions: Effects on ozone and elemental carbon concentrations in southern California, *Atmospheric Environment*, 43, 6328-6335, Copyright 2009, with permission from Elsevier Science.

vehicle emission inventories. Construction activities can also be a significant source of dust emissions, though this study focuses on diesel exhaust-related emissions only.

Estimates of emissions from construction activity are important to help weigh the effectiveness of various regulatory options when developing control strategies. To meet health-based air quality standards, planning agencies model air quality at high spatial resolution under future emission scenarios to demonstrate that standards will be attained. There is also a need for spatial resolution of emissions in studies that investigate exposure to air pollution at the community or neighborhood scale.

Emission inventories are a major source of uncertainty in air quality planning. Kean et al., (2000) reported estimates of off-road diesel NO_x and PM emissions based on fuel-use that were less than half of EPA's corresponding national estimates. A recent study of off-road engine emissions in California (Baker, 2008) found large uncertainties in estimates of equipment populations and activity. Comparing engine and activity survey data to both the California Air Resources Board OFFROAD and U.S. Environmental Protection Agency NONROAD models, Baker reported lower values for important factors such as equipment populations, hours of use, and rated horsepower. OFFROAD model estimates of the diesel construction equipment population in California were three times the values reported by Baker (2008). Engine usage and rated power output were reported to be over-estimated by factors of 40 and 10%, respectively, both of which would magnify the effect of an overstated engine population. Baker also found the relationship between the number of employees working in construction and diesel construction equipment populations to be weak at the county level. In short, estimates of construction equipment emissions suffer from large uncertainties in quantifying activity at state and national levels, and in the spatial allocation of this activity to finer spatial scales.

Estimates of off-road engine emissions based on fuel use and fuel-based emission factors do not require knowledge of equipment populations. Although there is variation in emission factors among equipment types, recent studies by Abolhasani et al. (2008), Frey et al. (2008a) and Durbin et al. (2007a), have characterized NO_x and other pollutant emission factors for construction equipment, on a per unit of fuel burned basis. Lewis et al. (2009) compare multiple estimates of construction emissions and describe applicable regulations. Additional research concerning construction emissions focuses on the activity patterns of off-road vehicles (Huai et al., 2005) and on measuring in-use emission factors of dust and PM_{10} in addition to $PM_{2.5}$ (Muleski et al., 2005). Reff et al. (2009) present a national $PM_{2.5}$ emission inventory and highlight the need for further study of off-road diesel mobile equipment.

The construction industry is concerned that requirements for retrofitting and/or replacing off-road diesel equipment will create economic hardship (Sandherr, 2007). Emission estimates from the OFFROAD model (CARB, 2007c) have been used to quantify potential air quality benefits of such control programs. There is a known inconsistency between underlying fuel use/engine activity data in the emission inventories for criteria pollutants such as NO_x and greenhouse gases such as CO_2. Staff are "working towards reconciling the emission estimates from the fuel usage approach and the models," (CARB, 2009a).

In this study, we evaluate differences in estimates of construction activity and emissions by location. An air quality model is used to assess the influence of revised emission inventories for the construction sector on air pollutants such as ozone and $PM_{2.5}$. Both region-wide emission totals and the spatial distribution of the emissions have important effects on air quality. This paper highlights the importance of reducing uncertainty in emission inventories for sectors that have not been studied as extensively as on-road vehicles (Sawyer et al., 2000) or electric power generation (Kim et al., 2006).

4.2 Methods

A widely used method (Samaras and Zierock, 1995; EPA, 2005b; CARB, 2007b) for calculating construction-related and other off-road mobile source emissions of air pollution starts from estimates of the number of pieces of equipment that are in service in a given area. Because off-road engines are not licensed and registered in the same way as on-road vehicles, engine populations are estimated based on annual new engine sales and estimates of equipment turnover. Engine populations are combined with rated power output of each engine, load factors, hours of use, and emission factors to estimate emissions of air pollutants such as VOC, NO_x, and exhaust PM.

$$E_i = N \times P \times L \times t \times F_i \quad (4.1)$$

In Eq (4.1), E_i is the emissions of pollutant i (g per day), N is the engine population (number of engines in use), P is the rated power output of the engine (kW), L is a load factor (average fraction of rated power output during operation), t is average operating hours per day, and F_i is the emission factor for pollutant i, expressed per unit of engine work output (g/kWh).

An alternative method combines fuel-use and mass-based emission factor data to estimate total emissions. Separate factors are used to distribute these emission totals across a domain of interest. Emission factors represent average emissions for each pollutant across the spectrum of equipment types and working conditions. Tax-exempt fuel use estimates represent total diesel fuel consumed by the construction industry in off-road engines but should not include fuel for construction support vehicles that travel on highways. Emissions are estimated as:

$$E_i = S \times F_i \quad (4.2)$$

In Eq (4.2), E_i is the emissions of pollutant i (g/day), and S is the fuel use (kg/day), and F_i is emission factor for pollutant i expressed per mass of fuel burned (g/kg).

Fuel Sales Data. The Energy Information Administration (EIA) conducts an annual survey of distillate fuel sales at the wholesale level, for various end use categories including construction activities. Fuel tax receipts and EIA survey data are reconciled with refinery production and net imports, thereby matching fuel consumption to reported fuel supply. Estimates of 2005 sales of off-highway distillate fuel used for construction in California were used in this research as the basis for a fuel-based emission inventory. Fuel consumption estimates of this type are available for all 50 states and the District of Columbia (EIA, 2006). As EIA fuel survey data are resolved only to the state level, spatial surrogates are needed to apportion construction activity and the

associated emissions to the county level and finer spatial scales. Potential surrogates are considered below.

Construction Employment Data. Employment data by county for the year 2005 reported by Baker (2008) were based on data from the California Employment Development Department. Data for 1990–2007 on both the number of establishments and employees in different sectors are available. Baker used the number of construction employees in each county as a surrogate to allocate construction equipment populations to the county level. Construction sector employment data does not correlate well with equipment populations. Baker reported that employment data only explained 12% of the variance associated with county-level equipment populations.

Construction Permit Data. The Construction Industry Research Board (CIRB) collects data from cities and counties across California on construction-related activity. These data support a variety of regulatory, business, and research needs. Archived construction permit records for 2005 were obtained from CIRB for use in this research (Bartolotto, 2009). The data included construction permit records for each California's 58 counties. More detailed data were obtained for 143 cities located within Los Angeles, Orange, and San Bernardino counties in southern California. Previous emission inventory development efforts have typically not made use of such fine-scale (i.e., sub-county level) data on construction activities.

Construction permit records specify total annual dollar value of construction projects in each locality. Construction activities are classified by CIRB as residential, commercial and industrial, public building, and public heavy-works construction. Data for public buildings and heavy-works were only available at the county level not at the city-level. The construction activity categories were summed to estimate total construction activity in each city and county.

By summing construction permit dollars an assumption is made that each sector of construction activity uses the same amount of fuel per dollar value of construction. While there is not a direct study of construction fuel use per dollar value of construction by sector, the Economic Input-Output Life Cycle Assessment (CMUGDI, 2008) reports emissions of diesel fuel related pollutants to be 5-7 times higher for highway, street, bridge and tunnel construction than for residential construction. Public works construction accounts for 11% of the total permit dollar values reported. Thus it is possible construction activity accounts for a much greater percentage of the total construction fuel use.

Although the contribution of each construction sector to total fuel use is uncertain, this uncertainty does not significantly affect the calculation of relative total fuel use by county. There is high correlation between residential construction activity and public works construction at the county level. Relative construction activity by county calculated with public works construction weighted 7-times as much as private construction displays a strong linear correlation, $r^2 = 0.99$, to relative construction by county calculated with equal weightings for each construction sector. Permit records for public works construction by city were not available, thus relative construction activity estimations based on private construction are subject to uncertainty regarding the distribution of public works projects.

An alternative database of construction permits is available from the California State Water Resource Control board (SWRCB, 2009). A storm water permit must be obtained from the SWRCB for construction projects that disturb >1 acre of land. While this database provides a useful alternative source of data on construction activity, it has some limitations. Construction activity is estimated by acreage, as opposed to dollars; thus, multistory projects are treated equal to single story projects that cover the same land area. It does not include highway construction or construction in cities with joint sewage/storm water treatment facilities. There is little information provided on how to allocate activity from multi-year projects. Storm water permit data are compared with other spatial surrogates discussed here, but are not used to estimate emissions.

Population Data. One of the main goals of construction activity is to provide residences, workplaces, and civil infrastructure to accommodate a growing population. Maintenance of existing infrastructure is another reason for construction activity. The demographic unit of the California Department of Finance is responsible for forecasting future population growth in California. County-level population forecasts were obtained for 2010 (DOF, 2007a), and compared with year 2000 county-level census data. Populations for each county in 2005 were estimated by linear interpolation. City-level population estimates were available for January 2007 and were compared to reported city populations from the 2000 census (DOF, 2007b; 2008).

Emission Inventories. The OFFROAD model (CARB, 2007c) was used to predict average 2005 summertime weekday emissions for diesel-powered construction equipment, including all rated power classes. Results were extracted by county, and included estimates of equipment population, fuel use, and emissions of total organic gases (TOG), CO, NO_x, SO_2, and PM.

The OFFROAD model estimates emissions using Eq. (4.1). In this work, the ratio of emissions outputs to fuel use outputs were used to back-calculate average emission factors for both the NONROAD (EPA, 2005a) and OFFROAD models.

Air Quality Modeling. The Community Multiscale Air Quality model (CMAQ; Byun and Schere, 2006) version 4.6 was used to evaluate the effects on air quality of changes to the construction emission inventory over a 6-day high ozone episode from 14-19 July 2005 in southern California. The analysis of particle concentrations uses the AE4 aerosol module (Binkowski and Roselle, 2003). The southern California model domain used here is centered on Los Angeles and extends 370 km south to north, and 550 km west to east. Figures 4.3 and 4.4 show maps of the modeling domain. Emission inventories for this study were provided by the California Air Resources Board (Jackson, 2007), and match information used in the 2007 Air Quality Management Plan for the South Coast Basin (SCAQMD, 2007a). Diurnal patterns were applied to emissions on a sector-by-sector basis. Separate diurnal patterns were applied on weekends vs. weekdays for sectors, such as gasoline and diesel vehicles, that have significantly varying activity patterns on weekends. For the baseline construction inventory emissions begin at 7AM and increase in intensity to 10 AM, then from 10 AM to 7 PM construction emissions remain at peak intensity and then decreased to zero emissions at 11 PM. Each sector's diurnal pattern was left unchanged from the baseline scenario to the adjusted scenarios except construction emissions. Construction emissions were changed slightly to begin at 6 AM and reach a constant peak intensity between 7 AM and 2 PM, and were tapered to zero by 7 PM.

Further details on the model, input data, and model evaluation against observations can be found in SCAQMD (2007a) and Millstein and Harley (2009b) and Appendix A.5.

A revised statewide annual construction emission estimate was determined using Eq. 4.2. Emission factors (g/kg fuel) used to create a new construction emission inventory are shown in Table 4.1. The revised estimate was based on fuel use reported by the EIA survey. To make a weekday modeling inventory, statewide emissions were distributed to the grid level based on the relative amount of county and city level CIRB permit data or relative population growth for cities where permit data was not available and then annual totals were divided by 250 weekdays. Total baseline and revised construction emissions estimates used in the model are shown in Table 4.2. Emission factors for SO_2 were held to the same SO_2/PM ratio as in the base case. Ultra-low sulfur diesel fuel standards were instituted in 2006 for off-road diesel in California; construction equipment emissions of SO_2 are not a focus of this work.

Table 4.1: Exhaust emission factors for diesel-powered combustion equipment.

Pollutant	Emission factors (g/kg)		
	This study	California OFFROAD model	EPA NONROAD model
NO_x ($\mu\pm\sigma$)	34.5±4.5[a]	42.9±4.9	34.1±4.1
PM ($\mu\pm\sigma$)	EPA value[b]	2.6±1.2	3.0±1.5
VOC ($\mu\pm\sigma$)	4.0±1.3[a]	7.2±3.6	3.7±2.6
CO ($\mu\pm\sigma$)	9.5±6.2[a]	18.8±6.6	17.9±10.1
$EC/PM_{2.5}$	0.63[c]	-	0.77[d]
$OC/PM_{2.5}$	0.32[c]	-	0.18[d]

[a] From in-use measurements of construction equipment (tier 0-2) presented in Abolhasani et al. (2008) and Frey et al. (2008a).
[b] 3.0±1.5, from EPA NONROAD model, (EPA, 2005b).
[c] Based on Caldecott Tunnel study, (Ban-Weiss et al., 2008b).
[d] From EPA speciate 4.0 (EPA, 2006), composite for HDDV vehicle exhaust.

Table 4.2: Baseline and revised emissions in selected southern California counties.

	Construction Emissions (10^3 kg/day)			
	Los Angeles	Orange	Riverside	San Bernardino
NO_x				
Baseline	75.1	38.0	18.9	14.6
Revised	12.0	4.3	8.8	4.2
Ratio[a]	0.16	0.11	0.47	0.29
Emis. Tot.[b]	524.8	143.8	145.6	210.3
$PM_{2.5}$				
Baseline	4.24	2.20	1.09	0.82
Revised	1.09	0.39	0.80	0.38
Ratio	0.26	0.18	0.74	0.47
Emis. Tot.[b]	53.3	15.4	16.4	29.8

[a] Ratio of revised to baseline construction emissions. The baseline emissions match information found in the 2007 Air Quality Management Plan for the South Coast Basin (SCAQMD, 2007a). The revised emissions are calculated based on Eq. 4.2 and use fuel inputs from the EIA survey and emission factors shown in Table 4.1. In the revised inventory, relative emissions by county were calculated based on CIRB permit data.
[b] This is the total of all emissions (not limited to construction emissions) in the southern California modeling domain in the baseline scenario.

4.3 Results

Fuel Use Estimates. EIA reports that total California diesel fuel used for construction equipment operating off-road in 2005 was 550 million kg. Recent surveys indicate relatively uniform construction activity across all seasons in California (Baker, 2008). Survey data from southern California shows 90 and 99% reductions in construction activity on Saturday and Sunday, respectively, compared to weekdays (Coe et al., 2003). Assuming 50 weeks with 5 workdays each we estimate 2.2 million kg/day of fuel is used on weekdays. The assumption here of zero weekend construction activity is a simplification that causes an over-estimation of weekday average fuel use. However, even if activity on each weekend day was assumed to be 10% of the weekday level, the weekday average fuel estimate would change by <5%.

Along with pollutant emissions, OFFROAD estimates fuel use for each type of equipment and location. The total diesel fuel use in California estimated by the OFFROAD model for construction equipment on an average weekday is 7.9 million kg/day, 3.6 times greater than the value based on the EIA survey.

Based on a survey of construction firms, Baker (2008) estimated statewide construction equipment populations, hours of activity, and rated horsepower that were approximately 30, 70, and 90% of the corresponding estimates in the OFFROAD model, respectively. The uncertainties associated with these factors could help to explain the higher predicted fuel use by the OFFROAD model.

Uncertainties in EIA survey data could contribute little to the difference in activity estimates. Overall, the EIA (2006) received responses from 91% of the fuel wholesalers that it solicited, indicating a comprehensive sample. To estimate sampling errors, EIA calculated the coefficient of variation at the state level for various fuel types. The EIA found the coefficient of variation was 4.7% for California non-residential distillate fuel sales (EIA, 2006). The uncertainty associated with the EIA survey is relatively small compared to the uncertainty in construction activity patterns or average equipment load levels. The relatively low uncertainty associated with reported fuel sales is a motivation for incorporating fuel sales, as opposed to activity estimates, into a method for calculating total emissions.

County Level Construction Activity. A comparison of six different surrogates used for county level allocation of construction activity is shown in Apendix A.1. The surrogates shown are population, population growth, OFFROAD model activity estimates, construction permit dollars, storm water construction permit acreage, and construction employment. These metrics are all expressed as fractions of the corresponding state total and they lead to different spatial distributions of construction activity.

Figure 4.1 shows relative county population growth and OFFROAD model-derived construction activity versus relative county construction permit dollars. It shows county-to-county variations in construction permit dollars are well correlated with differences in population growth (R^2 = 0.95) and less correlated with OFFROAD activity estimates (R^2 = 0.83) and absolute population estimates (R^2 = 0.84) (not shown).

Relative distributions of construction activity for the five largest counties in southern California are shown in Figure 4.2. Each bar plotted in the figure is the ratio of an alternative construction activity estimate to an estimate based on permit dollars. This figure thus compares the relative distribution of construction activity among counties. The four measures compared are population growth, the OFFROAD model, employment data, and storm water permit acreage. Permit dollar data and population growth are well correlated across the counties shown. Larger deviations from construction permit data are seen for each of the other methods, especially for Riverside and Orange counties.

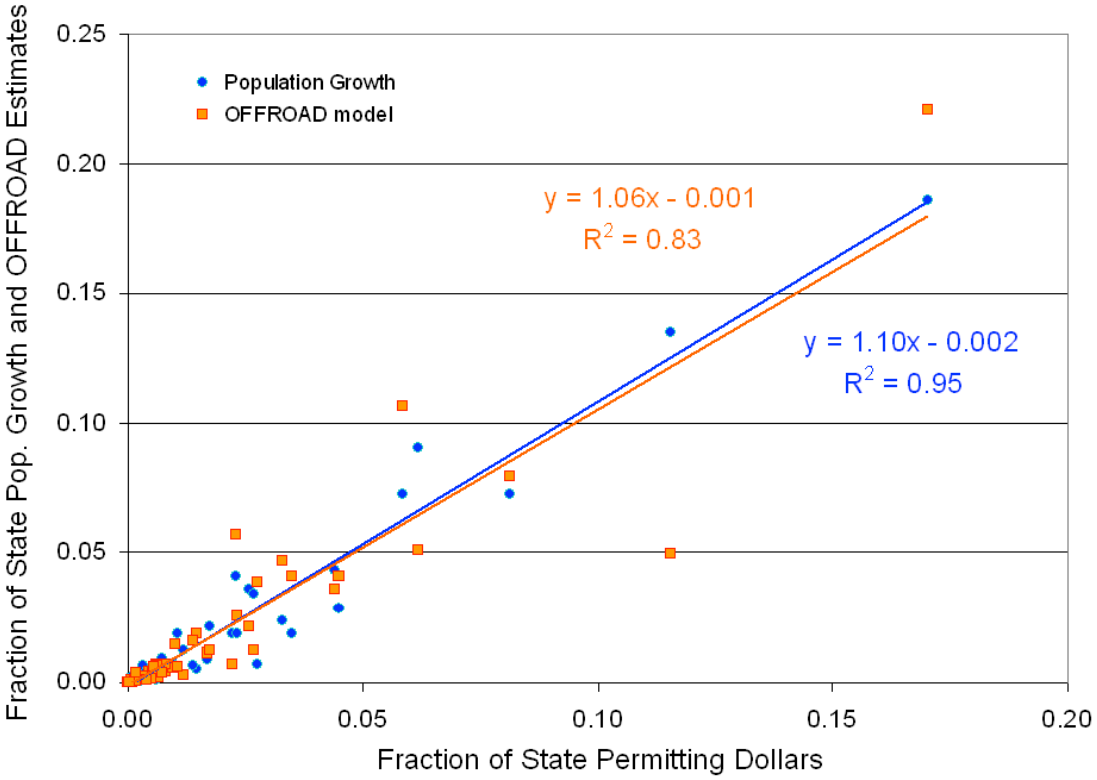

Figure 4.1: County fraction of population growth and OFFROAD construction activity as a function of permitting dollars.

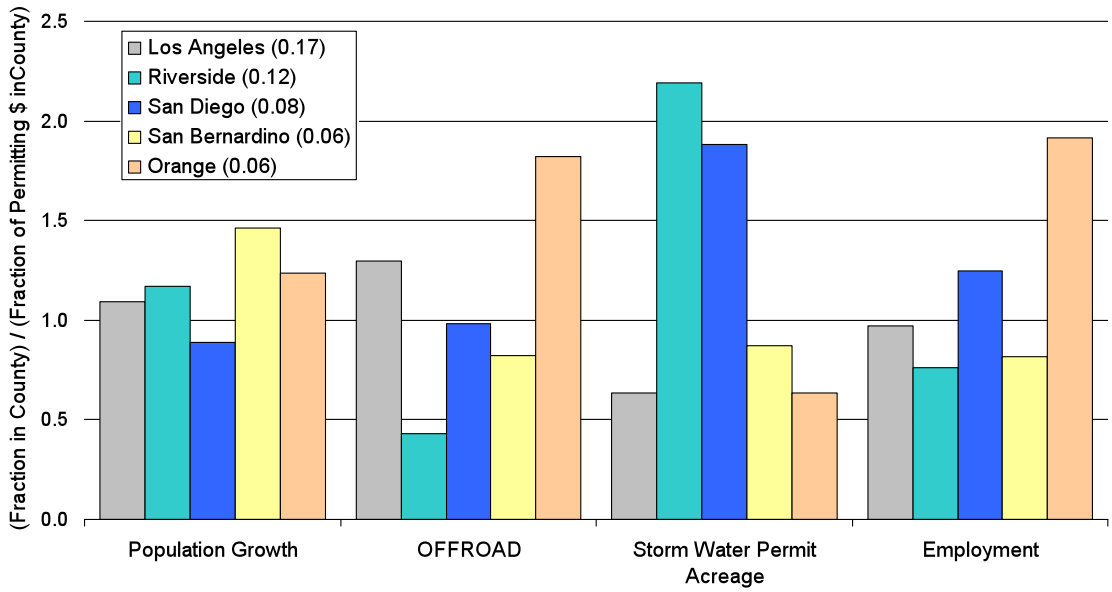

Figure 4.2: Fraction of population growth, OFFROAD construction activity, storm water permit acreage, and employment divided by the fraction of permitting dollars for selected southern California counties. A value of 1.0 would indicate relative county activity is the same as relative permitting dollars for that county. The numbers following the county names in the legend are the fraction of California permitting dollars for that county.

City Level Construction Activity. The OFFROAD model does not estimate activity at spatial scales smaller than counties. City level population data are compared here to city level construction permit data available for 143 cities located in Los Angeles, San Bernardino, and Orange counties. While cities vary in size, many of the cities considered here are small enough to fit within a single 5 by 5 km grid cell used in the emission inventories that support air quality modeling and planning efforts. Even larger cities usually extend over only a few grid cells. A city such as Los Angeles poses a special challenge: this unusually large city (>1200 km^2) encompasses forty-nine 5 by 5 km grid cells.

Similar analysis as above reveals strong correlation between construction permits and population growth ($R^2 = 0.79$). In contrast, city level population data in a single specified year does not correlate well with construction permit data ($R^2 = 0.27$). Appendix A.6 shows population and population growth plotted versus construction permits. Appendix A.2 shows southern California city level activity estimates based on construction permits, population growth, and population.

Emission Factor Estimates. Recent studies report measurements of in-use emissions from diesel-powered construction equipment. Frey et al. (2008a) and Abolhasani et al. (2008) report mass-based emissions of motor graders, backhoes, front-end loaders and excavators measured over various work cycles. Equipment emission factors are dependent on engine emission standards (tier level) at the time of manufacture, thus measured emission factors must be weighted to reflect the 2005 age mix of in-use equipment in California. Baker (2008) reported the age of surveyed equipment populations in California. Based on the phase-in years of the different tier regulations, it was assumed equipment manufactured prior to 1999 met tier 0 standards, newer equipment manufactured prior to 2004 met tier 1 standards, and the newest equipment met tier 2 standards. Based on the age distribution of in-use equipment reported by Baker (2008) 39, 33, and 28% of in-use construction vehicles met tier 0,1, and 2 standards, respectively. The average NO_x emission factor (E_f) was estimated to be 34.5±4.5 g kg^{-1} where,

$$E_f = \Sigma_i [(W_i)(F_i)] \quad (4.3)$$

W_i is the tier weighting (0.39, 0.33, or 0.28) and F_i is the average emission factor by tier of all equipment measured by Frey et al. (2008a) and Abolhasani et al. (2008). The standard deviation reported is measured across the full range of tested equipment.

Use of portable emission monitoring systems (PEMS) adds uncertainty in quantifying emissions. For example, Durbin et al. (2007b) evaluate PEMS measurements of NO_x and CO_2 against Federal Reference Methods. For PM, the system used by Frey et al. (2008a) and Abolhasani et al. (2008) relies on an optical method that can measure relative PM emission changes but does not translate readily to PM mass measurements. PM emission factors are available from older dynamometer test data, but have to be adjusted to reflect current emission regulations (EPA, 2004).

Emission factors can also be extracted from the OFFROAD and NONROAD models. Model-derived emission factors and standard deviations for NO_x, PM, VOC, and CO as of 2005 are shown in Table 4.1. These emission factors are calculated as the activity- weighted average of emission factors from the different types of construction equipment defined in the models. The

model-derived emission factors vary across construction equipment types, but the fuel use weighted emission factors do not vary much at the county level in OFFROAD output. The low variation of emission factors across counties indicates that OFFROAD assumes a similar mix of equipment types across counties. The OFFROAD and NONROAD models specify similar emission factors for PM, whereas the NO_x emission factor in OFFROAD is 24% higher than that in NONROAD and the average emission factor based on in-use measurements discussed above. The difference between the OFFROAD and the NONROAD average emission factor could be created by differences between the equipment mix assumed by the models or from differences between the emission factors of individual equipment types in each model.

Emission Estimates. Following Eq. 4.2, and using emission factors shown in Table 4.1, statewide NO_x and PM emissions from off-road diesel construction equipment were estimated to be 76 ± 11 and 6.6 ±3.3 (10^3 kg/day ±σ) for average weekdays, respectively, where the standard deviation is an estimate of uncertainty in the daily mean emissions that uses Gaussian error propagation to account for sampling uncertainty reported in the EIA fuel survey and variation across measured NO_x emission factors or NONROAD modeled PM emission factors. Corresponding OFFROAD model statewide emission estimates are 4.5 and 3.1 times the values reported here. Appendix A.3 shows county-level NO_x and PM construction emission estimates compared with OFFROAD estimates.

Air Quality Modeling. An air quality model was used to demonstrate the effects of revisions to the construction emission inventory in southern California. The base case inventory was changed in two ways. First, the total domain-wide construction emissions were changed to reflect the new estimates. Second, the spatial distribution of construction emissions was revised to reflect construction permit and population growth data at the city level. These changes were evaluated individually and combined together. Total emissions of NO_x and PM were lower in the revised inventory compared to the baseline (see Table 4.2). Both a lower amount of diesel fuel use and a lower NO_x emission factor contributed to the difference between baseline and revised emissions.

To summarize changes to the spatial distribution of emissions, construction activity decreased in Orange and Los Angeles Counties and increased in the inland counties of San Bernardino and Riverside. Table 4.2 shows the ratios of revised to baseline emissions are larger for the inland counties. A map of changes in the spatial distribution of construction-related emissions is shown in Appendix A.7.

Figure 4.3 shows changes in predicted elemental carbon (EC) concentrations for the various emission scenarios. Note that EC is more sensitive to the emission changes reported here than total fine particle ($PM_{2.5}$) mass, as $PM_{2.5}$ mass includes larger contributions from other non-diesel sources as well as secondary gas-to-particle conversion processes that do not affect EC. Panel B shows the effects of decreasing total construction activity while maintaining the same spatial distribution of emissions as in the base case. Construction emissions were scaled uniformly across the domain to match total emissions from the fuel-based approach. Panel C displays the effects of spatial redistribution of construction activity. In this case total construction emissions were equal to the base case, only the spatial distribution was altered. Panel D shows combined effects of both sets of revisions to construction emissions.

With the revised emissions estimates, EC concentrations are reduced the most in downtown Los Angeles and Orange County. While both spatial distribution and total emission changes are important, the total emission changes produce the larger effect. For example, domain-wide EC emissions from construction are 3.1 times greater in the base case compared to the fuel-based estimate. In comparison, the changes in EC emissions from the spatial redistribution of emissions range from 132% for Riverside County to
-44% for Orange County.

Differences in peak ozone between the base case and three cases with different construction emission estimates are shown in Figure 4.4. The reduction in construction emissions causes an increase in predicted ozone especially inland at locations such as Pomona and Riverside where peak ozone increases by 10-18 ppb depending on the conditions and day. The effects of changing the spatial distribution of construction emissions depend strongly on location. With all revisions to construction emissions considered together at once, peak ozone responses share a similar spatial pattern to the effects seen in panel B.

Modifying construction-related emissions has mixed effects on model accuracy. In general, the base case model has NO_x concentrations that are lower and PM concentrations that are higher than observations. By lowering construction activity overall and by shifting emissions from costal to inland counties, prediction skill for PM and EC improves but is degraded for NO_x relative to the base case. There are smaller changes to O_3 prediction skill. Appendix A.4 shows model performance statistics for NO_x, O_3, $PM_{2.5}$ and EC for the various scenarios. Assuming the new inventory more accurately represents construction emissions than the baseline inventory, the differences between the two scenarios show that the baseline emission inventory was adding to the overall positive bias in PM concentrations and partly obscuring an underestimate of NO_x emissions from other source categories.

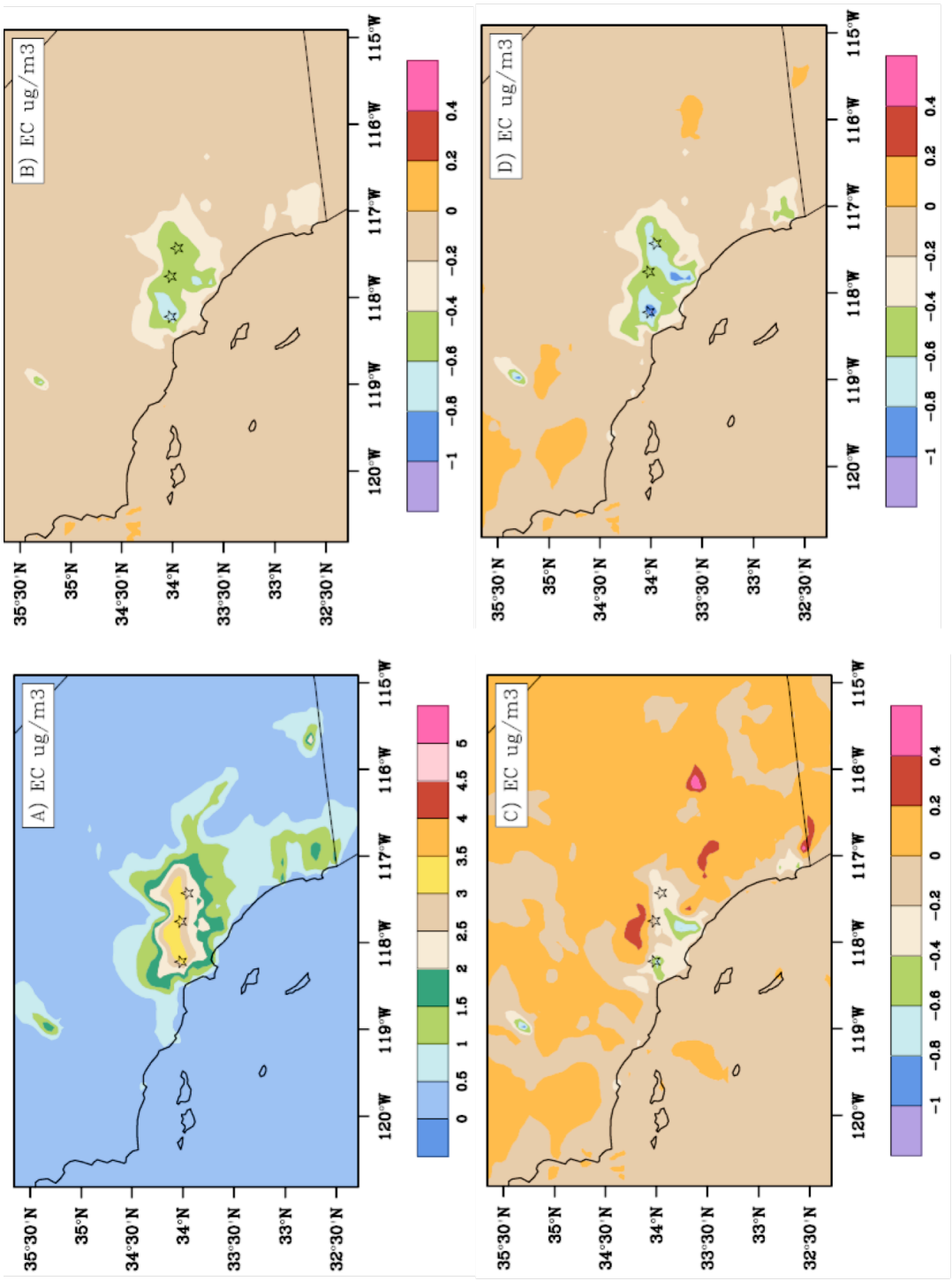

Figure 4.3: A) Average weekday EC in the base case at 1500 LT during the 6-day study period. B)–D) show changes in EC from base case. B) fuel-based estimates of emissions without changes in spatial distribution C) changes to spatial distribution of existing construction emissions to match permitting and population growth data D) combination of B and C. Starred locations are, from left to right, downtown Los Angeles, Pomona, and Riverside.

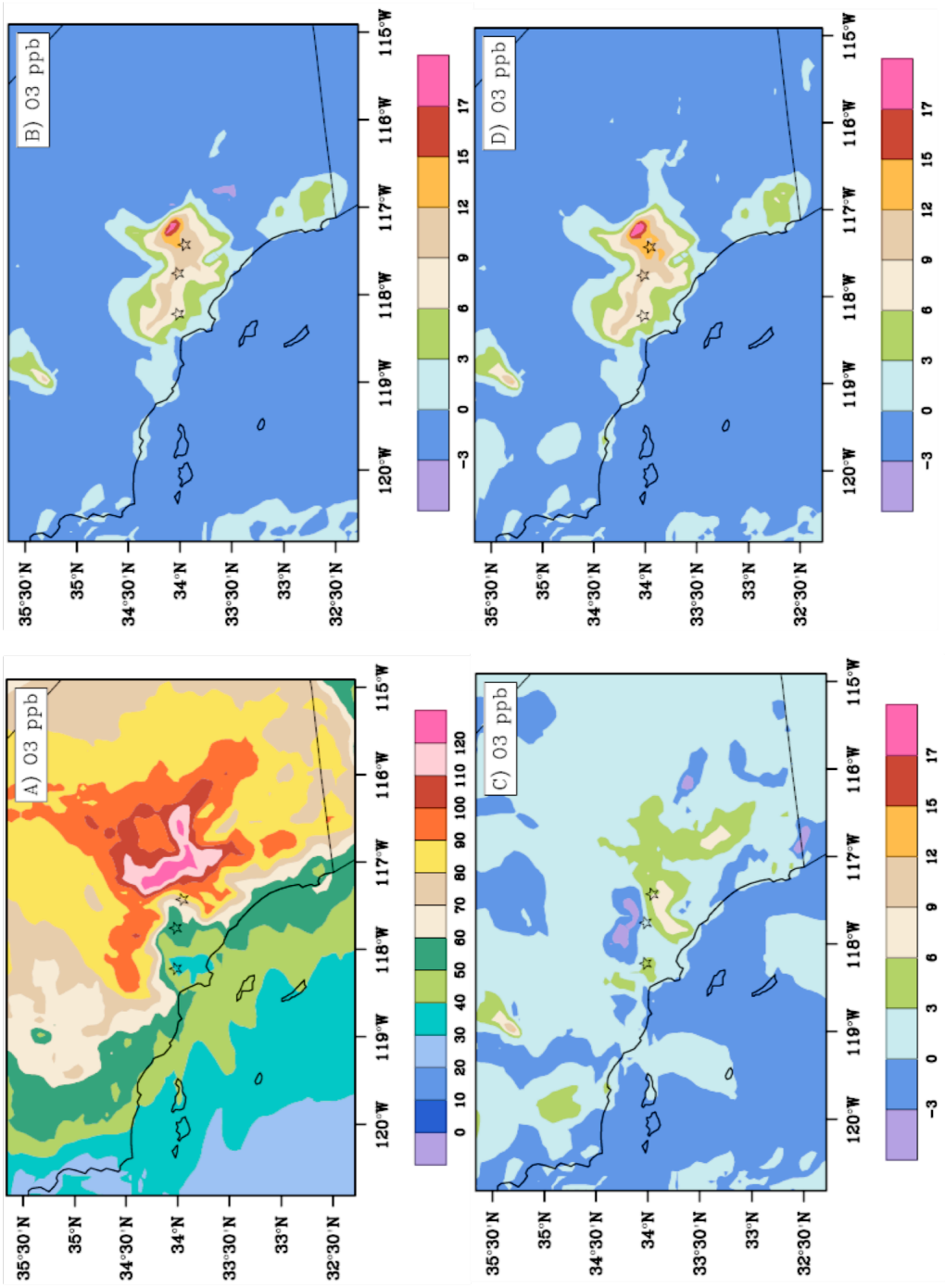

Figure 4.4: A) Average weekday ozone in the base case at 1500 LT during the 6-day study period. B)–D) show changes in ozone from base case. B) fuel-based estimates of emissions without changes in spatial distribution C) changes to spatial distribution of existing construction emissions to match permitting and population growth data D) combination of B and C. Starred locations are, from left to right, downtown Los Angeles, Pomona, and Riverside.

4.4 Discussion

Emission Inventory Methods. A central purpose of this work is to demonstrate emission inventory methods that rely on readily available data; the inventory methods described here provide a way to check emission inventory estimates developed using more specialized modeling tools. The differences between published diesel-powered construction equipment emission estimates (such as estimates from the OFFROAD model) and those reported here are large. The main source of disagreement is the overall amount of engine activity/fuel consumed. Additionally there is some difference between the NO_x emission factor incorporated in the OFFROAD model and the emission factor estimated here. Current emission allocations from state to county level appear to be within a factor of ~2, finer scale level allocations show larger differences for southern California.

Population growth was found to be spatially correlated with permitting records of construction activity. The EIA fuel survey provides national and state-level fuel sales by end-use category (EIA, 2006), and mass-based emission factors for diesel engines have been published recently in the technical literature (Abolhasani et al., 2008; Frey et al., 2008a; Frey et al., 2008b). Thus, the necessary data are available to estimate emission inventories for diesel-powered construction equipment across many regions of the country. The methodology presented here may be less applicable to regions that have little population growth or where diesel construction activity is concentrated in the public works sector relative to the residential and commercial sector. In these regions, records of construction permits may be essential to estimate the spatial distribution of construction emissions. Additional analysis would also be required for regions with strong seasonal changes to construction activity.

Emissions Modeling. A fuel-based approach for estimating construction-related emissions can be integrated into a more general emissions modeling framework. Emission processing programs, such as the Sparse Matrix Operator Kernel Emissions processing program (UNC, 2008), are generally used to distribute emission estimates from a county or state level to a model ready format (i.e., emissions per grid-cell). While SMOKE has incorporated a vehicle miles traveled method for on-road emissions, it is up to the user to define total off-road emissions and a surrogate for distributing these emissions to individual grid cells. In this case, the user could define total construction-related emissions based on fuel use data, and specify population growth as the surrogate for the spatial distribution of the emissions.

Discussion of Uncertainties. The fuel-based approach to estimating emissions is affected by various sources of uncertainty. There are only a limited number of studies focusing on measurement of in-use construction equipment emissions of NO_x. There are even fewer studies of PM emissions, including the relative abundance of EC, OC, and other constituents of fine particle mass.

Emission factors used here represent averages over all types of construction equipment and activity in the state or across a county, city, or model grid cell. Variations in emission factors will be less if the mix of construction equipment and equipment age is relatively constant across an area of interest. For example, in the OFFROAD model the standard deviation of emission factors across counties is small relative to the standard deviation of emission factors across equipment types. The relatively low standard deviation of emission factors across counties implies that, at

least at the county level, there is some homogeneity of equipment mix, without which the use of one average emission factor for different regions may not be justified.

There is additional uncertainty concerning fuel use estimates. If, out of convenience or necessity, off-road equipment were fueled with more expensive on-road diesel, this activity would not be counted by the EIA fuel survey. The process of using annual fuel consumption data to characterize a particular subset of days also adds uncertainty. Construction activity varies by season and by the day of week. Larger seasonal variation is likely outside of California where wintertime conditions may be more adverse.

There is not much data on variations in construction activity on short time scales. While some prior studies have focused on weekly and diurnal patterns in emissions (Chinkin et al., 2003; Harley et al., 2005; Chapter 3), construction activity patterns were not analyzed. Coe et al. (2003) report strong weekend decreases in construction activity and that 90% of construction working hours fall between 4 AM and 4 PM with ~1/4 of the work occurring before 8 AM.

Policy Implications. Construction activities generate air pollution including dust, gasoline and diesel engine exhaust, and VOC from paint, adhesives, and building materials. Air pollution emissions from off-road diesel-powered construction equipment appear to be significantly overstated in current emission inventories for California. Furthermore the assumed spatial distributions of activity and emissions appear outdated, at least for southern California. Engine retrofits or replacements for control of NO_x/PM emissions from off-road construction equipment may therefore not deliver overall air quality benefits that are as large as policy-makers have previously assumed.

Chapter 5

MODELING EFFECTS OF WEEKDAY-WEEKEND EMISSION DIFFERENCES

5.1 Introduction

Chapters 2 and 3 presented analyses of observed EC and fine particulate nitrate time series at urban locations across the U.S. Of particular relevance to this chapter are the observed responses in PM concentrations to changes in emissions that occur on weekends. While many sources have altered emission profiles on weekends, the largest contributions to overall changes in EC and NO_x emissions on weekends come from diesel engines, for which the overall level of activity on weekends is greatly reduced relative to typical weekday conditions (Dreher and Harley, 1998; Chinkin et al., 2003; Harley et al., 2005).

Considering atmospheric responses to changes in emissions that occur on weekends can be useful in evaluating the effects of pending or proposed regulations on emission sources, specifically as a way of testing understanding of how various air pollutants change in response to emission changes. Standard air quality model evaluation procedures quantify model biases and errors by comparing predictions with observed values for a historical base case. There are many possible sources of compensating error in these comparisons, however, so the credibility of model predictions remains suspect. The central issue of how models respond to emission changes is rarely considered as part of the base case model evaluation. A regular and predictable change in emissions, such as a weekly cycle, provides a test that can be used to evaluate the policy-relevant question of how air quality models and the real atmosphere respond to changes in emissions.

A well-known weekly cycle in ozone concentrations has been investigated extensively using both observed ozone time series and photochemical modeling analyses (Marr and Harley, 2002b; Yarwood et al., 2003; Murphy et al., 2007; Yarwood et al., 2008; Tonse et al., 2008). There has been less study of weekly cycles in PM constituents, and model-based studies of weekly cycles in PM constituents have not yet been published to my knowledge. In fact, weekly cycles in observed concentrations of fine particulate nitrate have only recently been clearly identified (Murphy et al., 2008; Chapter 3) Knowledge gained concerning nitrate responses to emission changes could be directly applicable to evaluation of potential control strategies relating to motor vehicles, as Ying et al. (2009) report that emissions from diesel engines are responsible for 40% of the total fine PM nitrate and that light-duty passenger vehicles account for another 20% in California.

In this chapter, air quality model predictions of weekly cycles in EC, nitrate, O_3, NO_x and NO_2 are evaluated. The focus of this evaluation is on nitrate, as the gaseous pollutants have been studied previously, and EC is a primary pollutant with expected linear emissions-concentrating relationships.

A key step in the formation of fine particulate nitrate is the conversion of NO_x to nitric acid (HNO_3). Nitrate in the particle phase is most commonly present as ammonium nitrate, which is often in or close to equilibrium with relevant gas phase species:

$$NH_3\,(g) + HNO_3\,(g) \Leftrightarrow NH_4NO_3\,(s) \qquad (5.1)$$

Ammonia is emitted directly to the atmosphere important sources include waste decomposition and microbial processes in soil. Gasoline engine exhaust is now a minor and decreasing source of ammonia emissions (Kean et al., 2009). Nitric acid is formed chemically in the atmosphere via a number of pathways. The main daytime pathway is reaction of NO_2 with the hydroxyl radical (OH):

$$OH + NO_2 \rightarrow HNO_3 \qquad (5.2)$$

At night when OH radical levels are low, other pathways dominate the formation of nitric acid, such as hydrolysis of N_2O_5 (Brown et al., 2006):

$$NO_2 + O_3 \rightarrow NO_3 + O_2 \qquad (5.3)$$
$$NO_2 + NO_3 \rightarrow N_2O_5 \qquad (5.4)$$
$$N_2O_5 + H_2O \rightarrow 2HNO_3 \qquad (5.5)$$

Formation of N_2O_5 occurs mainly at night because NO_3 undergoes rapid photolysis during the daytime. Initial attempts to measure the rate of homogeneous gas phase hydrolysis of N_2O_5 showed a strong dependence on the size of the experimental chamber, with the rate getting smaller with increasing chamber size. The dependence on surface area provided evidence for the importance of heterogeneous pathways (Sverdrup et al., 1987).

The rate of production of nitric acid from N_2O_5 is a function of both reaction kinetics and the available particle surface area. Additionally, Brown et al. (2006) describe the rate of N_2O_5 uptake as being a function of particle composition, where high sulfate composition increases the uptake rate. Other influences on the uptake coefficient may include levels of NO_3^- in particles, as well as organic coatings.

5.2 Methods

Air Quality Model. The Community Multiscale Air Quality model (CMAQ; Byun and Schere, 2006) version 4.6, with the SAPRC99 gas-phase chemical mechanism (Carter, 2000) is used to evaluate air quality in this study. Processes relating to secondary particle formation were modeled using the AE4 aerosol module (Binkowski and Roselle, 2003). Gridded hourly meteorological fields were developed using the Mesoscale Meteorological model (MM5) version 3.6.1 (SCAQMD, 2007a). Both meteorological input data and pollutant inflow boundary conditions for the air quality model are further described by Millstein and Harley (2009b).

The modeling domain (65 × 40 grid cells with 5 km horizontal resolution) is centered on the Los Angeles area in southern California, with the western boundary over the Pacific Ocean and the eastern boundary located in the Mojave Desert. The northern edge of the domain crosses north of Santa Barbara while the southern limit of the domain passes north of San Diego (see Figure 5.1). Fifteen vertical model layers were used in a telescoping scheme, with the lowest layer 36 m thick, and the topmost layer extending to a height of ~15 km above sea level. Two simulation periods are considered in this study: a summer high-ozone period running from 6 July through 29 August 2005, and a fall period extending from 30 October through 7 December 2005, when fine particle concentrations are high. During these time periods in 2005, wildfires did not have a major impact on air quality within the modeling domain. Both seasonal simulation periods considered in this research are over a month long, in contrast to past studies that have analyzed air quality during episodic events of short overall duration.

Baseline Emissions. Anthropogenic emission estimates for 2005 were developed by the South Coast Air Quality Management District and the California Air Resources Board, as described in the 2007 Air Quality Management Plan for the South Coast Air Basin (SCAQMD, 2007b). Baseline emissions from diesel-powered construction equipment were adjusted to account for overstated fuel use in this sector in the baseline inventory as described in Chapter 4. The spatial distribution of construction equipment emissions was also adjusted as these activities had moved on to new locations relative to those specified in the baseline inventory.

Additionally, the baseline chemical composition of NO_x emissions from on-road vehicles was revised to match the 5 and 1% NO_2/NO_x ratios reported for heavy-duty diesel and light-duty gasoline vehicles, respectively, in recent California highway tunnel experiments (Ban-Weiss et al., 2008a). Biogenic emissions were estimated using the BEIGIS model (Scott and Benjamin, 2003); separate day-specific estimates were available for each day of 2005 (Scott, 2009).

Weekend emission estimates for selected source categories were scaled to match the source activity patterns reported by Chinkin et al. (2003) for southern California. While the total weekend emissions were adjusted, the temporal patterns and spatial distributions of weekend emissions were left unchanged from the baseline. An important weekend change included in the

baseline inventory is the single midday activity peak for light duty vehicles opposed to the weekday commuting peaks. Table 5.1 presents total NO_x and $PM_{2.5}$ emissions along with weekend adjustment factors by source category. Diesel trucks are the single largest source of NO_x and experience large (~70%) weekend reductions. The three next most important NO_x emission categories in southern California are light duty vehicles, ships and commercial boats, and various point sources. Whereas point source emissions of NO_x and PM are reduced roughly by half on weekends, ship emissions are independent of day of week, and light duty vehicle emissions decrease only slightly on weekends. Thus diesel trucks are by far the most important contributor to weekend reductions in NO_x emissions. Although emissions from construction equipment are much smaller (roughly one tenth) than on-road diesel truck emissions, large weekend reductions in construction activity discussed in Chapter 4 imply that construction activities are the second largest contributor to weekend NO_x reductions.

Table 5.1: Air pollutant emissions on weekdays with Saturday and Sunday changes by source category. *(Totals presented here are from the full domain described in Chapter 4).*

	Weekday Emissions (10^3 kg)		Ratio to Weekday Emissions[a]	
Source Category	NO_x	$PM_{2.5}$	Saturday	Sunday
Diesel Trucks	474	18.9	0.35	0.30
Light Duty Motor Vehicles	293	6.5	0.91	0.81
Ships and Commercial Boats	170	12.8	1.00	1.00
Point Sources	144	32.6	0.48	0.48
Trains	81	2.3	0.97	0.97
Off-Road Equipment	80	3.9	0.87	0.87
Diesel Construction	41	3.7	0.10	0.00
Farm Equipment	36	2.0	0.50	0.50
Manufacturing and Industrial	26	1.0	0.97	0.97
Residential Fuel Combustion	19	1.5	1.00	1.00
Diesel Buses	17	0.3	0.99	0.89
Port Equipment	13	0.4	0.70	0.70
Recreational Boats	11	1.8	5.00	5.00
Lawn and Garden Equipment	11	1.0	0.53	0.53
Aircraft	9	4.6	1.00	1.00
Oil Drilling Equipment	8	0.3	0.85	0.85
Airport Support Equipment	7	0.2	0.50	0.50
Cooking	0	9.3	1.00	1.00
Other[b]	58	186.7	1.64	1.64
Total All Sources	**1495**	**290.0**	**0.73**	**0.69**

[a] The ratio of Saturday and Sunday to weekend NO_x emission is presented here. In general there was good agreement between NO_x and PM emission changes on weekends, as the reductions were due to changes in underlying source activity rather than changes in emission factors. The weekend increases in NO_x seen in the "other" category are due to changes in area source categories, PM emissions in the "other" category do not increase on weekends. Note that the "Total All Sources" weekend changes are also only relevant to NO_x, PM "Total All Sources" weekend changes can be calculated by a weighted sum.

[b] ~150 tons of dust is included in the $PM_{2.5}$ "Other" category.

The four largest combustion sources of primary $PM_{2.5}$ are point sources, diesel trucks, ships and commercial boats, and cooking. Weekly reductions in primary $PM_{2.5}$ emissions are strongly influenced by changes in point source emissions and diesel truck activity. Domain-wide totals of primary $PM_{2.5}$ emissions are dominated by dust emissions. Dust is added to the atmosphere through wind, farming operations and vehicle travel on both paved and unpaved roads. Speciation profiles of a number of PM source categories were updated as described in Chapter 4, (see A.5).

In addition to the baseline emission inventory, an "all-weekday" emission scenario was run that specified typical weekday emissions on all days of the week including weekends. This diagnostic simulation was used as a point of reference in evaluating the baseline emission inventory and associated weekday-weekend differences. This analysis removes some of the effects of atmospheric variability due to changing meteorological conditions, which is important given that the simulation periods used here include only 8 and 5 weekends during the summer and fall, respectively. A direct estimate of the response to weekend emission changes can be calculated at each time and grid cell as

$$R = 1 - \frac{B}{A} \tag{5.6}$$

where R equals the reduction in a pollutant or process rate as a result of weekend changes in emissions, B is the baseline quantity and A is the analogous quantity from the all weekday emission scenario.

Integrated reaction rate and integrated process rate analysis (IRR and IPR; Gipson, 1999) are used to quantify the effect of important reactions and physical processes affecting nitric acid concentrations. Process analysis adds a counter species to selected reactions, families of reactions, and physical processes, and integrates these process rates over a selected time period. Process analysis reports the net chemical production of a species over time as well as net transport due to advection and diffusion, and net loss due to other physical processes such as surface deposition. The sum of all the source and loss terms given by process analysis for a particular species is equal to the concentration change for that species between the start and end of the specified analysis time period. Process analysis was conducted for both the baseline and the all-weekday emission scenarios, and was used to evaluate weekend effects on HNO_3 production.

5.3 Results

Modeled and Observed Weekly Cycles. Figure 5.2 presents day of week variations in modeled and observed EC, nitrate, $PM_{2.5}$. Appendix B presents day of week variations in O_3, NO_x, NO_2 and HNO_3 as well as the PM constituents presented in Figure 5.2. Observed EC concentrations on Sundays are 0.67±0.09 and 0.72±0.09 of corresponding weekly averages for summer and fall seasons, respectively. Corresponding modeled EC concentrations on Sundays are 0.79±0.06 and 0.64±0.12. NO_x and ozone also show clear weekend changes with Sunday ozone ranging from 1.2-1.5, and Sunday NO_x ranging from 0.63-0.83 of corresponding weekly averages. Larger relative changes were modeled during the fall season for both NO_x and O_3, however, while NO_x levels remain high during the fall and winter, O_3 concentrations are relatively low.

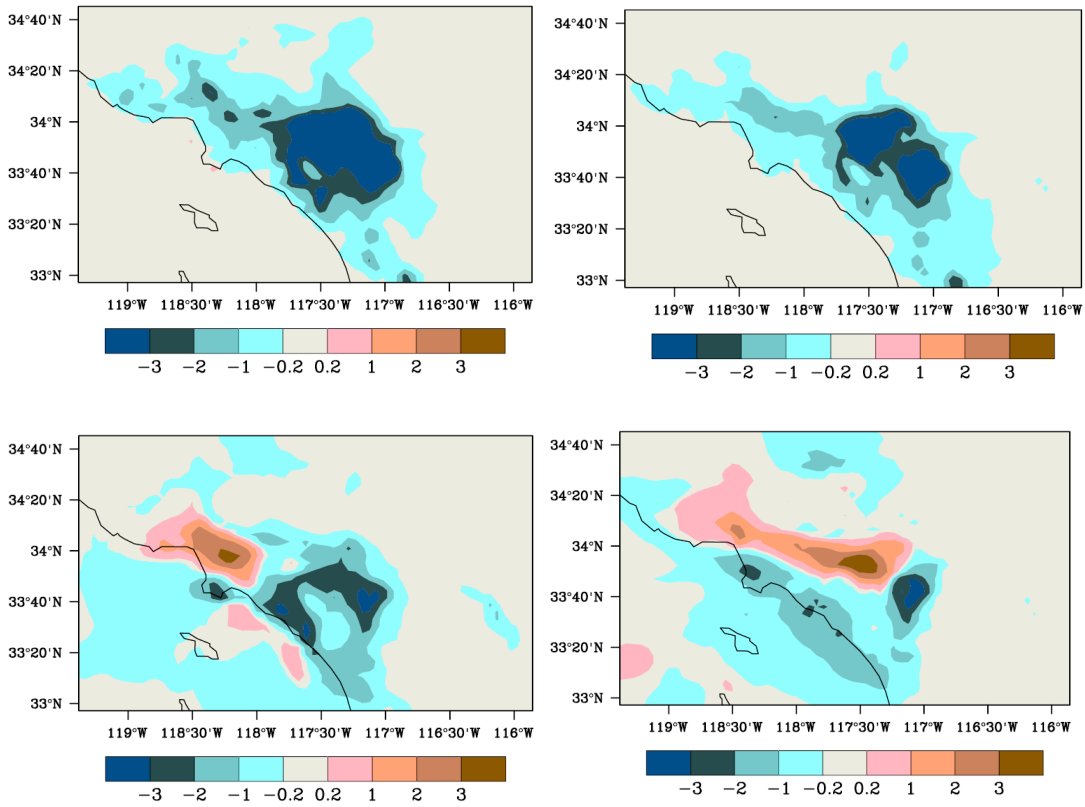

Figure 5.1: Difference between baseline and adjusted average daily nitrate concentrations ($\mu g/m^3$) during the summer (top) and fall (bottom). Left: Sunday. Right: Monday.

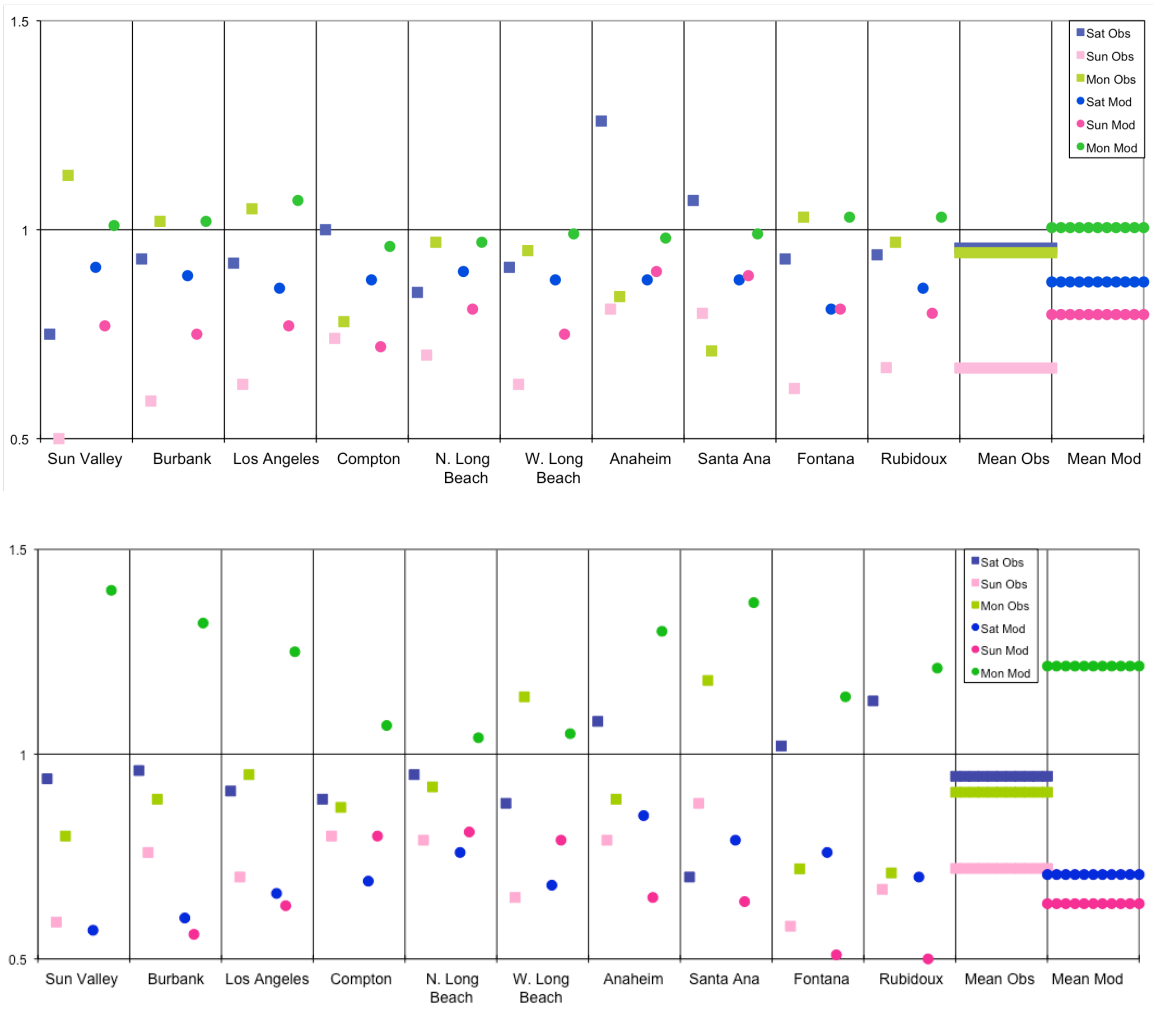

Figure 5.2a: Modeled and observed normalized 24-hour average concentrations of EC. Model concentrations normalized by 7-day moving average. Observed concentrations normalized by 21-day moving average with measurements every 3rd day. Top: summer, Bottom: fall.

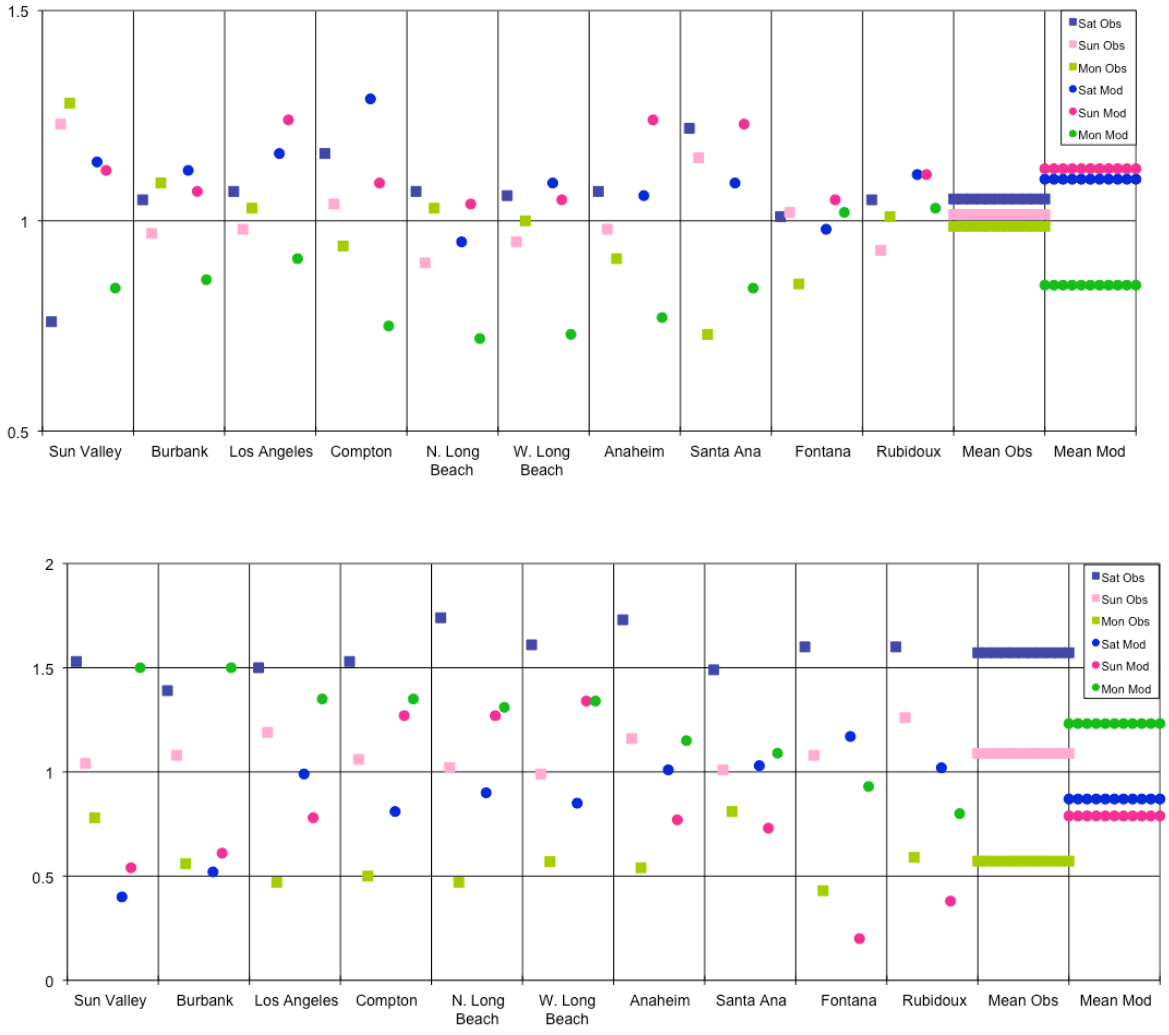

Figure 5.2b: Modeled and observed normalized 24-hour average concentrations of nitrate. Model concentrations normalized by 7-day moving average. Observed concentrations normalized by 21-day moving average with measurements every 3rd day. Top: summer, Bottom: fall.

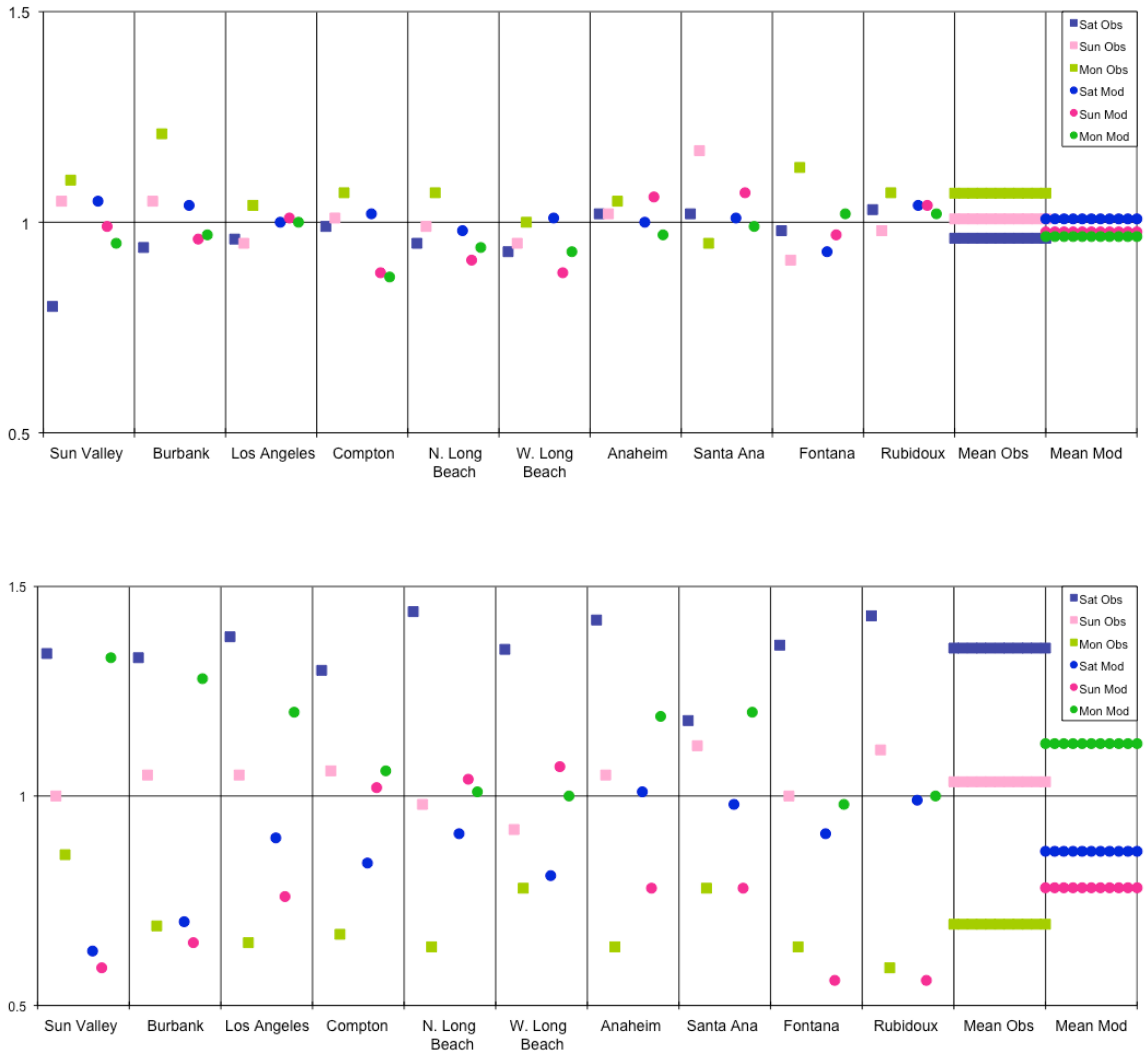

Figure 5.2c: Modeled and observed normalized 24-hour average concentrations of total $PM_{2.5}$. Model concentrations normalized by 7-day moving average. Observed concentrations normalized by 21-day moving average with measurements every 3rd day. Top: summer, Bottom: fall.

The response of nitrate to weekend reductions in NO_x emissions was variable and depended on the season. The summer MATES-III observations were too infrequent (once every 3rd day) to provide clear evidence of a weekly cycle in nitrate. Time-resolved nitrate observations at Claremont, CA, discussed in Chapter 3, indicate summer nitrate reductions on Sundays and Mondays (see Figure 3.1). Figure 5.1 presents the difference between baseline and all-weekday emissions model scenarios. A negative value indicates that modeled nitrate concentrations were lower with weekend emission reductions compared to concentrations predicted using all-weekday emissions. Figure 5.1 shows that average nitrate was reduced across much of the domain as a result of weekend emission changes during the summertime. Nitrate reductions were larger inland than over downtown Los Angeles. Table 5.2 shows that domain-wide modeled HNO_3 production by time, season and major chemical pathway. Due to weekend emission changes, domain-wide production of HNO_3 on Saturday – Monday decreased by 12% during the summer. This result is consistent with summertime nitrate reductions discussed in Chapter 3.

During fall, MATES-III observations (see Figure 5.2) and observations from Claremont (Chapter 3) indicate nitrate reductions on Mondays and increases on Saturday. Modeled domain-wide production of HNO_3 decreases by 6% as a result of weekend emission changes during the fall (see Table 5.2). However, modeled nitrate concentrations are not reduced in all locations as a result of the HNO_3 reductions. As shown in Figure 5.1 modeled nitrate increases over downtown Los Angeles as a result of weekend emission changes. This increase spreads over a larger area, including east to Riverside, on Mondays.

Table 5.2a: Domain wide summer HNO_3 production by major pathway and time.[a]

Summer	**NO2 + OH -> HNO3**		
Saturday	Production (ppm)	Weekend Effect	% of Sat-Mon
12am - 6am	0.22	0.94	0.6
6am - 12pm	4.52	0.85	13.3
12pm - 6pm	4.33	0.79	12.7
6pm - 12am	0.36	0.94	1.1
Sunday			
12am - 6am	0.20	0.80	0.6
6am - 12pm	4.10	0.77	12
12pm - 6pm	4.36	0.74	12.8
6pm - 12am	0.37	0.93	1.1
Monday			
12am - 6am	0.23	0.96	0.7
6am - 12pm	5.09	0.98	14.9
12pm - 6pm	5.72	0.99	16.8
6pm - 12am	0.39	1.00	1.1
Totals	29.9	**0.87**	**88%**
Summer	**N2O5 + H2O (het) -> 2HNO3**		
Saturday	Production (ppm)	Weekend Effect	% of Sat-Mon
12am - 6am	0.52	1.03	1.5
6am - 12pm	0.01	0.93	0.0
12pm - 6pm	0.01	0.91	0.0
6pm - 12am	0.75	0.89	2.2
Sunday			
12am - 6am	0.60	0.96	1.8
6am - 12pm	0.01	0.90	0.0
12pm - 6pm	0.01	0.84	0.0
6pm - 12am	0.82	0.84	2.4
Monday			
12am - 6am	0.53	0.88	1.6
6am - 12pm	0.01	1.04	0.0
12pm - 6pm	0.01	1.00	0.0
6pm - 12am	0.97	0.99	2.8
Totals	4.25	**0.93**	**12%**

[a] The weekend effect is calculated as total baseline production divided by total production in the all weekday scenario.

Table 5.2b: Domain wide fall HNO_3 production by major pathway and time.[a]

Fall	**NO2 + OH -> HNO3**		
Saturday	Production (ppm)	Weekend Effect	% of Sat-Mon
12am - 6am	0.14	0.98	1.1
6am - 12pm	1.49	0.92	11.8
12pm - 6pm	1.59	0.90	12.6
6pm - 12am	0.21	1.01	1.7
Sunday			
12am - 6am	0.13	0.87	1.0
6am - 12pm	1.38	0.85	10.9
12pm - 6pm	1.46	0.85	11.6
6pm - 12am	0.25	1.03	1.9
Monday			
12am - 6am	0.16	1.00	1.3
6am - 12pm	1.58	0.99	12.5
12pm - 6pm	1.73	0.99	13.7
6pm - 12am	0.23	1.01	1.8
Totals	10.4	**0.93**	**82%**
Fall	**N2O5 + H2O (het) -> 2HNO3**		
Saturday	Production (ppm)	Weekend Effect	% of Sat-Mon
12am - 6am	0.30	1.03	2.3
6am - 12pm	0.02	1.08	0.2
12pm - 6pm	0.03	0.94	0.2
6pm - 12am	0.32	0.86	2.5
Sunday			
12am - 6am	0.32	1.02	2.6
6am - 12pm	0.03	1.06	0.2
12pm - 6pm	0.04	1.01	0.3
6pm - 12am	0.32	0.88	2.5
Monday			
12am - 6am	0.36	1.05	2.9
6am - 12pm	0.04	1.10	0.3
12pm - 6pm	0.04	1.00	0.4
6pm - 12am	0.46	0.98	3.6
Totals	2.28	**0.98**	**18%**

[a] The weekend effect is calculated as total baseline production divided by total production in the all weekday scenario.

Table 5.2 shows that domain-wide HNO_3 production is predicted to decrease due to weekend emission changes in both seasons. However, Figures 5.1 and 5.3 show that local conditions can lead the model to predict an increase in HNO_3 production due to weekend emission changes. Figure 5.3 compares production of HNO_3 in Los Angeles and Riverside during both seasons. Los Angeles is located in the middle of the heaviest area of NO_x emissions while Riverside is located downwind of major NO_x emissions sources. In response to weekend emission changes the model predicts an increase in the production of HNO_3 from reaction of NO_2 with OH radical in both seasons in Los Angeles. At Riverside the opposite is true, with the exception of weekend evenings when HNO_3 production increases during the fall.

The different responses at Los Angeles and Riverside suggest a possible mechanism that could lead to varying nitrate responses to NO_x reductions. In areas with high local NO_x emissions, weekend NO_x reductions lead to higher ozone levels. Associated with higher ozone is an increased pool of radicals that lead to increased production of HNO_3 from NO_2. The model suggests that in locations with high local NO_x emissions, the reaction of $NO_2 + OH \rightarrow HNO_3$ is sensitive to the increase to the pool of radicals as opposed to the reduction of total NO_x concentration levels. The opposite is true in regions with relatively low local NO_x emissions. In these regions, weekend NO_x reductions may not lead to increased ozone formation and the NO_x reductions may significantly deplete the pool of NO_2 for reaction with OH radical.

This mechanism does not fully explain the differences between the model nitrate and the observations of nitrate. The observational record indicates a trend of increased nitrate on Saturday and perhaps on Sunday followed by decreased nitrate on Monday. The model indicates increased weekend nitrate in urban locations during the fall, with the increase spreading to a larger area over Sunday and into Monday. Accurate modeling of the response of nitrate to weekend NO_x reductions may be relatively challenging compared to modeling the weekend response of EC or ozone due to the longer time period that nitrate concentrations are effected by weekend emission reductions. The effects of weekend emission changes on EC and ozone concentrations are relatively confined to Saturday and Sunday. Thus, EC and ozone concentrations on Sunday are most sensitive to emissions and meteorology on Sunday.

In contrast, nitrate on Sunday is sensitive to emissions from both Saturday and Sunday, and from meteorology and transport conditions over that time period as well. Figure 5.4 shows the weekend response of both nitric acid-forming pathways across the whole domain by time and season. During fall, nitric acid production from $OH+NO_2$ increases in regions with strong weekend ozone effects and decreases elsewhere. Figure 5.4 shows the strongest increases in fall HNO_3 production occur during Sunday daytime and that there are relatively small changes to HNO_3 production on Monday. Figure 5.1 shows increased nitrate over a larger area on Monday compared to Sunday. The combination of increased Monday nitrate with relatively little increase in HNO_3 production on Monday indicates that modeled Monday concentrations are sensitive to conditions, including emissions and meteorology on previous days.

During both summer and fall, HNO_3 production from N_2O_5 hydrolysis shows strong Sunday evening increases. Thus, weekend ozone increases lead to widespread increases in production of HNO_3 from N_2O_5 hydrolysis within urbanized areas. As reported in Table 3, however, N_2O_5 hydrolysis accounts for only 12 and 18% of total Saturday through Monday HNO_3 production

during summer and fall, respectively. The response of HNO_3 production from $OH+NO_2$ depends strongly on season. Generally, the reaction of $OH+NO_2$ produces less nitric acid as a result of weekend emission changes during the summer. Near central Los Angeles, however, only small changes to nitric acid production are seen during the summer.

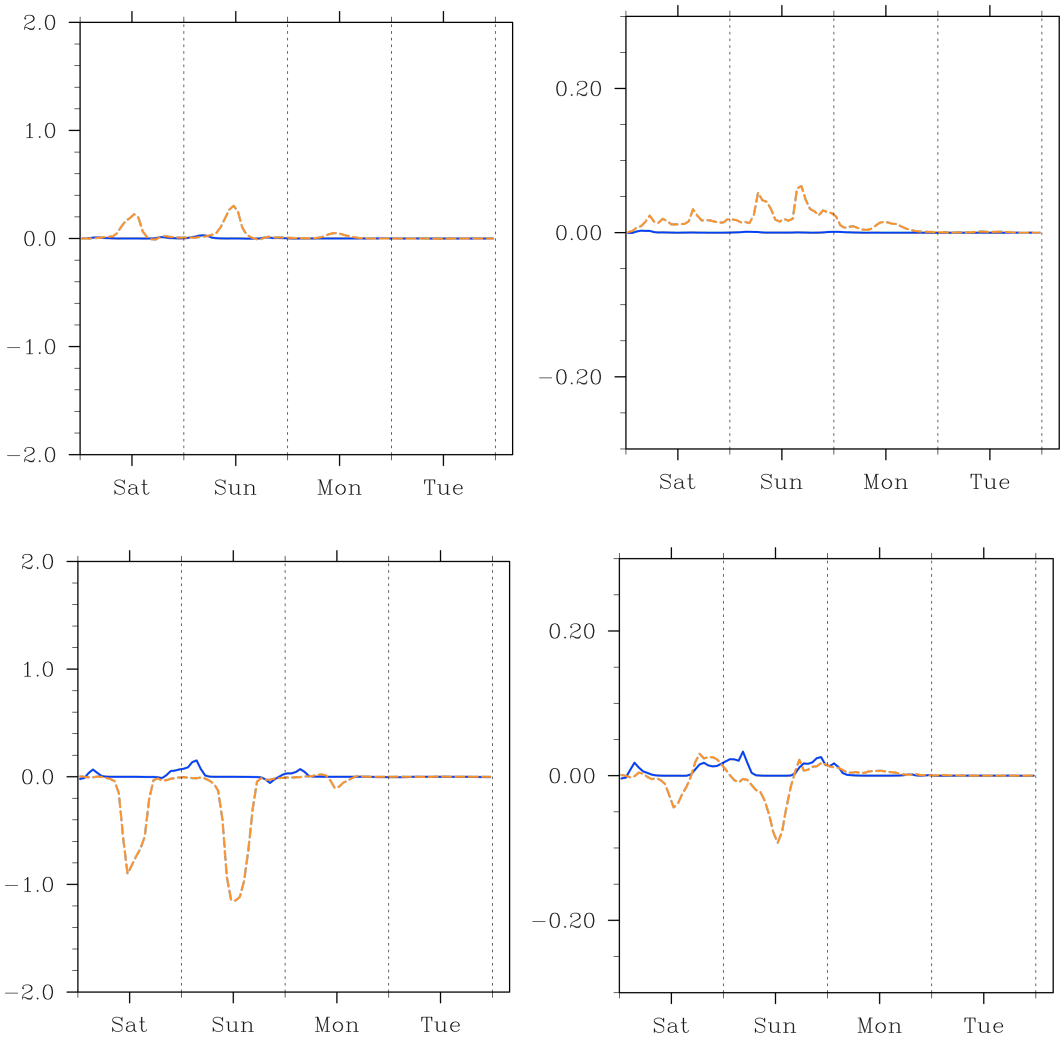

Figure 5.3: Hourly average difference (ppb) between the baseline and altered scenarios of HNO_3 production from OH + NO_2 (Orange, dashed), and N_2O_5 heterogeneous hydrolysis (Blue, solid) by season. Top panels: downtown Los Angeles. Bottom panels: Riverside. Left panels: summer. Right panels: fall.

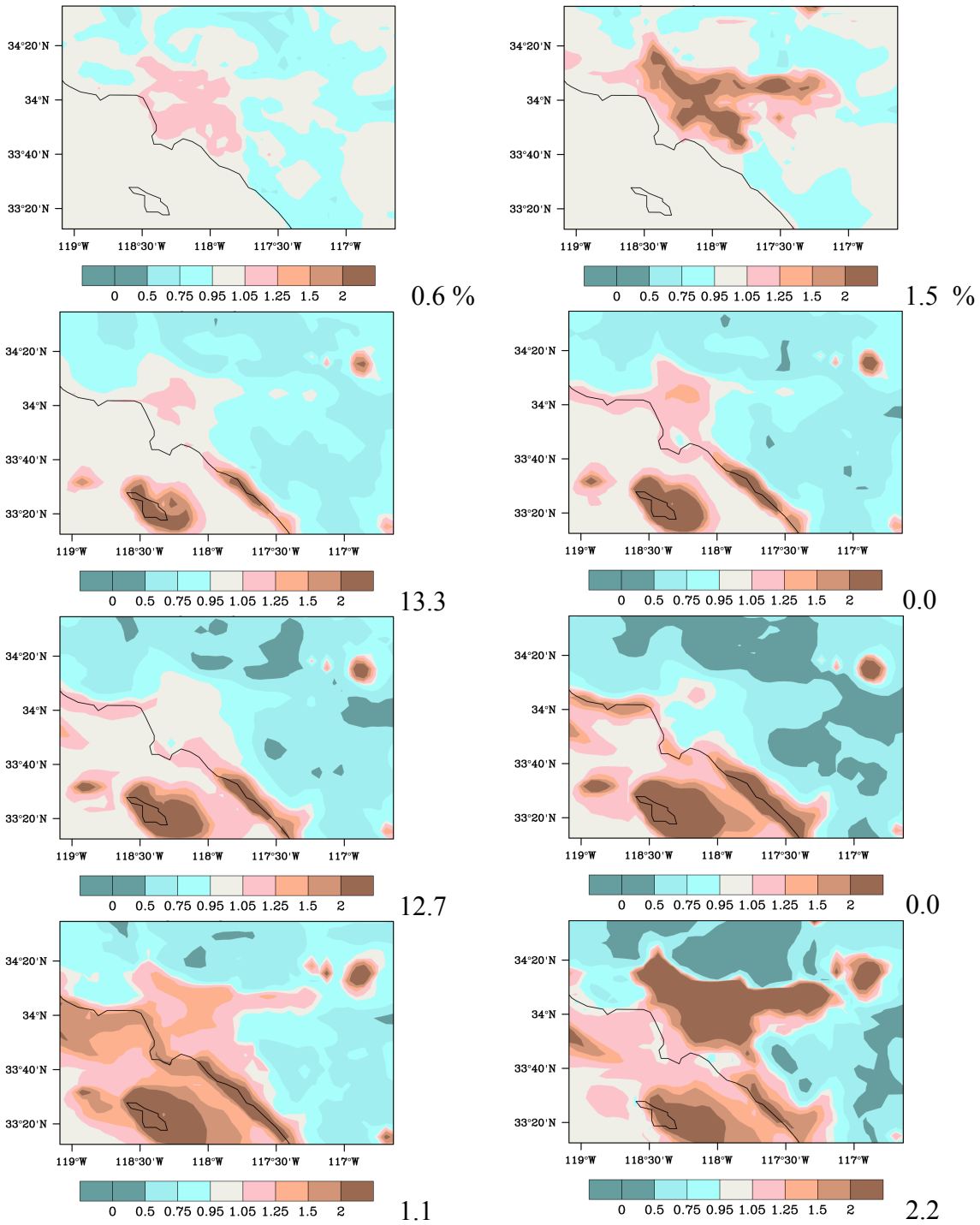

Figure 5.4a: Summer Saturday average ratio of baseline to adjusted scenario HNO_3 production by season. Values reported next to each panel are the percentage of total Saturday through Monday HNO_3 production from the reaction and time specified in the panel.
Left column: $NO_2 + OH \rightarrow HNO_3$. Right column: $N_2O_5 + H_2O \rightarrow 2HNO_3$.
From the top row to the bottom row, values were averaged over the time periods:
12AM - 6 AM, 6 AM – 12 PM, 12 PM – 6 PM, 6 PM – 12 PM.

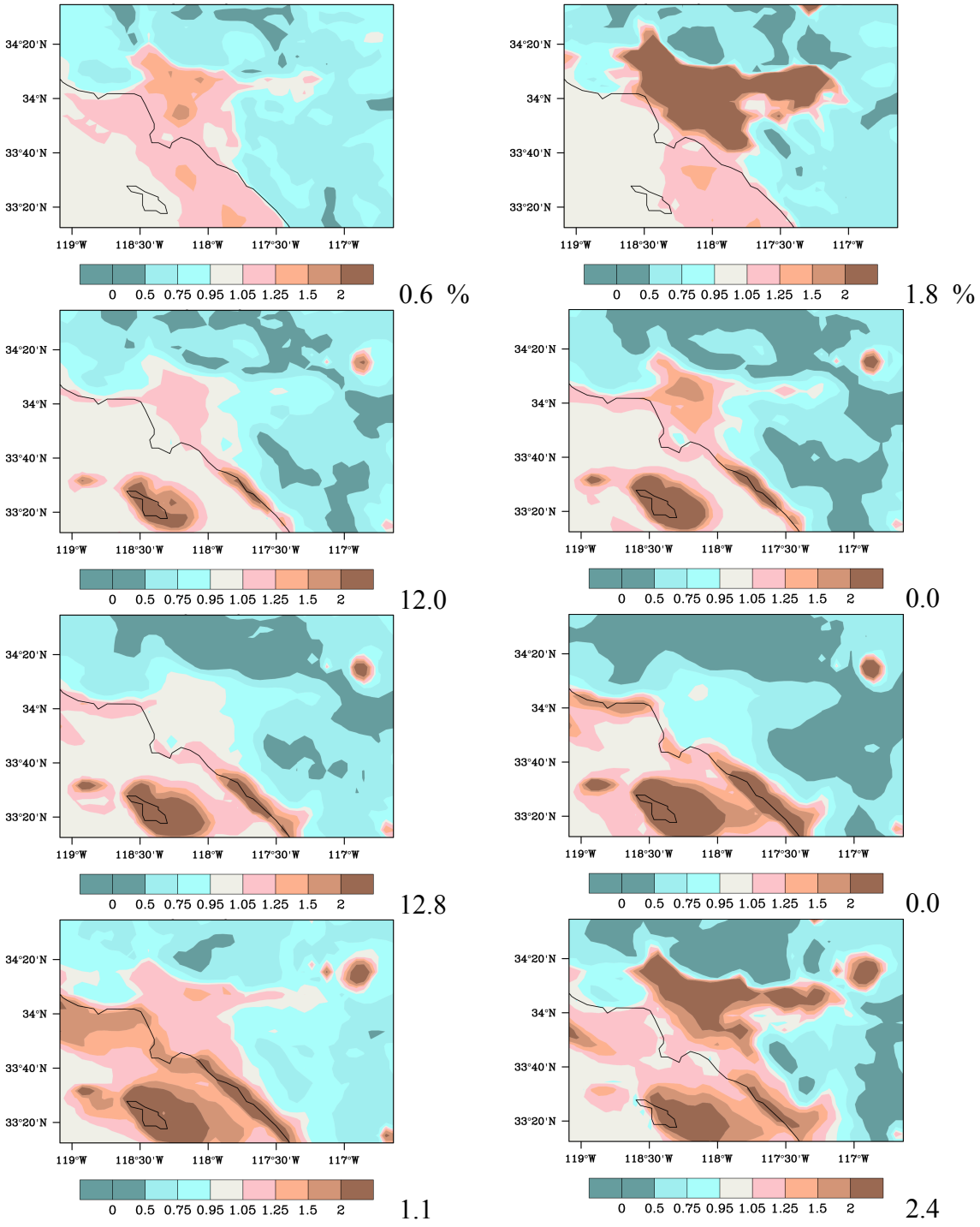

Figure 5.4b: Summer Sunday average ratio of baseline to adjusted scenario HNO_3 production by season. Values reported next to each panel are the percentage of total Saturday through Monday HNO_3 production from the reaction and time specified in the panel.
Left column: $NO_2 + OH \rightarrow HNO_3$. Right column: $N_2O_5 + H_2O \rightarrow 2HNO_3$.
From the top row to the bottom row, values were averaged over the time periods:
12AM - 6 AM, 6 AM – 12 PM, 12 PM – 6 PM, 6 PM – 12 PM.

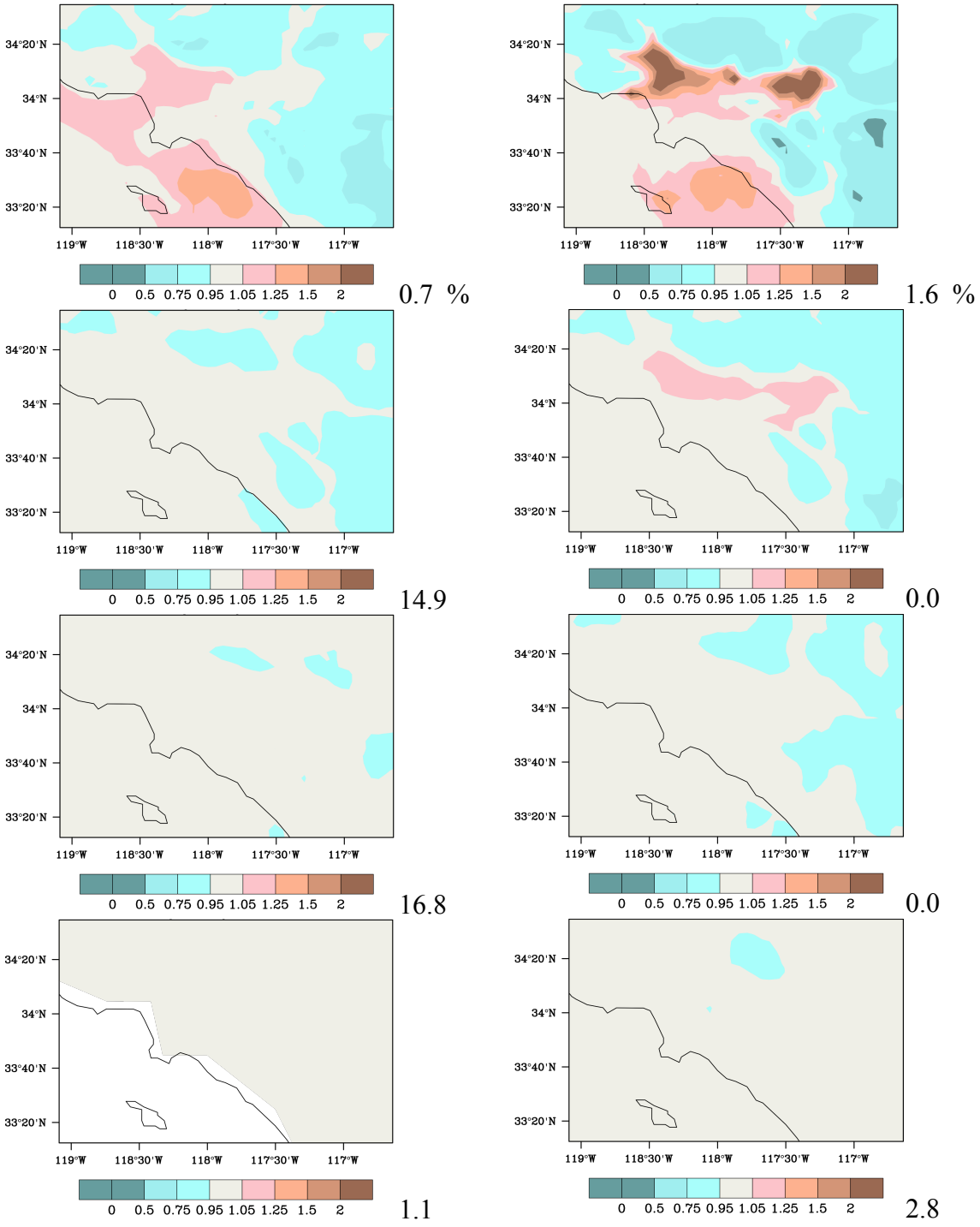

Figure 5.4c: Summer Monday average ratio of baseline to adjusted scenario HNO_3 production by season. Values reported next to each panel are the percentage of total Saturday through Monday HNO_3 production from the reaction and time specified in the panel.
Left column: $NO_2 + OH \rightarrow HNO_3$. Right column: $N_2O_5 + H_2O \rightarrow 2HNO_3$.
From the top row to the bottom row, values were averaged over the time periods:
12AM - 6 AM, 6 AM – 12 PM, 12 PM – 6 PM, 6 PM – 12 PM.

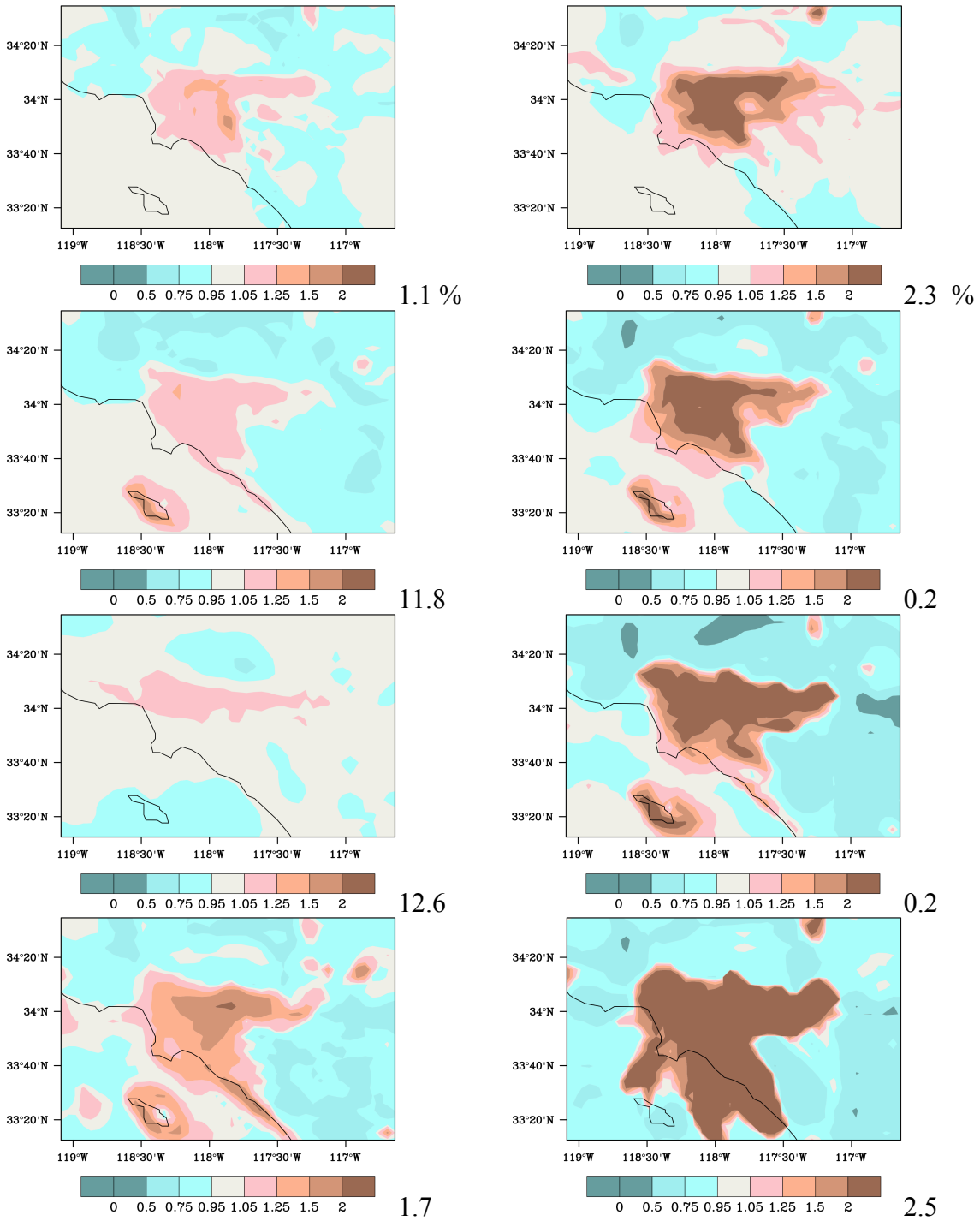

Figure 5.4d: Winter Saturday average ratio of baseline to adjusted scenario HNO_3 production by season. Values reported next to each panel are the percentage of total Saturday through Monday HNO_3 production from the reaction and time specified in the panel.
Left column: $NO_2 + OH \rightarrow HNO_3$. Right column: $N_2O_5 + H_2O \rightarrow 2HNO_3$.
From the top row to the bottom row, values were averaged over the time periods:
12AM - 6 AM, 6 AM – 12 PM, 12 PM – 6 PM, 6 PM – 12 PM.

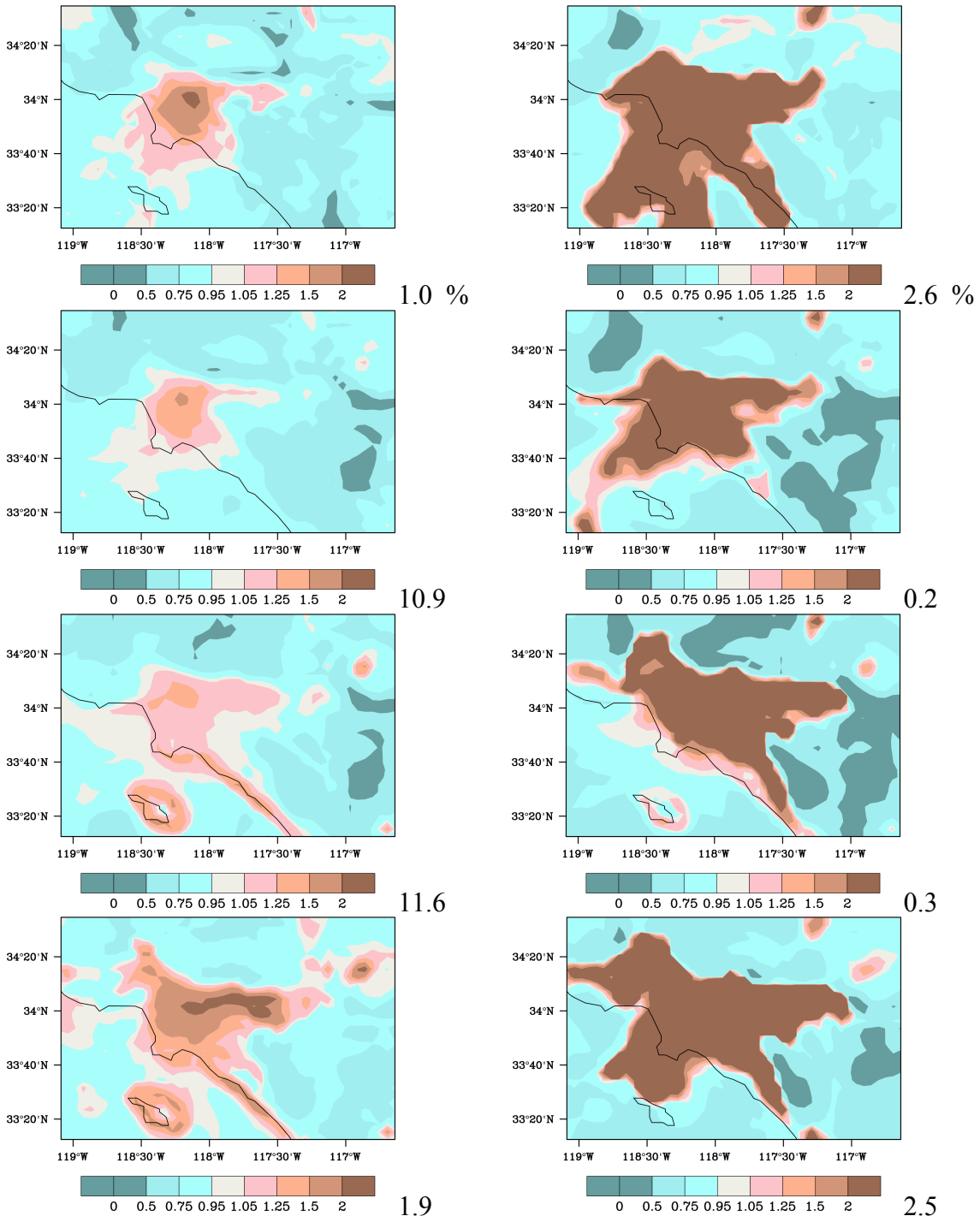

Figure 5.4e: Winter Sunday average ratio of baseline to adjusted scenario HNO_3 production by season. Values reported next to each panel are the percentage of total Saturday through Monday HNO_3 production from the reaction and time specified in the panel.
Left column: $NO_2 + OH \rightarrow HNO_3$. Right column: $N_2O_5 + H_2O \rightarrow 2HNO_3$.
From the top row to the bottom row, values were averaged over the time periods:
12AM - 6 AM, 6 AM – 12 PM, 12 PM – 6 PM, 6 PM – 12 PM.

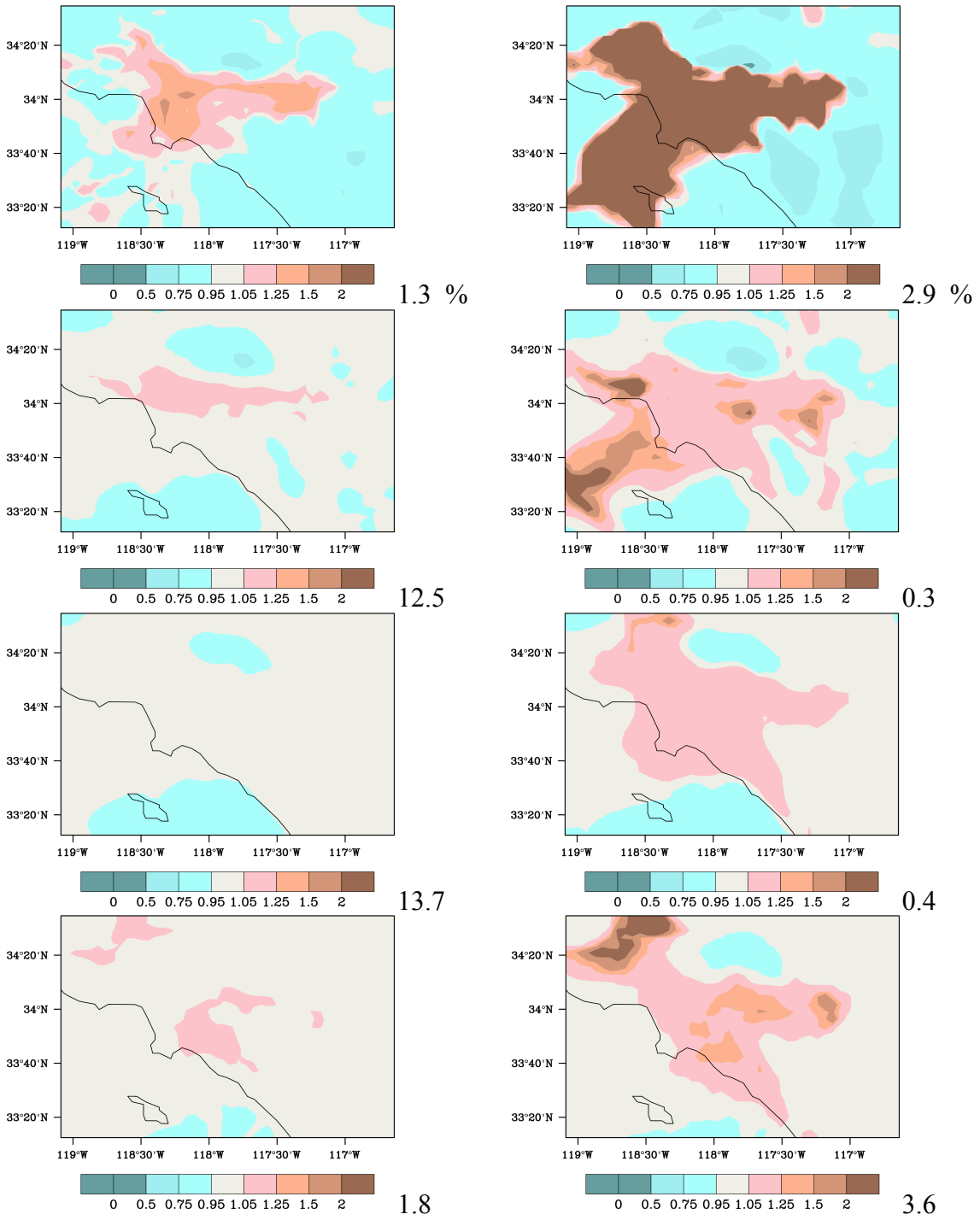

Figure 5.4f: Winter Monday average ratio of baseline to adjusted scenario HNO_3 production by season. Values reported next to each panel are the percentage of total Saturday through Monday HNO_3 production from the reaction and time specified in the panel.
Left column: $NO_2 + OH \rightarrow HNO_3$. Right column: $N_2O_5 + H_2O \rightarrow 2HNO_3$.
From the top row to the bottom row, values were averaged over the time periods:
12AM - 6 AM, 6 AM – 12 PM, 12 PM – 6 PM, 6 PM – 12 PM.

5.4 Summary and Policy Implications

The effects of weekend emission reductions on fine particulate nitrate were explored in this chapter. While intuitively one expects lower NO_x emissions will lead to decreases in fine particle nitrate, offsetting chemical effects may lead to a non-linear response of nitrate concentrations to changes in NO_x emissions. These chemical effects are present in both the daytime and nighttime pathways to nitric acid formation. The offsetting chemical effects can counteract the effect of reduced NO_2 concentrations on nitric acid production and result in nitrate decreases in urban areas that are smaller than expected based on the extent of NO_x emission reductions. Like ozone, secondary particulate nitrate exhibits nonlinear source-receptor relationships that make it hard to understand and control this air pollutant. The effectiveness of policies aimed at reducing nitrate through NO_x emission controls will vary depending on local conditions. NO_x reductions may have an adverse effect on nitrate concentrations in regions with high primary NO_x emissions and strong ozone weekend effects during fall and winter months.

The air quality model results presented in this chapter indicated summertime nitrate reductions similar to those found in the observational record, as reported in Chapter 3. Both model predictions and observations show weekend nitrate effects lasting through to Monday, as opposed to weekend effects on ozone and EC, which are mostly limited to Saturday and Sunday. In analyzing the observed record, it was essential to have high time resolution data (daily or better) over a year or longer before weekend signals in the data were apparent. Clear weekend signals emerged in the air quality model results when meteorology was held constant and the simulations were repeated using all weekday emissions.

One important unresolved difference between the modeled and observed nitrate response to weekend emission reductions was found during the fall. The observations indicated nitrate increases on Saturday and perhaps Sunday followed by nitrate reductions on Mondays. The model did not show reduction in Monday nitrate during the fall over much of the urban regions in the Los Angeles area. Due to the sensitivity of nitrate concentration to conditions on previous days it is unclear whether modeled emissions, chemistry, or meteorology and transport contribute to the difference between modeled and observed response of nitrate to weekend emission reductions. Additional field campaigns designed to measure continuous nitrate concentrations over multiple locations throughout a single air basin would be useful for more detailed model and observation comparisons.

Chapter 6

EFFECTS OF ACCELERATED RETROFIT OF DIESEL ENGINES ON AIR QUALITY

6.1 Introduction

Heavy-duty diesel engines are an important source of air pollution on urban, regional, and national scales (Lloyd and Cackette, 2001; Sawyer et al., 2000; Yanowitz et al., 2000b). Although they account for only 2% of the on-road vehicle fleet and 4% of the vehicle-km traveled, heavy-duty trucks are responsible for over half of nitrogen oxide (NO_x) and exhaust particulate matter (PM) emissions from on-road mobile sources (Kirchstetter et al., 1999). The importance of diesel engine emissions has been growing since 1990 due to success in controlling light-duty gasoline engine emissions, the failure of early efforts to control diesel NO_x emissions, and a threefold higher growth rate of diesel fuel sales compared to gasoline (EIA, 2006; Harley et al., 2005).

In contrast to earlier diesel emission control strategies that relied on combustion modifications and improved engine designs, current control strategies now typically include exhaust after-treatment (Johnson, 2006). Diesel particle filters (DPF) include a platinum catalyst upstream of the particle filter; the catalyst promotes oxidation of nitric oxide (NO) present in the exhaust to

nitrogen dioxide (NO_2). NO_2 in turn is used as an oxidizing agent to remove carbon particles from the filter to prevent it from plugging. Urea-based selective catalytic reduction (SCR) is a possible approach to controlling NO_x emissions from heavy-duty engines. A reason for using urea instead of ammonia is that urea can be stored in liquid form and is safer and easier to handle. Controls such as DPF and SCR systems have not yet been widely deployed on diesel engines in the U.S. Nationally, new heavy-duty diesel engines must meet more stringent exhaust PM and NO_x emission limits starting with the 2007 and 2010 engine model years, respectively. However, because of the long service life and slow rate of turnover for heavy-duty engines, the California Air Resources Board (CARB) has adopted an in-use emissions control rule that requires heavy-duty vehicle owners to retrofit or replace older engines (CARB, 2008a). This program is intended to accelerate reductions in diesel exhaust emissions that would otherwise occur more gradually due to fleet turnover, as shown in Figure 6.1. As a result, all on-road heavy-duty diesel trucks operating in California are expected to meet current new-engine exhaust PM emission standards by 2014. The adoption of best available control technology for NO_x will proceed at a slower pace. It is estimated that by 2014, half of the in-use trucks operating in California will meet current new-engine emission standards for NO_x (CARB, 2008a).

Diesel emission regulations are technology neutral and various approaches are possible. SCR systems are a viable option for retrofit on in-use engines to reduce NO_x emissions (CARB, 2008a). Other approaches to diesel NO_x emission control include lean NO_x traps (LNT) that react NO_x with unburned hydrocarbons, and NO_x storage catalysts that adsorb NO_x chemically under lean conditions, and then desorb NO_x periodically under rich conditions (Johnson, 2004). Side effects of the new emission controls may include reduced engine efficiency and changes in emissions of certain pollutants such as nitrogen dioxide (NO_2), nitrous acid (HONO), and ammonia (NH_3) (Jeong et al., 2008; Johnson et al., 2009).

To date the main concern about DPF systems appears to be increased primary NO_2 emissions. For example, Carslaw (2005) and Carslaw et al. (2005; 2006) showed that at many sites throughout London, NO_2 concentrations did not decrease along with NO_x between 1997-2003, and the increase in the measured NO_2/NO_x ratio could be linked to the use of DPFs and an increase in the fraction of light-duty diesel vehicles. Jenkin et al. (2008) reported a 7% increase in mean O_3 mixing ratios when modeling the effects of increases in NO_2/NO_x emission ratios in southern England.

The diesel engine replacement/retrofit program in California will lower exhaust PM emissions, but will also increase the NO_2/NO_x emission ratio from <10 to ~35% over a relatively short time period (i.e., by 2014). Since the schedule for reducing diesel NO_x emissions is more gradual compared to that for exhaust PM, increases in concentrations of NO_2 and related pollutants may be observed. Therefore, the objective of this study is to assess the impacts of diesel engine emission controls on ambient air quality, by comparing future emission scenarios for 2014 with and without the accelerated diesel engine replacement/retrofit program. To make these comparisons, an Eulerian photochemical air quality model is applied to southern California for both summer (high ozone) and fall (high PM and NO_2) conditions. Air quality endpoints assessed here include O_3 and NO_2 in the gas phase, as well as fine particulate nitrate and elemental carbon mass.

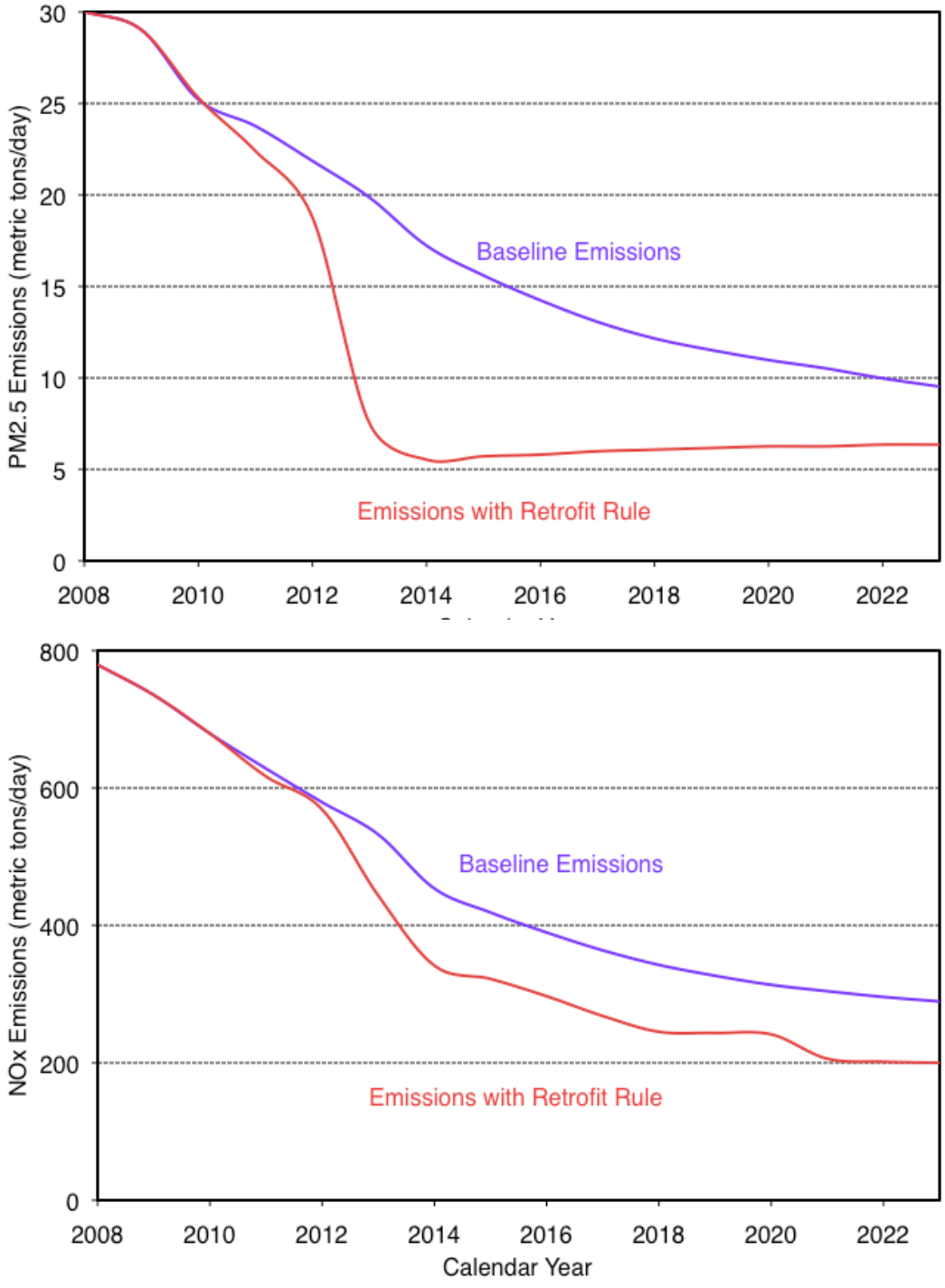

Figure 6.1: On-road heavy-duty diesel engine exhaust particulate matter and nitrogen oxide emission trends (California state totals), with and without a new rule to accelerate retrofit/replacement of older engines. Source: (Jaw et al., 2009).

6.2 Methods

Air Quality Model. The Community Multiscale Air Quality model (CMAQ; Byun and Schere, 2006) version 4.6, with the SAPRC99 gas-phase chemical mechanism (Carter, 2000) is used to evaluate air quality for baseline (2005) and two alternative future (2014) emission scenarios. The choice of future year (2014) in this study was determined by the schedule for completing installation of particle filters on (or replacing) all older on-road heavy-duty diesel engines in California. As described in Chapter 5, processes relating to secondary particle formation were modeled using the AE4 aerosol module (Binkowski and Roselle, 2003) and gridded hourly meteorological fields were developed using the Mesoscale Meteorological model (MM5) version 3.6.1 (SCAQMD, 2007a). Further details are found in Chapter 5 and Millstein and Harley (2009b).

The modeling domain (centered on Los Angeles, with 65 × 40 grid cells with 5 km horizontal resolution) is the same as described in Chapter 5. Figure 6.2 shows the modeling terrain and locations with particle and gas measurements. As in Chapter 5, two simulation periods, one summer (6 July – 29 August) and one fall period (30 October – 7 December), are considered in this study.

Baseline Emissions. The same baseline emissions as described in Chapter 5 were used in this study. These anthropogenic emissions were originally developed by the South Coast Air Quality Management District and the California Air Resources Board, as described in the 2007 Air Quality Management Plan for the South Coast Air Basin (SCAQMD, 2007b). Changes to diesel-powered construction equipment, the diesel NO_2/NO_x emission ratio, and weekday/weekend emissions were included as described in Chapter 5.

Baseline anthropogenic emissions for fall 2005 and summer/fall 2014 simulation periods were estimated by adjusting summer 2005 emission estimates using scaling factors for each pollutant and source category derived from tabulated seasonal planning inventories for 2005 and 2014 (SCAQMD, 2007b) so that:

$$E_i^{new} = E_i^{2005summer} \times \frac{SC_i^{new}}{SC_i^{2005summer}} \qquad (6.1)$$

Where E is the model emission set for a particular source category, for example diesel trucks, for either the new time period or the baseline summer 2005 and over species i (NO_x, $PM_{2.5}$, reactive organic compounds, CO, or SO_2). SC is the estimated emission totals for the south coast air basin in the seasonal planning inventories of species i for the specified time period (SCAQMD, 2007b).

Biogenic emissions were estimated using the BEIGIS model (Scott and Benjamin, 2003); separate day-specific estimates were available for each day of 2005 (Scott, 2009). Biogenic emissions were unchanged in the 2014 simulations.

The forecasts of future anthropogenic emissions in southern California reflect the effects of population growth and all emission control rules adopted prior to 2006. Baseline emission forecasts for 2014 do not include the effects of the new rule requiring in-use diesel engine

retrofits. The effects of other recently adopted rules requiring emission reductions at ports (CARB, 2006) and reductions of greenhouse gas emissions (CARB, 2008b) are also not included here. The 2014 emission inventory factors in growth in the number of trucks on the road, as well as fleet turnover which acts by replacing older trucks with new ones that meet current new-engine emission standards for PM and NO_x. Thus significant (~50%) reductions in diesel truck emissions are forecast to occur between 2005 and 2014 even without the in-use engine retrofit/replacement rule, as shown in Figure 6.1.

Emissions for 2014 Retrofit Scenario. Additional reductions in PM and NO_x emissions due to accelerated retrofits and engine replacements, beyond what can be expected from fleet turnover, have been estimated by Jaw et al. (2009) and are shown in Figure 6.1. Emissions of NO_x from on-road diesel vehicles are reduced by 22% relative to the baseline 2014 emission scenario. Similarly, exhaust PM emissions are reduced by 64%. These scaling factors were derived from the ratio of 2014 emissions for the two cases shown in Figure 6.1, with small adjustments to account for emissions from lighter vehicles (below 6 350 kg = 14 000 lb gross vehicle weight) that will not be subject to retrofits. Minor contributions to total CO and VOC emissions in the 2014 baseline inventory from on-road diesel engines were left unchanged in the retrofit scenario.

The NO_2/NO_x emission ratio for on-road heavy-duty diesel engines was set at 5% (per Ban-Weiss et al., 2008a) in the baseline 2014 emission scenario. The ratio was increased to 35% (Herner et al., 2009) in the 2014 retrofit scenario, reflecting universal use of DPF systems to control exhaust PM emissions. Some increase in NO_2/NO_x emission ratio may occur by 2014 even without the accelerated retrofit program, though this effect on fleet-average emissions will be small because any new DPF-equipped trucks must also meet low-NO_x emission standards that apply to new engines. Retrofit of DPF systems on older engines with higher NO_x emission rates has more potential to increase the fleet-average NO_2/NO_x emission ratio.

6.3 Results and Discussion

As shown in Figure 6.1, in the baseline scenario, both NO_x and $PM_{2.5}$ emissions from heavy duty vehicles are forecast to decrease with a characteristic time (half-life) of 7-8 years, reflecting the combined effects of growth in travel and fleet turnover in the on-road heavy-duty vehicle sector. The 7-8 year turnover rate corresponds to a 9-10% per year reduction in emissions of both pollutants, which is a higher rate than has been achieved in past years. For example, Ban-Weiss et al. (2008b) found that heavy-duty diesel NO_x and PM emission factors measured on-road decreased between 1997 and 2006 by 3 and 5% per year, respectively, and these numbers do not account for growth in diesel fuel use over the same period which offset some of the reductions.

The retrofit rule is likely to speed up the rate of diesel engine emission reductions significantly. The recent economic downturn may mean that the effects of the retrofit rule have been underestimated. Growth in diesel truck travel and fleet turnover are both likely to have been reduced relative to past trends due to the major downturn in the economy that has occurred since 2007. Presuming a rebound in fleet turnover rate lags a rebound in fleet truck travel the retrofit rule may have a larger impact than shown in Figure 6.1 if truck traffic rebounds by 2014 with an older fleet than predicted.

After 2014, growth in vehicle travel leads to small increases in PM emissions in the retrofit scenario, and the difference in PM emissions between the two scenarios therefore decreases in later years. In the retrofit scenario, NO_x reductions occur at a slower pace than for PM reductions, as shown in Figure 6.1. Exhaust PM and NO_x emissions from the affected diesel engines are reduced in the retrofit scenario by 68 and 25%, respectively, below 2014 baseline values.

Table 6.1 shows domain-wide anthropogenic emissions by scenario and season. While the reductions in on-road diesel engine emissions discussed above are significant, especially for exhaust PM, the overall reductions in anthropogenic emissions between the 2014 baseline and retrofit scenarios are less dramatic. In the 2014 baseline scenario (without retrofits), on-road diesel vehicle emissions account for 26 and 23% of total NO_x and EC emissions, respectively, shown in Table 6.1. For the 2014 retrofit scenario, diesel vehicles are responsible for 21% of total NO_x emissions, and 9.5% of total EC emissions. Note in Table 6.1 that forecast changes in emissions between 2005 and 2014 reflect increased emphasis on controlling diesel engine emissions, and therefore include greater relative reductions in NO_x compared to CO and VOC. In contrast, through the 1990s, mobile source emissions of CO and VOC decreased more rapidly than NO_x (Kirchstetter et al., 1999; Parrish et al., 2002).

Air quality model predictions for 2005 were compared to routine surface observations for gaseous pollutants, and to observations from 11 special study sites from the Multiple Air Toxics Exposure Study (MATES-III; SCAQMD, 2008), where speciated 24-h average fine particle concentrations were measured every third day. The network of special study $PM_{2.5}$ observation sites used for model evaluation is shown in Figure 6.2. As shown in Table 6.2, there are no large systematic biases in model predictions of the pollutants examined here for 2005 (fine particulate EC and nitrate; O_3 and NO_2 in the gas phase), though the possibility of compensating errors cannot be excluded.

More detailed comparisons of model predictions with observations are shown in Figure 6.3 on a site-by-site basis. Figure 6.3c shows $PM_{2.5}$ concentrations consistently above the annual average $PM_{2.5}$ standard of 15 $\mu g/m^3$ during both the summer and fall seasons. At most locations, there is reasonable agreement for both seasons and all pollutants considered here. As expected, absolute EC and NO_2 concentrations are higher during fall, whereas O_3 concentrations are higher during summer. EC concentrations are over-predicted during the summer at Compton and North Long Beach; both sites are located close to the ports of Los Angeles and Long Beach. Fall season predictions at these locations match the observations more closely. EC concentrations at Fontana are significantly under-predicted in both seasons. These under-predictions are pervasive, not isolated to a few days or extreme events. A search of satellite imagery of the surrounding area revealed a large inter-modal freight facility located 1 km to the west; that facility is very likely to be contributing to the elevated EC concentrations observed at Fontana. Diesel NO_x emissions from this facility are also affecting concentrations of O_3 and NO_2 observed at Fontana: in both summer and fall there are signs of ozone titration (and therefore decreased O_3 and increased NO_2) apparent in Figure 6.3. The comparison of model to observational results at Burbank is suggestive of an underestimation of EC and similar ozone titration effects to those seen at Fontana during the fall but not summer. The Burbank site is located about 500 m away from an interstate highway (I-5) that is a major truck route in and out of the Los Angeles basin. For both

Fontana and Burbank, the 5 km horizontal resolution of the emission inventory and the air quality model are not sufficient to resolve plume-scale dispersion near major freight-handling facilities and highways, even if emissions from these sources were known with high precision.

Table 6.1: Air pollutant emission estimates by year, season, and scenario in southern California[1] (metric tons per day, t/d).

Year	Scenario	CO	NO_x	NMOC[2]	NH_3	$PM_{2.5}$	EC[3]
2005	Summer Baseline	3949	990	1285	111	121	23
2005	Fall Baseline	3784	1042	852	113	124	24
2014	Summer Baseline	2358	632	1059	93	110	17
2014	Fall Baseline	2198	668	636	93	114	18
2014	Summer Retrofit	2358	597	1059	93	106	15
2014	Fall Retrofit	2198	632	636	93	110	16

[1] Emissions for typical weekday conditions for the southern California modeling domain shown in Figure 6.2.
[2] The reported values for non-methane organic compounds (NMOC) include anthropogenic emissions only. Biogenic VOC contribute an additional 395±97 and 118±42 t/d in summer and fall, respectively.
[3] Elemental carbon (EC) emissions are also included as part of fine particle ($PM_{2.5}$) emissions in the previous column.

Table 6.2: Seasonal mean normalized differences (% ± standard deviation) in concentrations of fine particulate elemental carbon and nitrate, and in ozone and nitrogen dioxide in the gas phase.[a]

	EC	NO_3^-	O_3[b]	NO_2	$PM_{2.5}$
2005 baseline vs. 2005 observed values[c]					
Summer	+13±36	–20±23	+16±12	+23±32	+19±17
Fall	–4±29	+10±29	+14±32	–6±25	+17±34
2014 baseline vs. 2005 baseline[c]					
Summer	–23±3	–15±11	+9±8	–32±8	-9±3
Fall	–23±2	–2±5	+36±14	–26±8	-6±2
2014 retrofit vs. 2014 baseline[c]					
Summer	–12±2	+2±2	+3±2	–4±3	-1±0.3
Fall	–14±2	+6±2	+7±3	–2±3	-1±0.3

[a] The seasonal weekday 24-hour average concentration was found at each location shown in Figure 6.2 for each model run and the set of observations. At each location a normalized difference between the listed pair of scenarios was calculated and the differences were averaged across all the locations. The standard deviation reported is the standard deviation of normalized differences across all locations for each set of scenarios. The comparisons of O_3 and NO_2 were limited to a smaller set of locations as shown in Figure 6.3.

[b] Ozone seasonal averages were taken as the average of all weekday concentrations between 10 AM and 6 PM.

[c] "2005 baseline" = 2005 baseline model run; "2014 baseline" = 2014 baseline model run; "2014 retrofit" = the 2014 model run with the new regulations applied. "Observed Values" = particles measured from MATESIII, gas measurements from routine air quality measurements in southern California.

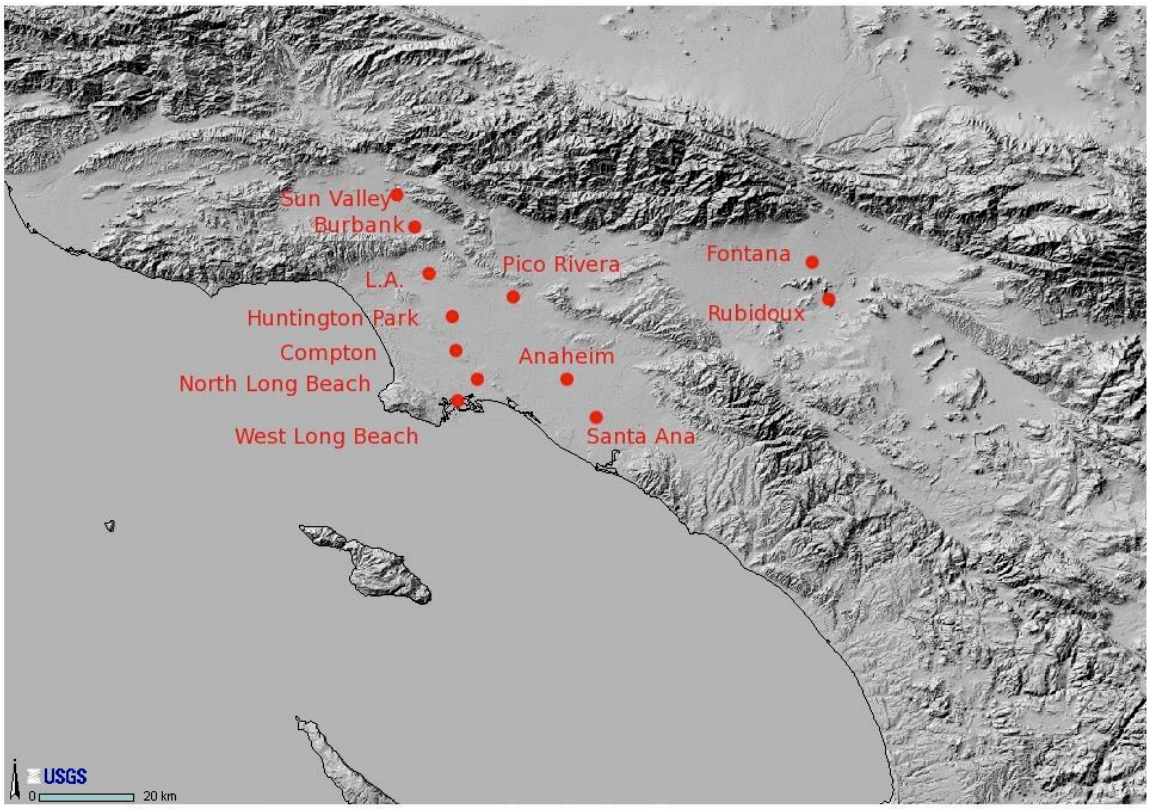

Figure 6.2: Map of southern California air quality model study domain, including MATES-III surface observation sites.

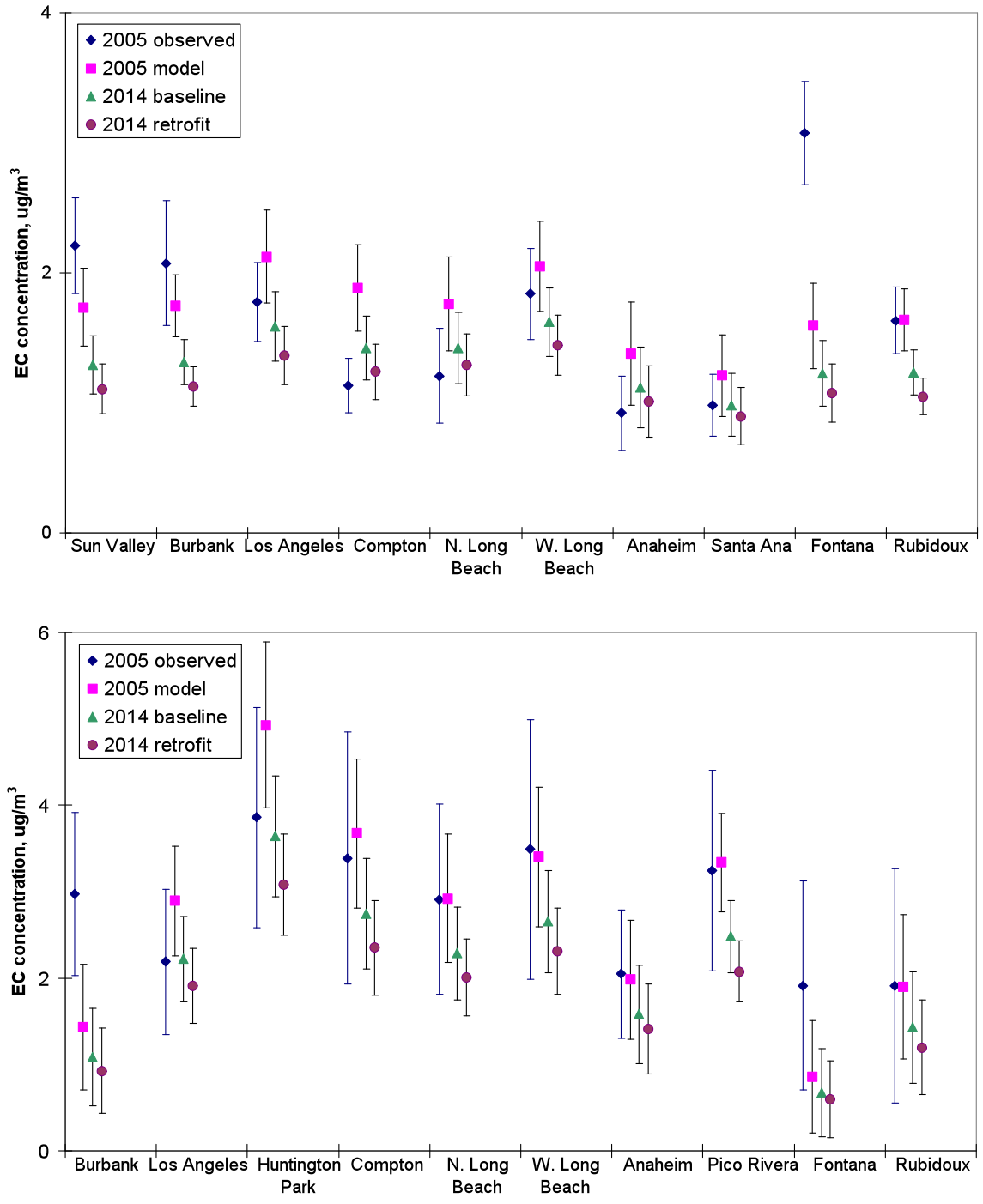

Figure 6.3a: Average weekday (μ ± standard deviation) observed and modeled elemental carbon (EC) concentrations. All values shown are 24-h averages. Measurement site locations are shown in Figure 6.2. Top panel: summer. Bottom panel: fall.

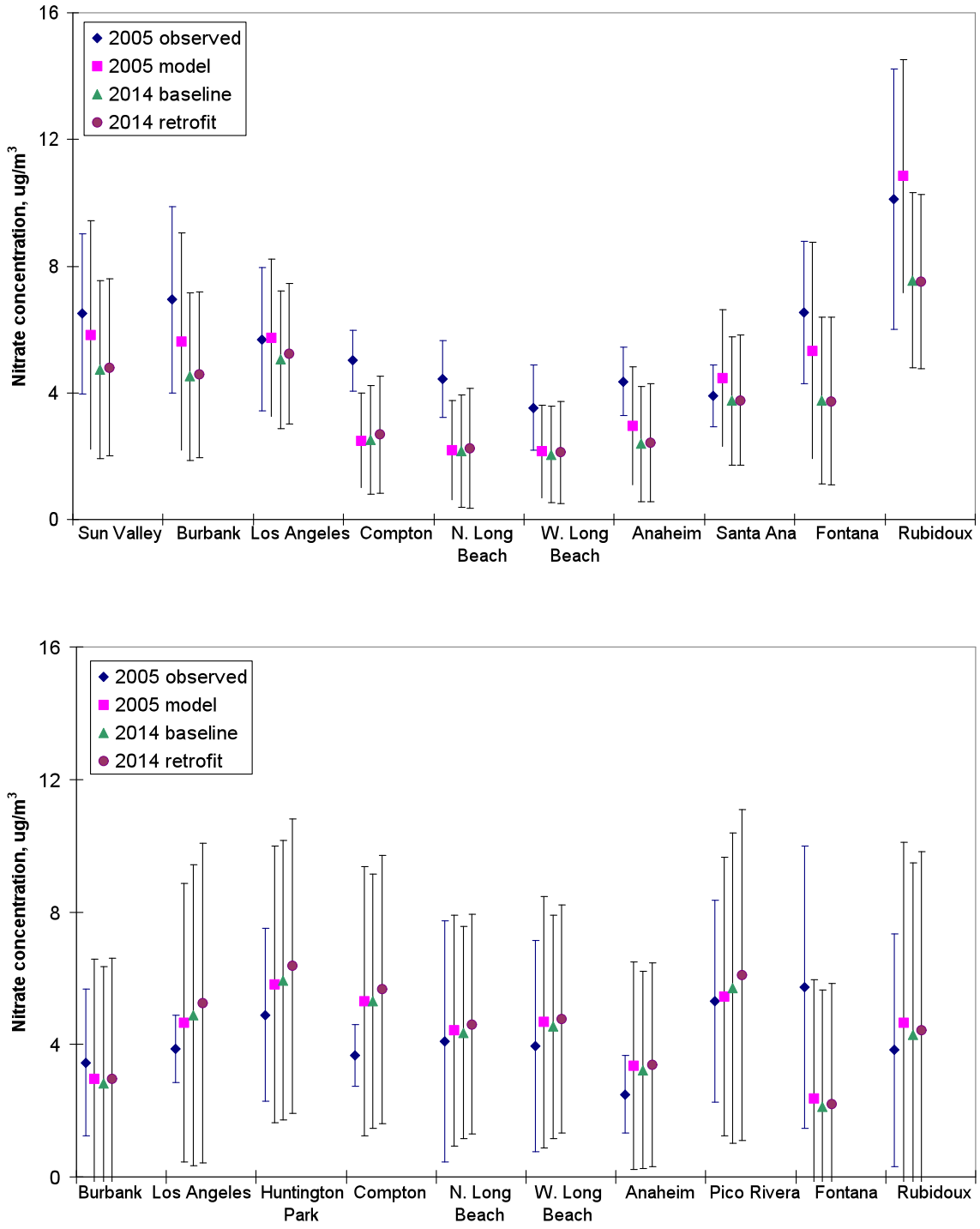

Figure 6.3b: Average weekday (μ ± standard deviation) observed and modeled fine particulate nitrate concentrations. All values shown are 24-h averages. Measurement site locations are shown in Figure 6.2. Top panel: summer. Bottom panel: fall.

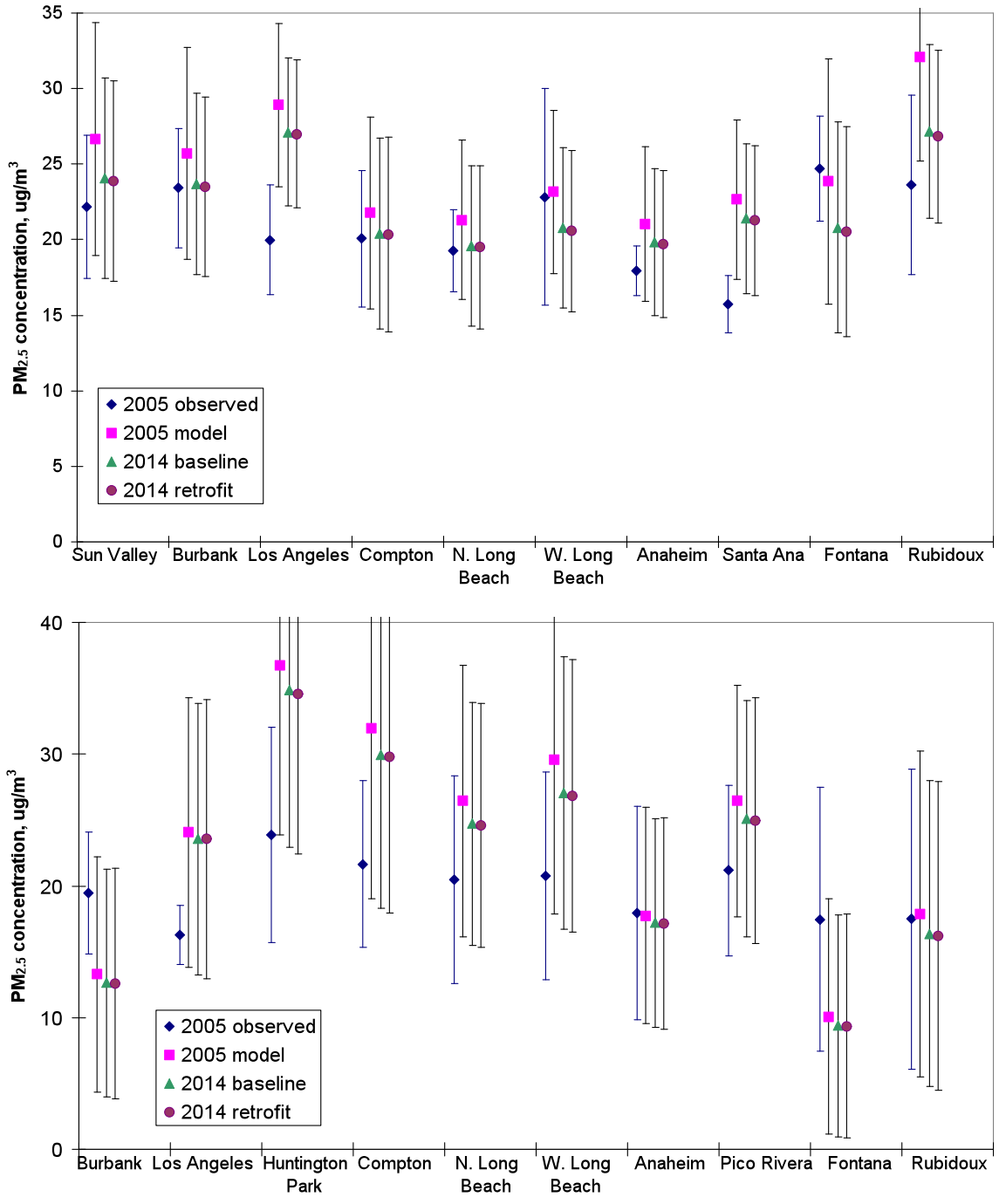

Figure 6.3c: Average weekday (μ ± standard deviation) observed and modeled $PM_{2.5}$ concentrations. All values shown are 24-hour averages. Measurement site locations are shown in Figure 6.2. Top panel: summer. Bottom panel: fall.

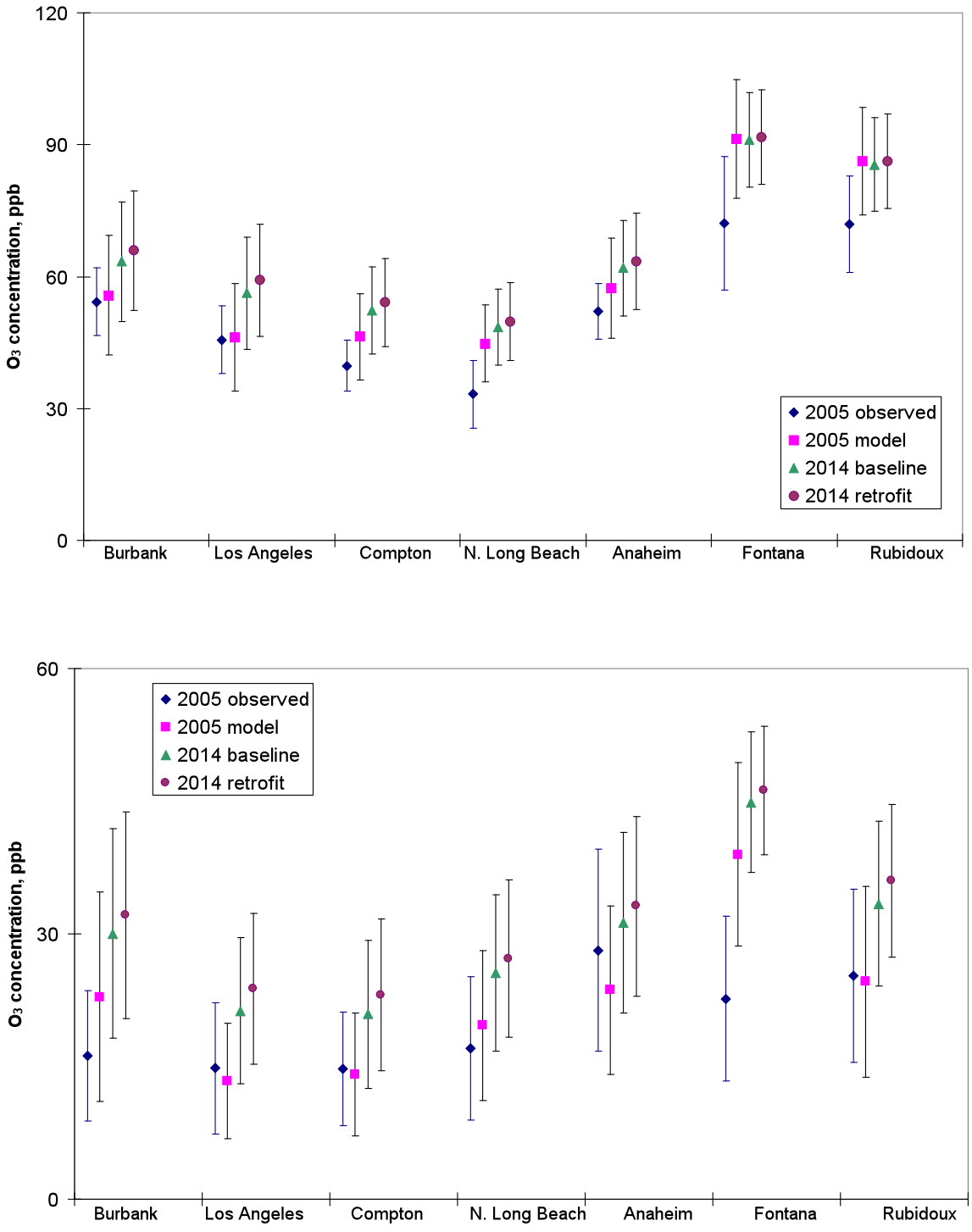

Figure 6.3d: Average weekday (μ ± standard deviation) observed and modeled ozone (O_3) concentrations. All values shown are 8-h averages for the period 10 AM-6 PM local time. Measurement site locations are shown in Figure 2. Top panel: summer. Bottom panel: fall.

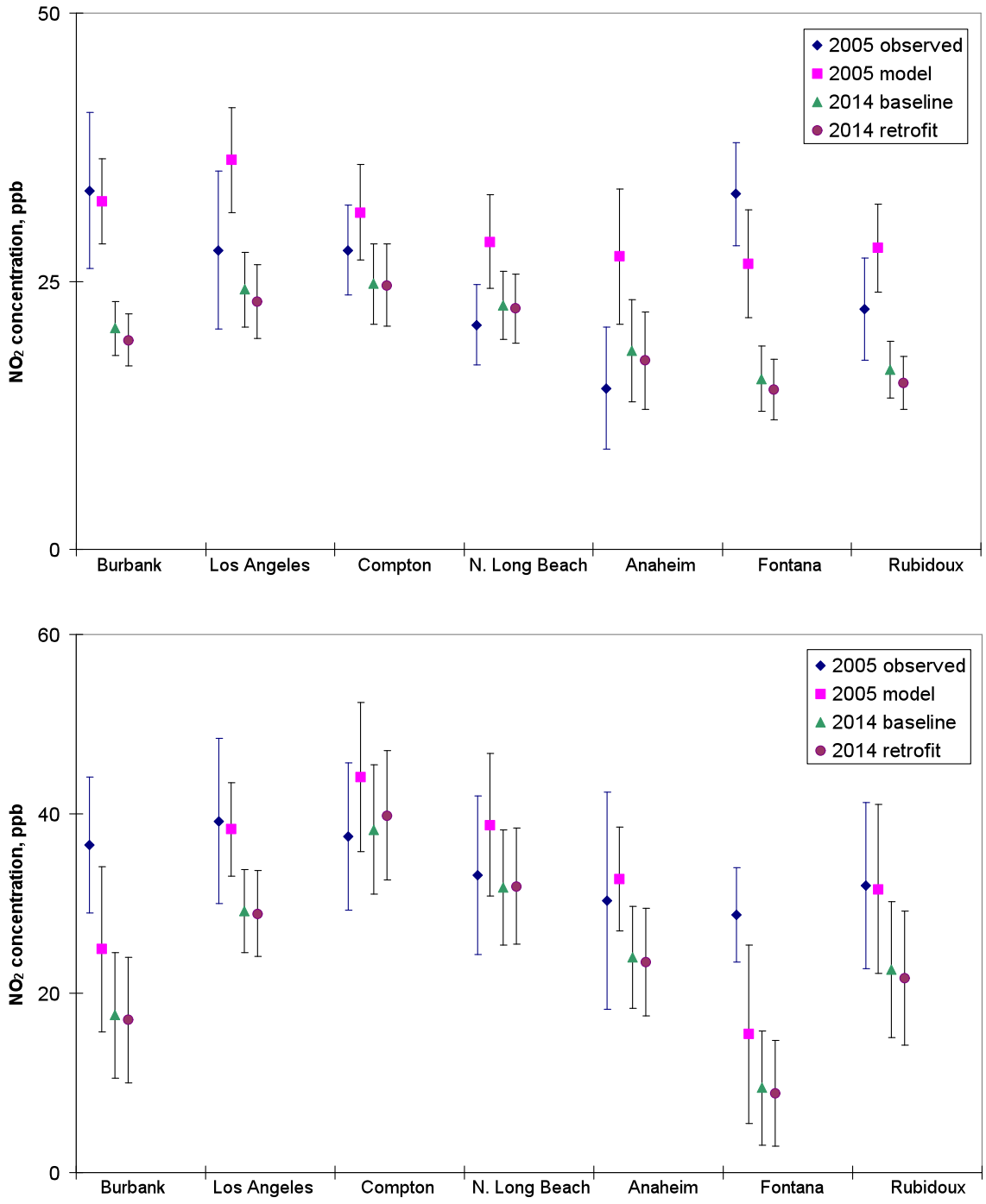

Figure 6.3e: Average weekday (μ ± standard deviation) observed and modeled nitrogen dioxide (NO_2) concentrations. All values shown are 24-hour averages. Measurement site locations are shown in Figure 2. Top panel: summer. Bottom panel: fall.

Both 2014 scenarios yield lower particulate EC and nitrate, and higher O_3 concentrations relative to 2005, in response to changes in PM and NO_x emissions. Relative to the 2014 baseline, reductions of 12±2% and 14±2% in average EC concentrations are predicted for the diesel retrofit scenario, in summer and fall respectively. Changes to other pollutants were small relative to the changes in EC, for example decreases to total $PM_{2.5}$ averaged at 1±0.3%. As shown in Table 6.2, the reductions in EC due to the retrofit program are smaller than reductions that are expected due to changes in emissions from all sources between 2005 and 2014 without any retrofits.

Decreases in EC are the largest and most likely to be observable ambient effect of the in-use diesel engine retrofit rule. Direct on-road measurements of diesel engine emissions over the next 5 years in California should be able to detect changes in exhaust PM emissions as well as in NO_x mass and speciation.

Figure 6.4 shows predicted spatial distributions of daily average (or 8-h average in the case of ozone) pollutant concentrations for the 2014 baseline emission scenario. Figure 6.4 also shows further changes to these concentrations that may result from diesel retrofits. Starred locations shown in Figure 6.4 are Los Angeles and Riverside/Rubidoux further to the east. The largest absolute reductions in EC from the in-use diesel retrofit program occur around central Los Angeles and near the port where truck traffic is high. These locations not only have high average EC levels but also relatively high population density. The use of regional scale metrics such as tons of statewide emissions reduced per day do not show the collocation of EC reductions and population density. The undesirable effects of diesel retrofits on O_3 concentrations are also largest near central Los Angeles, an upwind VOC-limited region where NO_x reductions can lead to O_3 increases. Larger relative increases in ozone are forecast to occur during fall when absolute O_3 concentrations are lower (see Table 6.2 and Figure 6.3).

While increases in O_3 concentrations also are predicted in densely populated areas, the O_3 increases are smaller in a relative sense for both seasons, when compared to expected decreases in EC. However, whether the predicted increases in ozone levels and decreases in EC levels lead to public health benefits is uncertain. Diesel particulate pollution is classified as a toxic air pollutant by California. Elevated levels of $PM_{2.5}$ and ozone are associated with a number of health effects, including aggravated asthma and premature death (CARB, 2007a).

A recent study by Jarrett et al. (2009) examined the long-term risk of mortality of exposure to increased levels of both ozone and $PM_{2.5}$. The study included data from ~450 thousand subjects across almost 100 metropolitan areas in the U.S. and included an 18 year follow-up period with ~120 thousand deaths. Jerrett et al. (2009) found a significant increase in the relative risk of death from cardiovascular causes with increased ambient $PM_{2.5}$ concentrations and a significant increase in the risk of death from respiratory causes with increased ambient ozone. However, Jerrett et al. (2009) found that when all causes of death are considered, there is a significant increased risk of mortality due to increases in $PM_{2.5}$ and there is not a significant increase of mortality risk due increases in ozone.

Another important issue regarding the health effects of the in-use diesel regulations is the relationship between ambient concentrations and intake-relevant exposure. Exposure to

pollutants depends on a person's breathing rate and the local concentration of pollutants the person is breathing. Thus, a person's activity patterns and daily travel patterns influence their exposure to pollution given a given ambient outdoor pollution level. Marshall et al. (2006) use an activity and travel survey of ~25,000 people in the South Coast Air Basin to estimate intake rate of outdoor air pollutants. Marshall et al. (2006) found the ratio of average intake-relevant exposure concentrations to average ambient concentrations was 1.5 and 0.18 for diesel $PM_{2.5}$ and ozone, respectively. Thus, ambient measurements of diesel $PM_{2.5}$ understate the true average exposure of the population to diesel $PM_{2.5}$ and ambient measurements of ozone overstate the true average exposure of the population to ozone. In further analysis of population exposure, Marshall (2008) found that low-income and non-white populations were disproportionately exposed to diesel $PM_{2.5}$ pollution. The target of diesel particulate matter by the in-use diesel regulations is appropriate given the high relative intake relevant exposure and the disproportionate exposure of lower-income non-white populations to diesel $PM_{2.5}$.

Changes to NO_2 concentrations reported in Table 6.2 require careful interpretation as there are competing underlying effects. During summer, NO_2 concentrations decrease by 4±3%. By 2014 about half of all in-use diesel trucks are supposed to have been retrofitted with NO_x after-treatment devices, thus reducing total NO_x emissions. This reduction in total NO_x offsets the effect of DPF retrofits on older trucks, which lead to increased primary NO_2 emissions. During the fall when photochemical activity levels are lower, small increases in average NO_2 concentrations are seen near central Los Angeles and the port area.

Figure 6.5 shows average weekday diurnal profiles of NO_2 concentrations for both 2014 emission scenarios and seasons at Los Angeles and Rubidoux. The diurnal plots show that the differences between NO_2 concentrations in the retrofit scenario and the base case are larger at night during both seasons. However, peak NO_2 levels near Los Angeles are not lower under the retrofit program and increased exposure to direct NO_2 emissions from DPF-equipped engines remains as a possible concern. At the air basin scale, retrofitting of NO_x control equipment on in-use diesel engines plays an important role in mitigating the effect of increased NO_2 emissions due to retrofit of diesel particle filters on older engines.

Both 2005 and 2014 emission inventory estimates are uncertain. The most important uncertainties relevant to the present study are the changes in on-road diesel emissions that will occur by 2014 with and without the retrofit program. Emissions from other source categories (e.g., on-road gasoline engines, off-road mobile sources, road/soil dust emissions in the fine mode, biomass burning) also help to determine the relative importance of on-road diesel engine emissions and their control. Another important issue, not addressed here, is the longer-term durability of new and retrofit emission control systems on in-use diesel engine emissions beyond 2014 when most of the installed emission control systems will still be relatively young.

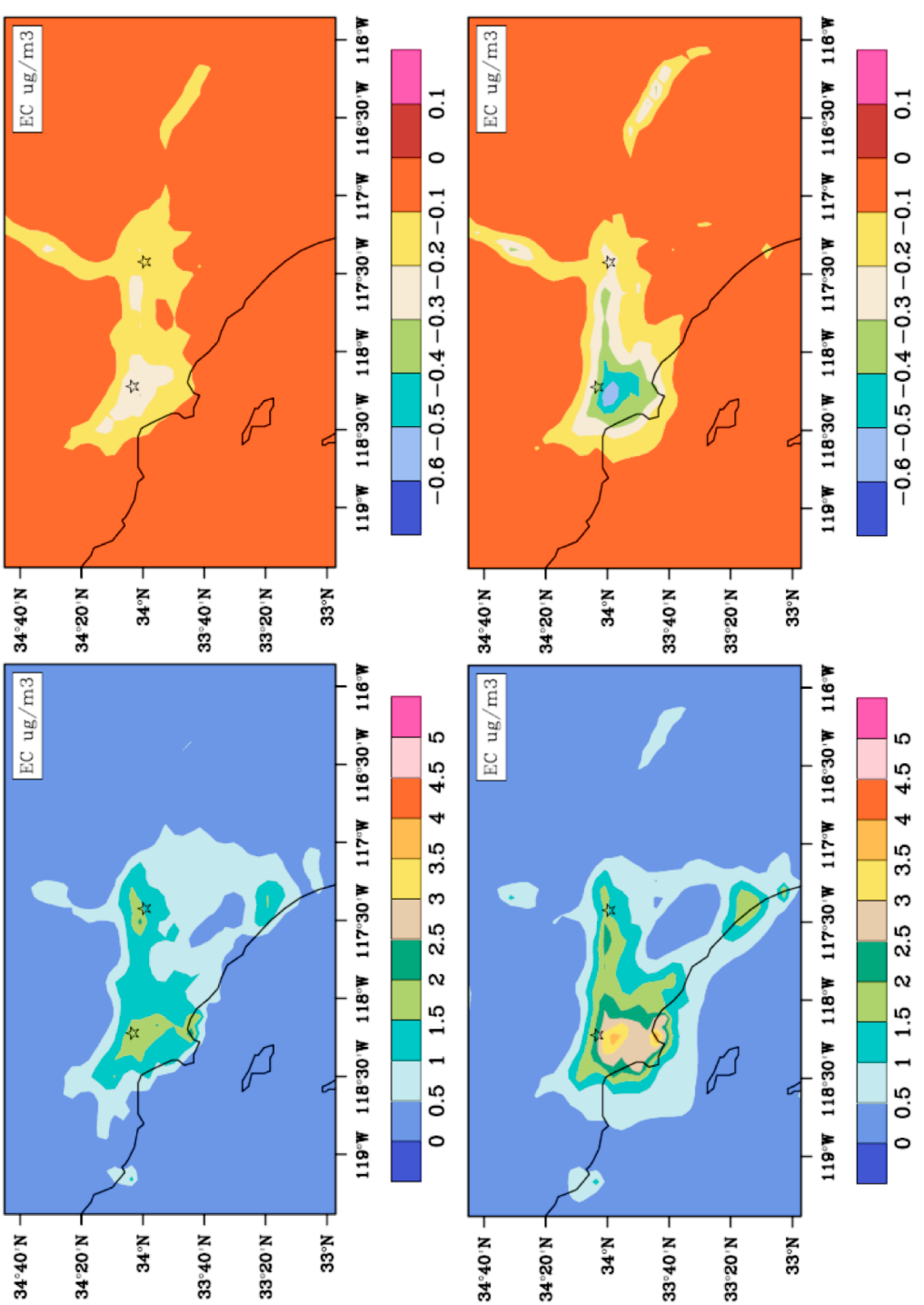

Figure 6.4a: Left panel: Average modeled summer (top) and winter (bottom) concentrations of EC. All weekday hours were averaged. Right panel: Difference between 2014 retrofit scenario and the 2014 baseline scenario. *The stars are (from west to east) downtown Los Angeles and Rubidoux.*

Note: For ease of viewing Figure 6.4a-c is presented in grayscale as Figure 6.4d-f.

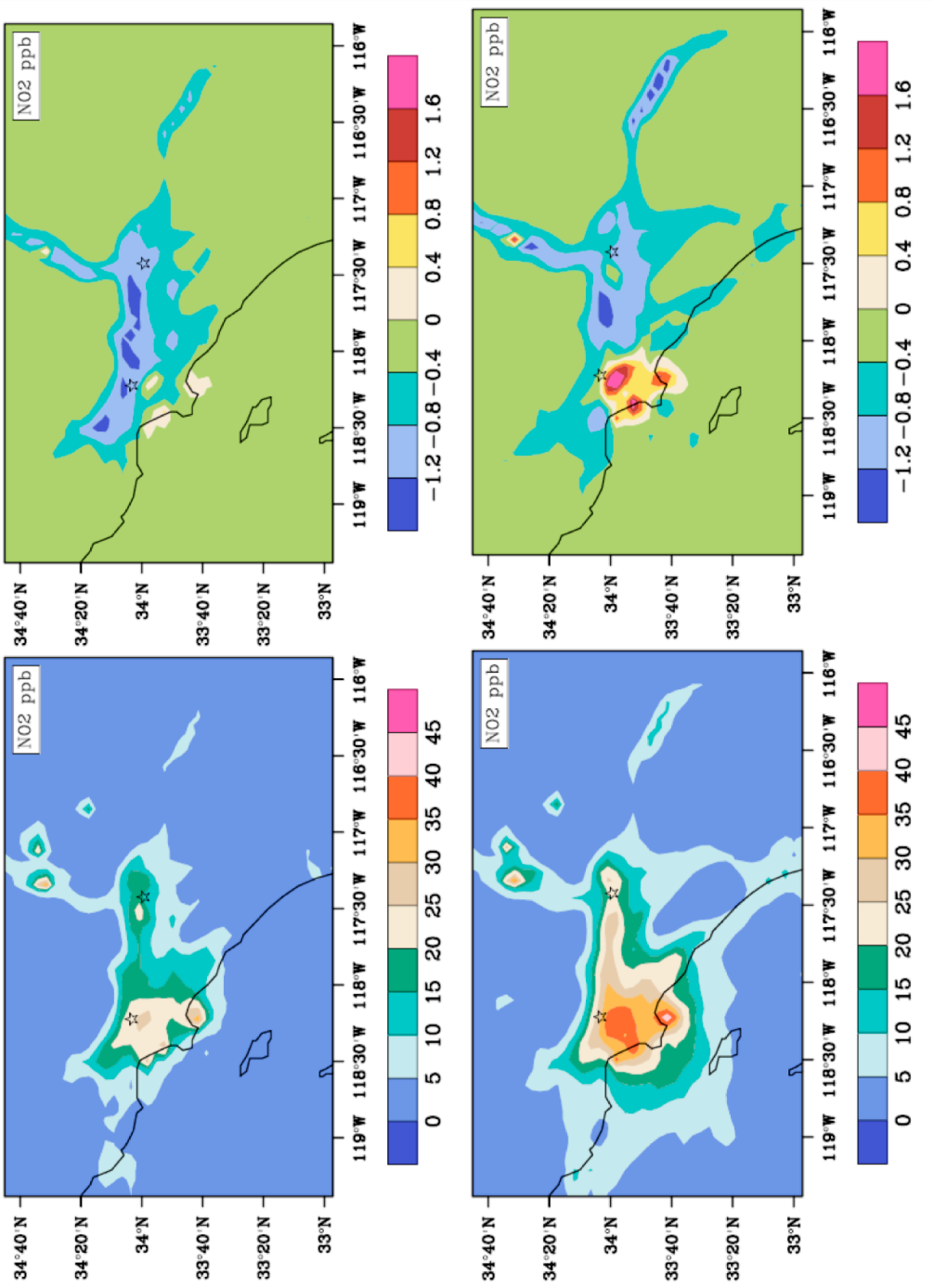

Figure 6.4b: Left panel: Average modeled summer (top) and winter (bottom) concentrations of NO_2. All weekday hours were averaged. Right panel: Difference between 2014 retrofit scenario and the 2014 baseline scenario. *The stars are (from west to east) downtown Los Angeles and Rubidoux.*

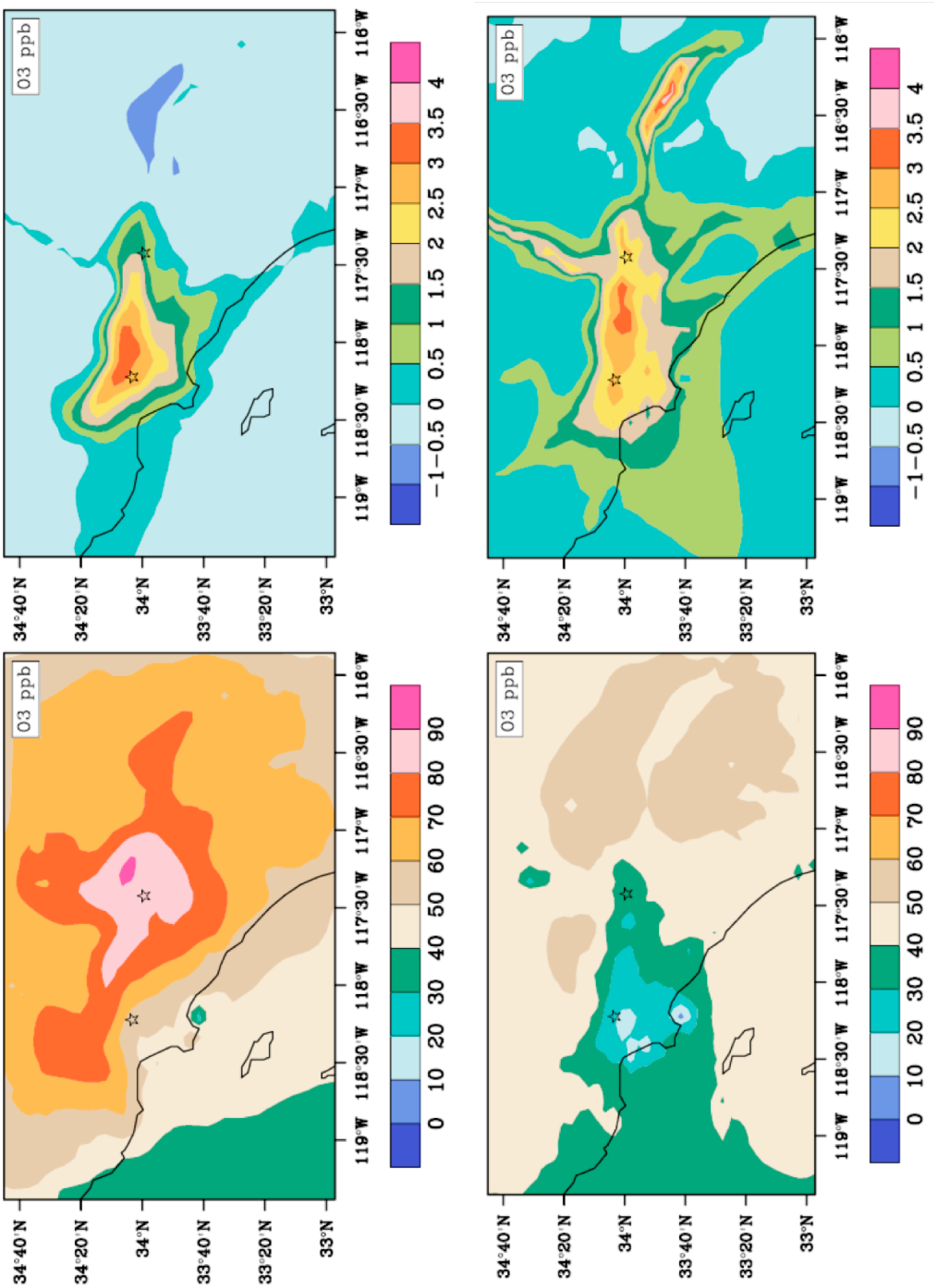

Figure 6.4c: Left panel: Average modeled summer (top) and winter (bottom) concentrations of O_3 concentrations were averaged over weekday hours 10 am – 6 pm local time. Right panel: Difference between 2014 retrofit scenario and the 2014 baseline scenario. *The stars are (from west to east) downtown Los Angeles and Rubidoux.*

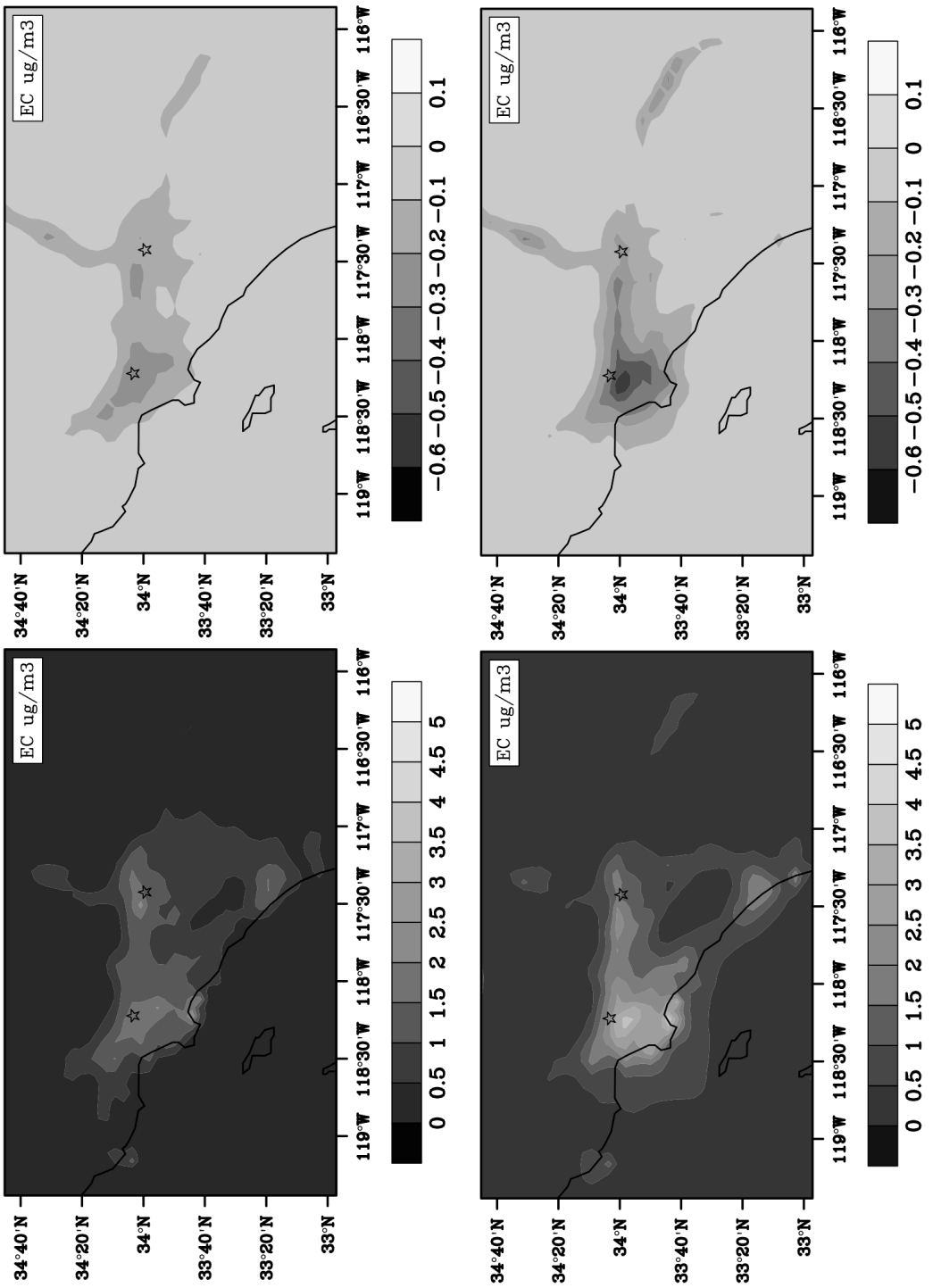

Figure 6.4d: Left panel: Average modeled summer (top) and winter (bottom) concentrations of EC. All weekday hours were averaged. Right panel: Difference between 2014 retrofit scenario and the 2014 baseline scenario. *The stars are (from west to east) downtown Los Angeles and Rubidoux.*

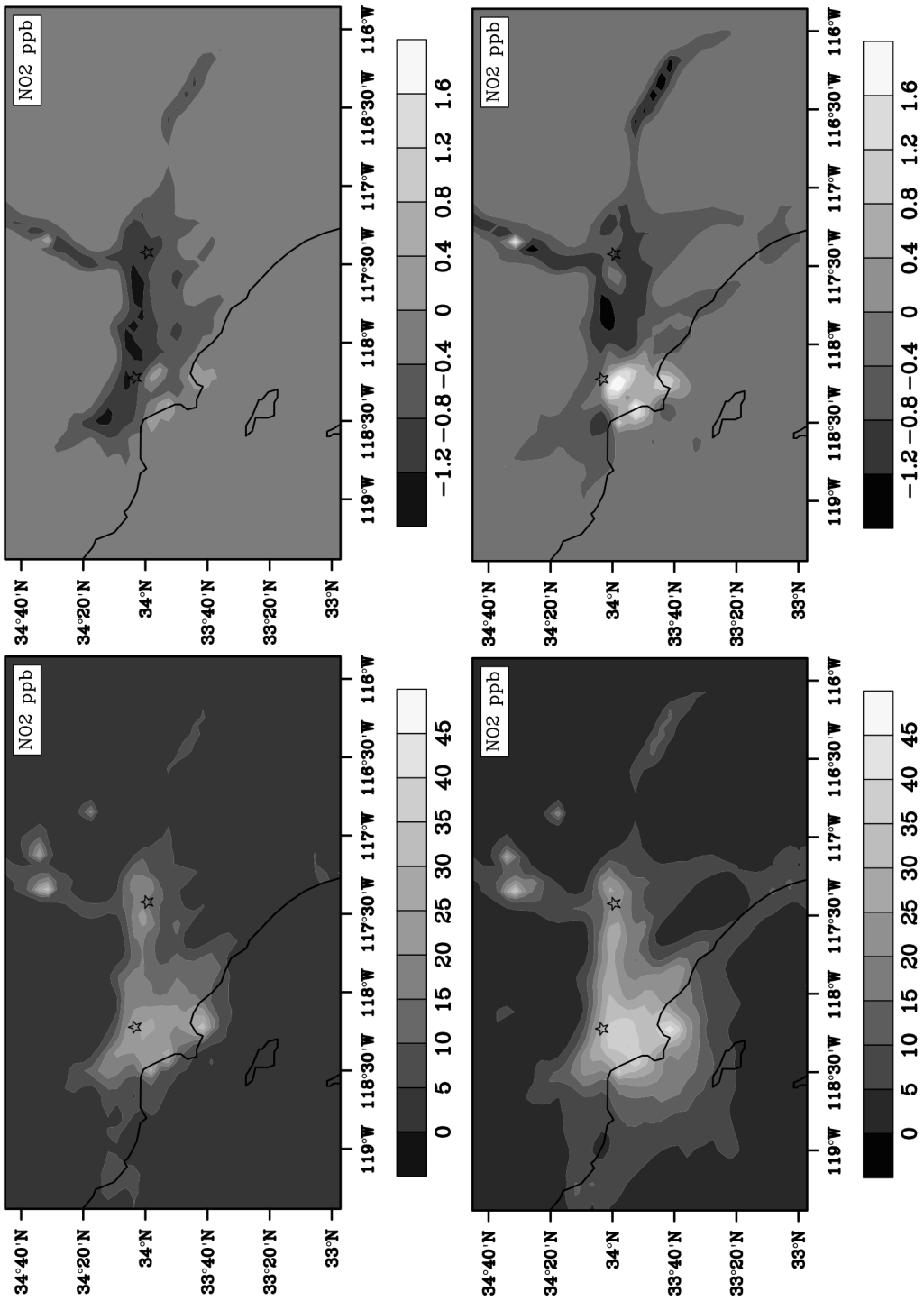

Figure 6.4e: Left panel: Average modeled summer (top) and winter (bottom) concentrations of NO_2. All weekday hours were averaged. Right panel: Difference between 2014 retrofit scenario and the 2014 baseline scenario. *The stars are (from west to east) downtown Los Angeles and Rubidoux.*

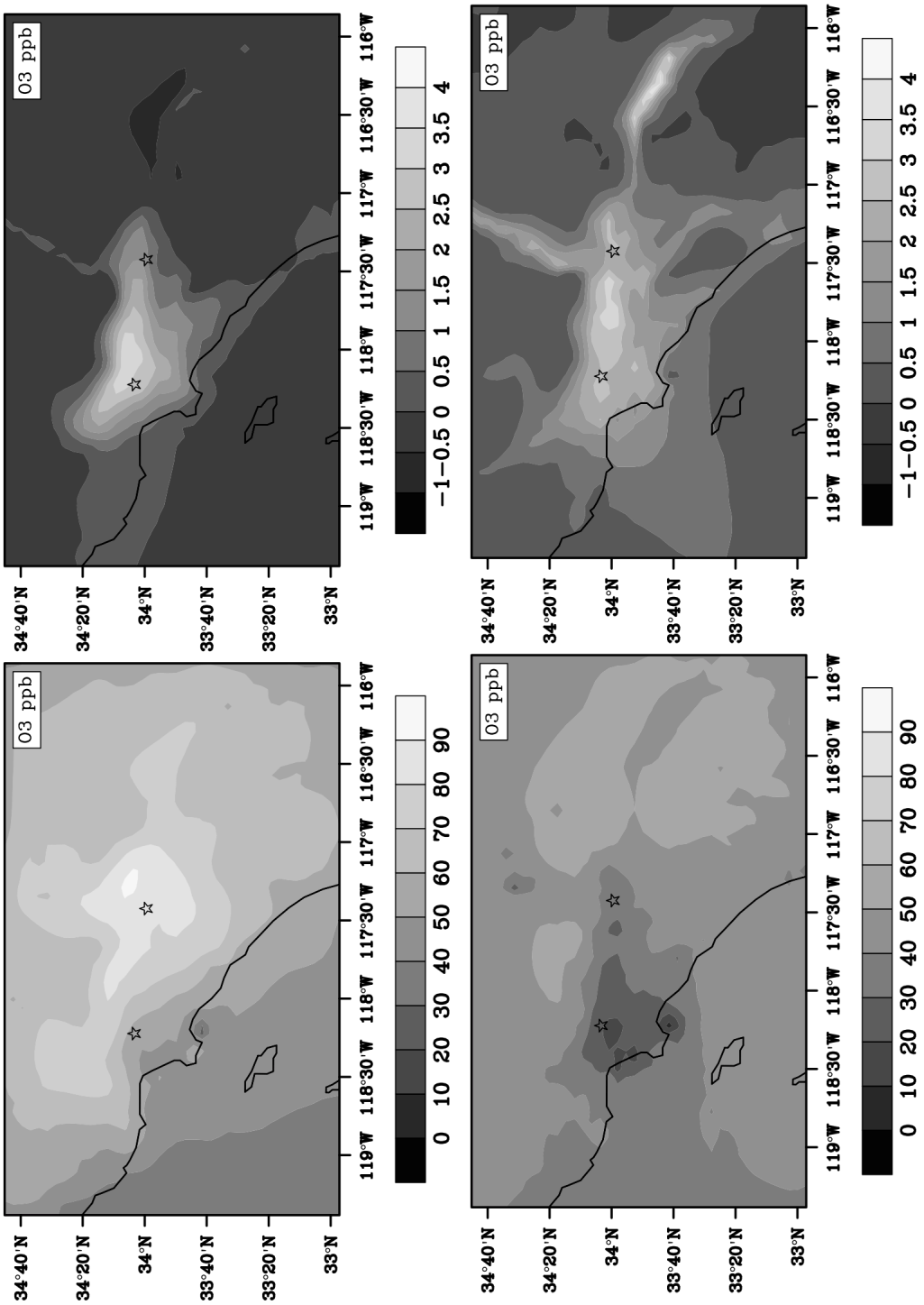

Figure 6.4f: Left panel: Average modeled summer (top) and winter (bottom) concentrations of O_3 concentrations were averaged over weekday hours 10 am – 6 pm local time. Right panel: Difference between 2014 retrofit scenario and the 2014 baseline scenario. *The stars are (from west to east) downtown Los Angeles and Rubidoux.*

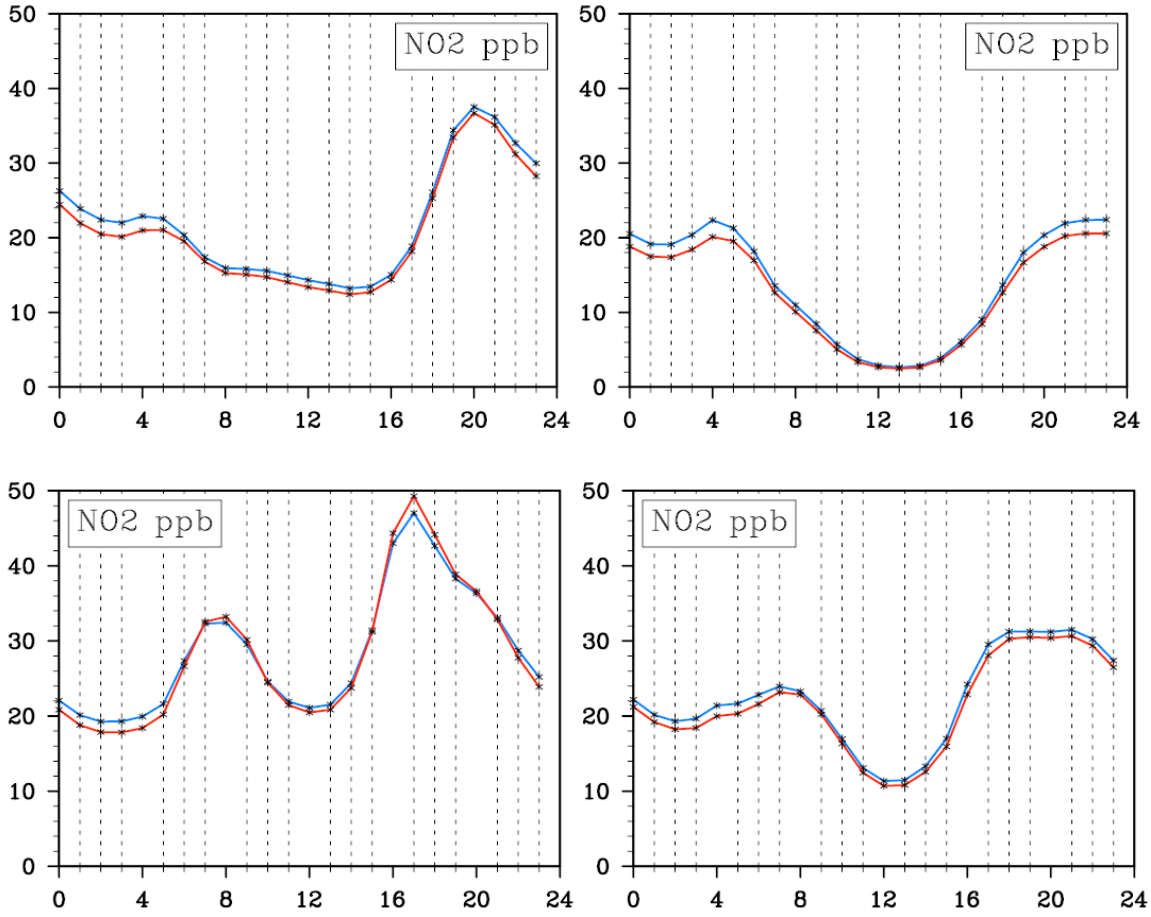

Figure 6.5: Average weekday diurnal NO_2 concentrations for summer (top) and fall (bottom) in 2014. (Blue: 2014 base case, Red: 2014 retrofit scenario). Left: downtown Los Angeles. Right: Rubidoux.

6.4 Summary and Conclusions

This study investigated effects on air quality of a control strategy that accelerates control of emissions from on-road heavy-duty diesel engines. In-use trucks will be required to meet current new-engine emission standards on a schedule that ranges from 2012 to 2023 depending on pollutant and model year. By 2014, all heavy-duty diesel trucks are expected to meet stringent PM emission standards, and about ~50% of in-use trucks will be required to have low NO_x emissions as well. The likely retrofit control system for exhaust PM, known as a diesel particle filter or particle trap, typically oxidizes NO present in the exhaust to NO_2 to help oxidize carbon particles that accumulate on the exhaust filter. As a result, the ratio of NO_2/NO_x emissions from diesel trucks equipped with particle traps can increase dramatically. The increase in primary NO_2 emissions may degrade air quality in some respects, as an undesired side-effect of controlling diesel exhaust PM emissions.

In this study we found that if retrofits of in-use diesel engines for control of both exhaust PM and NO_x emissions proceed as planned, significant reductions in atmospheric concentrations of diesel exhaust particulate matter will be realized, with a possible accompanying increase in ambient ozone. Although the effects of the retrofit program on near-road NO_2 concentrations deserve further study, ambient NO_2 concentrations should generally decrease along with decreased total NO_x emissions from diesel engines, despite a higher NO_2/NO_x ratio in primary emissions.

The health effects of the in-use diesel regulations are challenging to quantify given the varying health effects of ozone and $PM_{2.5}$ and the uncertainty regarding ozone mortality effects. The negative consequences of increased ozone due to slowly decreasing NO_x emissions should not be ignored. The ozone increases found here and the slow rate of diesel NO_x reductions expected after 2014, shown in Figure 6.1, indicate that more aggressive NO_x reductions would be required to see reduced ozone levels in 2014. However, the strong evidence of increased mortality from increased ambient $PM_{2.5}$ concentrations, the relatively high intake-relevant exposure to diesel $PM_{2.5}$ compared to ozone, and the environmental justice issues concerning diesel $PM_{2.5}$ emissions, indicate the in-use diesel regulations are well positioned to help address important air quality problems.

Chapter 7

CONCLUSIONS

7.1 Summary of Major Findings

Reductions in emissions that occur on weekends, for example from heavy-duty diesel trucks, provide a test case for whether atmospheric responses to changes in emissions can be observed and explained. Ozone responses have already been studied extensively. The response of ozone to weekend emission reductions is non-linear and depends on the relative concentration levels of NO_x and VOC. In areas with high local NO_x emissions ozone may increase with an increase of radical chemistry and with less titration of ozone by NO. In areas with high VOC, and limited NO_x emissions, ozone will decrease, as there is less NO_x to fuel the photolytic cycle. Compared to the understanding of ozone much less is known about changes in particle mass and composition that may occur in response to emission reductions on weekends. The study of PM response to weekend emission changes is limited in part due to a sparse observational record for PM, with most of the available measurements limited to 24-h averages of particle mass. Typical sampling frequencies have been once every 3-6 days, which is poorly suited to studying atmospheric responses to weekly emission cycles. Data from four PM "supersites" equipped with continuous online measurement methods were analyzed in this research. These measurements provided long-term (1 year or more) records of diurnal and day-to-day variations in fine particulate black carbon and nitrate.

Yearlong records of black carbon (BC) concentrations measured at St. Louis, Pittsburgh, and Fresno were analyzed. BC concentrations were highest at Fresno, with daily maxima up to 9 $\mu g/m^3$ compared to maxima at St. Louis and Pittsburgh of ~3 $\mu g/m^3$. Recurring reductions in BC concentrations on Sundays, relative to 7-day moving averages, of 22±6 and 25±5% were observed at Fresno and St. Louis, respectively. Smaller weekend reductions in BC were observed at Pittsburgh and they were not statistically significant.

Frequency domain (spectral) analysis of hourly BC time series at Fresno and St. Louis was used to apportion variance in measured concentrations to annual, weekly and diurnal time scales. Seasonal differences that recur on annual time scales accounted for 35 and 9% of the total variance in BC at Fresno and St. Louis, respectively. The weekly cycle accounted for 2 and 3% of the variance, and the diurnal cycle accounted for 6 and 4% of the variance at Fresno and St. Louis, respectively.

Time series of fine particulate nitrate concentrations were analyzed at the three sites mentioned above as well as Claremont, CA, an inland site in the Los Angeles basin. As expected, nitrate levels varied by site and season. In general, nitrate concentrations were higher during the fall and winter, and higher in California than elsewhere. Claremont was found to experience relatively high fine particle nitrate levels during all seasons.

Weekly cycles in nitrate were observed at three of the sites that were analyzed. Weekly minima were observed on Mondays, with mean reductions relative to 7-day moving averages of 23±12, 29±23, and 16±9% at Fresno, Claremont and St. Louis, respectively. Similar reductions in nitrate were observed on Sundays at Fresno and St. Louis. The mean reductions in nitrate were similar to those reported on weekends for BC, but the changes in nitrate had larger associated uncertainties and indicated a delayed response to weekend changes in emissions. The delayed response was more evident during colder months of the year, with summer season data showing a more rapid (i.e., same-day) atmospheric response to weekend emission reductions. There was also indication in the observational record of Saturday increases nitrate at Fresno, Claremont and St. Louis, and Sunday increases at Claremont. These increases suggest the possibility of a weekend effect for particle nitrate similar to that of ozone. Alternatively, the increased Saturday nitrate concentrations could be carried over from of slow build up nitrate concentrations through the week.

At Pittsburgh there was no evidence of weekly cycles in particulate nitrate even though significant weekend NO_x reductions were observed at this site. An interaction between nitrate and sulfate was investigated as a potential explanation for the lack of weekly nitrate cycle. Sulfate concentrations were found to decrease by 26±16 and 23±21% on Saturdays during the spring and summer months, respectively. Sulfate reductions can lead to higher ammonia gas concentrations if ammonium moves from being associated with sulfate aerosol to the gas phase. In turn, increased ammonia availability can lead to higher nitrate aerosol. It was found however that these sulfate reductions increased the ratio of fully neutralized sulfate to bisulfate (i.e., a less acidic aerosol resulted), but the sulfate reductions were not large enough to increase free ammonia concentrations and thereby increase concentrations of ammonium nitrate in the particle phase. So it was concluded that the lack of a weekly cycle in nitrate at Pittsburgh could not be explained by sulfate-nitrate interactions. Instead the relatively low nitrate concentrations and variability on other time scales make atmospheric responses to lower NO_x on weekends hard to detect in this case.

The next phase of this research involved use of an Eulerian air quality model to study atmospheric responses to emission changes. An important and uncertain input to such models is the gridded emission inventory that specifies emissions by location, time, pollutant, and source category. In developing emission inventory input files to support air quality modeling, a large

contribution to total NO_x and PM emissions from diesel-powered construction equipment was noted. Emissions for this source category were estimated by California Air Resources Board staff using the OFFROAD mobile source emissions model. An alternative inventory was developed based on surveys of diesel fuel sales in the construction sector and in-use measurements of exhaust emission factors. Estimates from California's OFFROAD model for NO_x and PM emissions from construction equipment were 4.5 and 3.1 times the new fuel-based emission estimates developed in this research. A comparison of the OFFROAD inputs to a recent survey of diesel construction equipment, showed OFFROAD estimated ~3 times the amount of construction equipment, and ~1.5 times the amount of construction activity compared to the survey. If OFFROAD used values of equipment population and activity similar to the survey, much of the discrepancy between the fuel use estimate and the OFFROAD model would be removed.

An updated spatial allocation of construction activity based on construction permit data indicated 2.3 and 0.44 times the original OFFROAD model derived shares of total statewide construction activity occurring in Riverside and Orange counties. In general the construction permit data showed greater construction activity at inland locations in southern California, and less activity near the coast. Construction permit data were used to evaluate alternative approaches for spatial allocation of these emissions. It was found that population growth could explain 95% of the variance in construction permit data at the county level in California. Air quality model tests showed that changes to the construction inventory led to large changes in O_3 (up to 15 ppb increases above baseline model predictions). EC estimates decreased by as much as 1 $\mu g/m^3$ using the new inventory compared to the original.

Adopting the revised estimates of construction equipment emissions, the air quality modeling was extended to include longer duration summer and fall seasonal simulations of air quality in southern California. The baseline year was 2005 when the most recent major air quality field studies took place. Using estimates of day-specific emissions for both seasons, including weekday-weekend emission changes, predicted and observed decreases in EC and NO_x on Sundays relative to weekly averages were 20-30 and 17-23%, respectively. Modeled and observed ozone concentrations increased 23-50% relative to weekly averages. Large site-to-site and week-to-week variability in nitrate response in both the model simulations and observations prevented definitive comparisons for this pollutant.

By comparing the baseline model results to separate reference simulations that were conducted with anthropogenic emissions set to typical weekday emission levels on all 7 days of each week, the effects of weekend emission reductions were isolated. This comparison showed similar predicted nitrate reductions on Mondays at Claremont as observed at this site in the analysis presented in Chapter 3. Process analysis indicated that weekend NO_x emission reductions could have counterproductive effects on nitrate in regions with strong ozone weekend effects and high anthropogenic emission rates. The heterogeneous reaction of N_2O_5 to form HNO_3 increased in response to weekend NO_x emission reductions, especially during the fall. The rate of HNO_3 formation from the gas-phase NO_2+OH reaction varied by location and season, with downtown Los Angeles showing an increase in HNO_3 production through that pathway in response to weekend emission changes.

The air quality model was also used to evaluate the effects of new California regulations requiring installation of exhaust PM filters on all in-use heavy-duty diesel trucks and buses by 2014. These filters will reduce PM emissions, but lead to increased NO_2/NO_x emission ratios. Relative to a baseline emission scenario for 2014 without the diesel emission retrofit requirements, reductions in EC concentrations of 12±2 and 14±2% were found for the summer and fall, respectively. EC concentrations were more sensitive to control of diesel emissions than fine particle mass. Corresponding reductions in $PM_{2.5}$ were 1±0.3 and 1±0.3% in the summer and fall, respectively. Increases in O_3 of 3±2 and 7±3% were predicted in summer and fall as well. Although primary emissions of NO_2 increased, ambient NO_2 concentrations decreased by 2-4%, reflecting effects of additional retrofit controls on diesel NO_x emissions. While providing insight into ambient air quality, the 5X5 km grid size may obscure issues regarding local increases of primary NO2 emissions in areas with heavy truck traffic. In those locations, the model will also underestimate reductions of diesel $PM_{2.5}$. Increases of 2±2 and 6±2% in particle nitrate were predicted during the summer and fall respectively. Overall, significant reductions of ambient diesel particle matter are predicted to occur as a result of the new emission regulations; accompanying these reductions are some increases in ozone and particulate nitrate.

7.2 Recommendations for Further Research

Formulation of effective air quality improvement policies requires accurate emission inventories. Further analysis and improvement of emission inventories is needed, as large uncertainties persist in current emission estimates. Both on-road and off-road diesel engines are especially worthy of additional study. For example, in Chapter 4, new estimates of construction equipment estimates were developed that were factors 3-5 times lower than current official inventories for California. Uncertainty in the construction equipment inventory could be reduced further with additional in-use measurements of emissions from construction equipment. Model calculations employing the new construction inventory represent NO_x less accurately implying other errors in the model inventory remain to be discovered. Inventories of emissions from other mobile sources, such as trucks, railroad locomotives, and ships, both ocean-going and recreational, are also uncertain.

Emissions from diesel source categories are forecast to change dramatically in future years due to new emission control rules. It will be important and useful to verify whether in-use emissions from diesel engines decrease as expected over the next decade. Inventories of light and heavy-duty vehicle emissions are typically based on estimations of miles traveled and are thus not constrained by fuel sales data. Vehicle emission inventories could be improved by combining statewide fuel use data with spatially resolved activity estimates based on truck counts. NO_x and speciated PM measurements of in-use emissions from ships are needed to define their relative contribution to emissions in coastal areas and to help with evaluation of proposed and adopted emission control strategies at ports.

This thesis focused on two major constituents of fine particle mass, namely nitrate and black or elemental carbon, both of which are closely linked to diesel engine exhaust emissions. Organic aerosol is also an important contributor to ambient $PM_{2.5}$ concentrations (Zhang et al., 2007). Typically, air quality models under-predict organic aerosol concentrations relative to observations. Representing the formation and transport of secondary organic aerosol is especially

challenging (Hallquist et al., 2009). Further research is needed to identify the key precursor VOC emission sources and mechanisms by which secondary organic aerosol is formed.

Recent on-road measurements of gasoline and diesel engine emissions (Ban-Weiss et al., 2008a) highlight the importance diesel trucks as a source of direct emissions of formaldehyde and other carbonyls. Current inventories of carbonyl emissions could be improved through comparison to an inventory based on fuel-use information and measured emission factors. The oxidation catalyst present as part of most diesel particle filters, soon expected to be standard equipment on diesel trucks as described in Chapter 6, has been observed to reduce VOC emissions (Herner et al., 2009). Additional research is recommended to quantify the effects on air quality of DPF installation on new and in-use heavy-duty diesel engines. For example, VOC emission reductions from diesel engines could help to reduce formation of ozone and secondary organic aerosol.

Significant reductions in emissions from diesel engines are likely over the next decade. Ambient air monitoring networks are not well-configured to show the effects of emissions changes on ambient air quality or human health. Analysis of continuous observations of fine particle nitrate, elemental and organic carbon, ultrafine particle number and size distribution, and speciated NO_y, could provide insight into exposure and health effects. Measurement locations should not be limited to ambient sites, but could span the range of distances from high source locations. This would allow research into local effects of statewide programs such as the effects of increased primary NO_2 emissions from the in-use diesel regulations.

Appendix A

Appendix A presents material related to Chapter 4. Details of metrics used to estimate the spatial distribution of off-road construction diesel fuel use are presented at the county and city levels in A.1 and A.2. Emission estimates by county are presented in A.3. A comparison of model output to observations is shown in A.4. Additional details about PM speciation profiles applied to modeled emissions can be found in A.5. A regression between city level permitting data and population data is shown in A.6. Presented in A.7 are maps of the spatial distribution of construction activity as estimated in Chapter 4 and by the OFFROAD model.

A.1: County fraction of state total: Construction permitting dollars, population, population growth, OFFROAD and employment.

County	CIRB Permits[a]	SW Permits[b]	Pop[c]	Pop Growth[d]	OFFROAD[e]	Employment[f]
Alameda	3.5E-02	7.8E-03	4.1E-02	1.9E-02	4.1E-02	4.8E-02
Alpine	1.3E-04	1.0E-04	3.6E-05	2.1E-05	1.1E-05	9.1E-05
Amador	1.5E-03	1.5E-03	1.0E-03	9.9E-04	8.7E-04	1.0E-03
Butte	4.5E-03	4.8E-03	5.9E-03	5.2E-03	4.4E-03	4.8E-03
Calaveras	3.1E-03	2.3E-03	1.2E-03	1.4E-03	2.0E-03	1.8E-03
Colusa	6.4E-04	7.9E-04	5.8E-04	9.5E-04	1.2E-04	2.5E-04
Contra Costa	3.3E-02	2.8E-02	2.8E-02	2.4E-02	4.7E-02	3.3E-02
Del Norte	4.3E-04	3.7E-04	8.0E-04	6.6E-04	3.5E-04	4.8E-04
El Dorado	8.1E-03	1.6E-02	4.8E-03	6.1E-03	4.2E-03	6.4E-03
Fresno	2.6E-02	2.5E-02	2.4E-02	3.6E-02	2.2E-02	2.4E-02
Glenn	8.1E-04	4.6E-04	7.9E-04	8.2E-04	2.0E-04	4.2E-04
Humboldt	2.0E-03	8.1E-04	3.6E-03	1.6E-03	2.4E-03	3.4E-03
Imperial	7.1E-03	1.2E-02	4.6E-03	9.1E-03	3.5E-03	2.1E-03
Inyo	1.8E-03	1.5E-04	5.1E-04	2.0E-04	1.2E-03	6.3E-04
Kern	2.3E-02	4.2E-02	2.1E-02	4.1E-02	5.7E-02	1.9E-02
Kings	3.1E-03	3.5E-03	4.0E-03	6.8E-03	1.1E-03	1.4E-03
Lake	1.7E-03	3.4E-04	1.7E-03	1.8E-03	2.7E-03	1.3E-03
Lassen	6.4E-04	1.8E-04	9.8E-04	7.6E-04	3.1E-04	5.5E-04
Los Angeles	1.7E-01	1.1E-01	2.7E-01	1.9E-01	2.2E-01	1.7E-01
Madera	6.6E-03	2.8E-03	3.9E-03	7.4E-03	2.0E-03	3.3E-03
Marin	6.1E-03	7.4E-04	6.9E-03	1.0E-03	7.4E-03	9.7E-03
Mariposa	5.5E-04	1.9E-04	5.0E-04	3.9E-04	7.5E-04	4.2E-04
Mendocino	1.7E-03	9.1E-04	2.5E-03	1.3E-03	1.7E-03	2.3E-03
Merced	1.2E-02	9.9E-03	6.6E-03	1.2E-02	2.9E-03	3.4E-03
Modoc	3.1E-04	3.1E-05	2.8E-04	2.3E-04	6.8E-05	2.3E-04
Mono	2.4E-03	2.9E-04	3.8E-04	3.6E-04	8.3E-04	8.1E-04
Monterey	9.4E-03	8.3E-03	1.1E-02	5.8E-03	5.7E-03	7.7E-03
Napa	5.1E-03	2.5E-03	3.7E-03	3.5E-03	3.7E-03	4.6E-03
Nevada	3.1E-03	4.0E-03	2.7E-03	2.0E-03	2.7E-03	4.5E-03
Orange	5.8E-02	3.7E-02	8.3E-02	7.2E-02	1.1E-01	1.1E-01
Placer	2.2E-02	4.6E-02	8.2E-03	1.9E-02	7.4E-03	1.9E-02
Plumas	7.3E-04	4.6E-03	5.8E-04	1.9E-04	2.6E-04	1.0E-03

Riverside	1.2E-01	2.5E-01	5.2E-02	1.4E-01	5.0E-02	8.8E-02
Sacramento	4.4E-02	2.3E-02	3.7E-02	4.3E-02	3.6E-02	5.0E-02
San Benito	5.0E-04	3.4E-04	1.6E-03	2.0E-03	1.2E-03	2.1E-03
San Bernardino	6.2E-02	5.4E-02	5.3E-02	9.1E-02	5.1E-02	5.1E-02
San Diego	8.1E-02	1.5E-01	8.2E-02	7.2E-02	8.0E-02	1.0E-01
San Francisco	2.8E-02	2.6E-03	2.2E-02	7.3E-03	3.9E-02	1.8E-02
San Joaquin	2.7E-02	2.4E-02	1.8E-02	3.4E-02	1.2E-02	1.8E-02
San Luis Obispo	8.1E-03	7.3E-03	7.1E-03	4.3E-03	7.0E-03	9.6E-03
San Mateo	1.5E-02	2.4E-03	2.0E-02	5.1E-03	1.9E-02	1.8E-02
Santa Barbara	9.9E-03	3.7E-03	1.1E-02	6.6E-03	1.5E-02	1.1E-02
Santa Clara	4.5E-02	5.5E-03	4.8E-02	2.9E-02	4.1E-02	4.8E-02
Santa Cruz	6.2E-03	4.0E-04	7.2E-03	2.3E-03	6.9E-03	7.7E-03
Shasta	5.5E-03	3.3E-03	4.9E-03	5.4E-03	6.5E-03	5.9E-03
Sierra	8.7E-05	7.2E-04	1.0E-04	-1.5E-05	6.5E-05	1.5E-04
Siskiyou	1.4E-03	4.9E-04	1.3E-03	4.9E-04	7.5E-04	1.1E-03
Solano	1.7E-02	3.1E-02	1.1E-02	8.8E-03	1.2E-02	1.4E-02
Sonoma	1.4E-02	8.4E-03	1.3E-02	6.7E-03	1.6E-02	1.7E-02
Stanislaus	1.7E-02	1.1E-02	1.4E-02	2.2E-02	1.2E-02	1.5E-02
Sutter	4.8E-03	4.5E-03	2.5E-03	4.5E-03	1.7E-03	1.9E-03
Tehama	1.6E-03	3.9E-04	1.7E-03	1.9E-03	6.3E-04	1.0E-03
Trinity	3.3E-04	0.0E+00	3.9E-04	4.0E-04	1.2E-04	2.5E-04
Tulare	1.0E-02	1.1E-02	1.1E-02	1.9E-02	6.0E-03	7.6E-03
Tuolumne	1.7E-03	2.8E-04	1.6E-03	7.7E-04	3.5E-03	1.9E-03
Ventura	2.3E-02	1.9E-02	2.2E-02	1.9E-02	2.6E-02	2.1E-02
Yolo	7.3E-03	5.7E-03	5.1E-03	7.1E-03	3.5E-03	6.3E-03
Yuba	4.1E-03	4.70E-03	1.9E-03	3.9E-03	1.2E-03	1.1E-03
State Totals	$84.5 billion[aa]	95,834 acres	36.6 million[bb]	5 million[cc]	340 tons NO_x[dd]	888,691[ee]

[a] Fraction of statewide permitted construction spending taking place in each county based on construction project locations.
[b] Fraction of statewide storm water permitted construction acreage taking place in each county based on construction project locations and year of permit.
[c] Fraction of statewide California Department of Finance estimated population (average of 2000 census and 2010 estimates).
[d] Fraction of statewide California Department of Finance estimated population change (difference of 2010 estimates and 2000 census).
[e] Fraction of statewide NO_x emissions estimated by the OFFROAD model for year 2005.
[f] Fration of statewide construction employment (2005) reported by ERG.

[aa] Annual total
[bb] Population
[cc] Population growth
[dd] Weekday average
[ee] Total employees

A.2: City fraction of state total: Construction permitting dollars, population, and population growth.[a]

City	Permits[b]	Pop[c]	Pop Growth[d]
Adelanto	3.0E-03	7.2E-04	2.4E-03
Agoura Hills	4.2E-04	6.2E-04	7.2E-04
Alhambra	9.2E-04	2.4E-03	8.8E-04
Anaheim	3.2E-03	9.2E-03	4.3E-03
Apple Valley	3.3E-03	1.9E-03	4.3E-03
Arcadia	1.3E-03	1.5E-03	8.6E-04
Artesia	2.0E-04	4.7E-04	3.0E-04
Avalon	2.2E-05	9.3E-05	6.1E-05
Azusa	3.9E-05	1.3E-03	9.9E-04
Baldwin Park	3.1E-04	2.2E-03	1.4E-03
Barstow	2.2E-04	6.4E-04	7.5E-04
Bell	8.5E-05	1.0E-03	5.7E-04
Bell Gardens	1.6E-04	1.2E-03	6.6E-04
Bellflower	4.9E-04	2.0E-03	1.1E-03
Beverly Hills	2.4E-03	9.6E-04	5.7E-04
Big Bear Lake	4.0E-04	1.6E-04	2.1E-04
Bradbury	4.2E-05	2.5E-05	2.1E-05
Brea	9.8E-04	1.1E-03	1.2E-03
Buena Park	1.0E-03	2.2E-03	1.1E-03
Burbank	3.8E-03	2.9E-03	1.9E-03
Calabasas	2.3E-03	6.3E-04	5.9E-04
Carson	1.5E-03	2.6E-03	2.2E-03
Cerritos	1.2E-03	1.5E-03	8.8E-04
Chino	3.3E-03	2.2E-03	3.8E-03
Chino Hills	1.8E-03	2.1E-03	3.2E-03
Claremont	5.7E-04	9.8E-04	8.0E-04
Colton	5.0E-04	1.4E-03	1.1E-03
Commerce	4.0E-04	3.6E-04	2.3E-04
Compton	6.2E-04	2.6E-03	1.5E-03
Costa Mesa	1.4E-03	3.0E-03	1.2E-03
Covina	3.6E-04	1.3E-03	7.1E-04
Cudahy	1.6E-05	6.8E-04	4.1E-04
Culver City	2.3E-04	1.1E-03	4.7E-04
Cypress	7.9E-04	1.3E-03	6.8E-04
Dana Point	9.3E-04	9.8E-04	4.5E-04
Diamond Bar	7.9E-04	1.6E-03	9.7E-04
Downey	1.7E-03	3.0E-03	1.5E-03
Duarte	1.8E-04	6.1E-04	4.1E-04
El Monte	6.5E-04	3.3E-03	2.6E-03
El Segundo	1.0E-03	4.5E-04	2.6E-04
Fontana	8.9E-03	4.8E-03	1.4E-02
Fountain Valley	4.6E-04	1.5E-03	6.8E-04

Fullerton	8.6E-04	3.6E-03	2.9E-03
Garden Grove	1.0E-03	4.6E-03	1.8E-03
Gardena	3.8E-04	1.6E-03	1.0E-03
Glendale	1.9E-03	5.5E-03	3.0E-03
Glendora	6.8E-04	1.4E-03	7.7E-04
Grand Terrace	8.1E-05	3.3E-04	2.0E-04
Hawaiian Gardens	6.6E-05	4.2E-04	2.9E-04
Hawthorne	5.9E-04	2.4E-03	1.2E-03
Hermosa Beach	6.3E-04	5.2E-04	2.2E-04
Hesperia	7.6E-03	2.3E-03	6.3E-03
Hidden Hills	1.5E-04	5.4E-05	4.1E-05
Highland	1.8E-03	1.4E-03	2.0E-03
Huntington Beach	2.3E-03	5.4E-03	3.2E-03
Huntington Park	1.8E-04	1.7E-03	8.7E-04
Industry	1.3E-03	2.1E-05	6.5E-06
Inglewood	1.8E-03	3.2E-03	1.6E-03
Irvine	1.5E-02	5.4E-03	1.6E-02
Irwindale	4.9E-04	4.4E-05	5.5E-05
La Canada Flintridge	8.8E-04	5.7E-04	2.5E-04
La Habra	3.8E-04	1.7E-03	8.7E-04
La Mirada	7.6E-04	1.3E-03	8.7E-04
La Palma	5.7E-05	4.3E-04	1.8E-04
La Puente	1.6E-04	1.1E-03	5.5E-04
La Verne	1.6E-04	8.9E-04	4.4E-04
Laguna Beach	9.8E-04	6.7E-04	3.5E-04
Laguna Hills	3.4E-04	8.8E-04	9.1E-04
Laguna Niguel	8.7E-04	1.8E-03	1.2E-03
Laguna Woods	4.6E-05	4.9E-04	1.5E-04
Lake Forest	5.3E-04	2.1E-03	5.2E-03
Lakewood	7.7E-04	2.2E-03	1.0E-03
Lancaster	8.4E-03	3.8E-03	6.6E-03
Lawndale	1.8E-04	8.9E-04	4.5E-04
Loma Linda	9.4E-04	6.0E-04	8.6E-04
Lomita	1.2E-04	5.6E-04	2.6E-04
Long Beach	4.9E-03	1.3E-02	7.8E-03
Los Alamitos	1.8E-04	3.2E-04	1.5E-04
Los Angeles	6.4E-02	1.1E-01	8.2E-02
Lynwood	3.7E-04	1.9E-03	7.9E-04
Malibu	4.7E-04	3.6E-04	3.0E-04
Manhattan Beach	1.2E-03	9.7E-04	6.9E-04
Maywood	1.6E-04	7.9E-04	4.6E-04
Mission Viejo	1.0E-03	2.6E-03	1.3E-03
Monrovia	5.4E-04	1.0E-03	5.9E-04
Montclair	5.2E-04	9.7E-04	9.5E-04
Montebello	3.6E-04	1.7E-03	8.6E-04

Monterey Park	7.9E-04	1.7E-03	1.1E-03
Needles	6.9E-05	1.5E-04	2.5E-04
Newport Beach	3.7E-03	2.2E-03	3.7E-03
Norwalk	8.1E-04	2.9E-03	1.4E-03
Ontario	2.6E-03	4.6E-03	3.9E-03
Orange	1.4E-03	3.7E-03	2.5E-03
Palmdale	6.6E-03	3.9E-03	7.6E-03
Paramount	3.2E-04	1.5E-03	6.8E-04
Pasadena	3.1E-03	3.9E-03	3.4E-03
Pico Rivera	4.3E-04	1.8E-03	9.3E-04
Placentia	3.6E-04	1.4E-03	1.3E-03
Pomona	1.2E-03	4.3E-03	3.2E-03
Rancho Cucamonga	5.4E-03	4.6E-03	1.2E-02
Rancho Palos Verdes	3.6E-04	1.1E-03	4.6E-04
Rancho Santa Margarita	2.2E-04	1.3E-03	6.2E-04
Redlands	2.7E-03	1.9E-03	2.1E-03
Redondo Beach	1.7E-03	1.8E-03	1.0E-03
Rialto	4.7E-04	2.6E-03	1.9E-03
Rolling Hills	1.1E-04	5.2E-05	2.4E-05
Rolling Hills Estates	1.1E-04	2.1E-04	1.0E-04
Rosemead	4.1E-04	1.5E-03	9.8E-04
San Bernardino	3.0E-03	5.4E-03	5.2E-03
San Clemente	2.7E-03	1.8E-03	4.6E-03
San Dimas	4.6E-04	9.8E-04	5.0E-04
San Fernando	2.0E-04	6.7E-04	3.9E-04
San Gabriel	4.8E-04	1.1E-03	7.2E-04
San Juan Capistrano	1.0E-03	9.7E-04	6.7E-04
San Marino	1.7E-04	3.6E-04	1.3E-04
Santa Ana	2.0E-03	9.4E-03	3.8E-03
Santa Clarita	3.0E-03	4.7E-03	6.8E-03
Santa Fe Springs	2.0E-03	4.7E-04	3.6E-04
Santa Monica	3.2E-03	2.4E-03	1.8E-03
Seal Beach	7.5E-04	6.9E-04	4.6E-04
Sierra Madre	8.6E-05	2.9E-04	1.1E-04
Signal Hill	5.0E-04	3.0E-04	5.0E-04
South El Monte	1.5E-04	5.9E-04	3.2E-04
South Gate	4.7E-04	2.7E-03	1.4E-03
South Pasadena	2.8E-04	6.8E-04	3.6E-04
Stanton	1.1E-04	1.0E-03	3.8E-04
Temple City	3.6E-04	9.5E-04	5.8E-04
Torrance	2.9E-03	3.9E-03	2.7E-03

Tustin	1.3E-03	1.9E-03	1.3E-03
Twentynine Palms	5.3E-04	7.2E-04	3.3E-03
Upland	1.7E-03	2.0E-03	1.8E-03
Vernon	1.7E-04	2.5E-06	1.1E-06
Victorville	7.2E-03	2.7E-03	1.0E-02
Villa Park	2.4E-04	1.7E-04	7.4E-05
Walnut	6.2E-05	8.6E-04	5.7E-04
West Covina	6.8E-04	3.0E-03	2.0E-03
West Hollywood	1.6E-04	1.0E-03	4.5E-04
Westlake Village	1.3E-03	2.4E-04	1.3E-04
Westminster	7.0E-04	2.5E-03	1.1E-03
Whittier	8.2E-04	2.3E-03	8.3E-04
Yorba Linda	2.9E-03	1.8E-03	2.4E-03
Yucaipa	1.7E-03	1.4E-03	2.8E-03
Yucca Valley	7.8E-04	5.6E-04	1.1E-03

[a] The fraction of activity attributed to unincorporated areas was distributed equally across each city with in that county.
[b] Fraction of statewide permitted construction spending taking place in each city based on construction project locations.
[c] Fraction of statewide California Department of Finance population estimate for each city for year 2007 (closest year to 2005) .
[d] Fraction of statewide California Department of Finance estimated population change (difference between 2007 estimates and 2000 census data).

A.3: State and county total NO_x and PM average weekday emission estimates.

	Estimates from this study 10^3 kg d^{-1} ($\pm\sigma$)		OFFROAD model 10^3 kg d^{-1}	
County	NO_x	PM	NO_x	PM
State Total	76.3 ±10.6	6.6 ±3.3	340.2	20.5
Alameda	2.7 ±1.2	0.23 ±0.15	13.9	0.87
Alpine	0.0098 ±0.0068	0.00085 ±0.00072	0.0038	0.00024
Amador	0.11 ±0.030	0.0097 ±0.0053	0.30	0.017
Butte	0.34 ±0.054	0.030 ±0.015	1.5	0.093
Calaveras	0.24 ±0.11	0.021 ±0.014	0.68	0.036
Colusa	0.049 ±0.029	0.0043 ±0.0032	0.041	0.0022
Contra Costa	2.5 ±0.56	0.22 ±0.12	15.9	0.88
Del Norte	0.033 ±0.0087	0.0029 ±0.0016	0.12	0.0071
El Dorado	0.62 ±0.13	0.054 ±0.028	1.4	0.089
Fresno	2.0 ±0.51	0.17 ±0.094	7.4	0.45
Glenn	0.06 ±0.022	0.0054 ±0.0032	0.067	0.0043
Humboldt	0.16 ±0.067	0.014 ±0.0087	0.80	0.049
Imperial	0.55 ±0.33	0.047 ±0.037	1.2	0.063
Inyo	0.14 ±0.13	0.012 ±0.013	0.41	0.019
Kern	1.7 ±0.77	0.15 ±0.099	19.4	0.92
Kings	0.24 ±0.18	0.021 ±0.018	0.38	0.022
Lake	0.13 ±0.029	0.012 ±0.0061	0.90	0.044
Lassen	0.049 ±0.010	0.0042 ±0.0022	0.11	0.0064
Los Angeles	13.0 ±1.97	1.1 ±0.57	75.1	4.6
Madera	0.50 ±0.21	0.044 ±0.028	0.66	0.040
Marin	0.47 ±0.37	0.041 ±0.038	2.5	0.16
Mariposa	0.042 ±0.0096	0.0036 ±0.0019	0.26	0.014
Mendocino	0.13 ±0.043	0.012 ±0.0067	0.59	0.036
Merced	0.90 ±0.50	0.078 ±0.058	1.0	0.061
Modoc	0.024 ±0.0053	0.0021 ±0.0011	0.023	0.0015
Mono	0.19 ±0.17	0.016 ±0.017	0.28	0.018
Monterey	0.72 ±0.20	0.063 ±0.035	1.9	0.12
Napa	0.39 ±0.089	0.034 ±0.018	1.2	0.077
Nevada	0.23 ±0.098	0.020 ±0.013	0.93	0.057
Orange	4.46 ±1.65	0.39 ±0.24	36.2	2.25
Placer	1.69 ±0.29	0.15 ±0.075	2.5	0.16
Plumas	0.055 ±0.037	0.0048 ±0.0040	0.090	0.0054
Riverside	8.8 ±2.2	0.77 ±0.42	17.0	1.06
Sacramento	3.35 ±0.54	0.29 ±0.15	12.1	0.76
San Benito	0.038 ±0.023	0.0033 ±0.0025	0.42	0.025
San Bernardino	4.7 ±1.6	0.41 ±0.24	17.4	1.06
San Diego	6.2 ±1.4	0.54 ±0.29	27.1	1.71
San Francisco	2.1 ±1.2	0.18 ±0.14	13.3	0.78
San Joaquin	2.0 ±0.71	0.18 ±0.11	4.2	0.27
San Luis Obispo	0.61 ±0.25	0.054 ±0.034	2.4	0.15
San Mateo	1.1 ±0.61	0.096 ±0.071	6.5	0.41
Santa Barbara	0.76 ±0.22	0.066 ±0.037	5.1	0.29

Santa Clara	3.4 ±1.0	0.30 ±0.17	13.9	0.88
Santa Cruz	0.47 ±0.26	0.041 ±0.030	2.3	0.14
Shasta	0.42 ±0.063	0.037 ±0.019	2.2	0.13
Sierra	0.0066 ±0.0075	0.00058 ±0.00071	0.022	0.0010
Siskiyou	0.11 ±0.055	0.0096 ±0.0066	0.26	0.014
Solano	1.3 ±0.44	0.11 ±0.067	3.9	0.24
Sonoma	1.0 ±0.45	0.091 ±0.059	5.5	0.34
Stanislaus	1.3 ±0.30	0.12 ±0.062	4.2	0.27
Sutter	0.36 ±0.16	0.032 ±0.021	0.56	0.036
Tehama	0.13 ±0.040	0.011 ±0.0063	0.21	0.013
Trinity	0.025 ±0.0067	0.0022 ±0.0012	0.041	0.0022
Tulare	0.80 ±0.41	0.069 ±0.049	2.0	0.13
Tuolumne	0.13 ±0.055	0.011 ±0.0072	1.2	0.063
Ventura	1.77 ±0.30	0.15 ±0.079	8.7	0.51
Yolo	0.56 ±0.088	0.048 ±0.025	1.2	0.073
Yuba	0.31 ±0.18	0.027 ±0.020	0.39	0.023

$\pm\sigma$ reflects uncertainty associated with emission factor estimates, sampling uncertainty reported in the EIA survey, and variation from county surrogates based on permitting dollars, population growth and employment. The larger uncertainties of predicted PM emissions compared to predicted NOx emissions reflect larger variation in emission factors from the NONROAD model compared to variation in the measured NO_x in-use emission factors.

A.4: Bias and error presented for each of the four emission scenarios: baseline, baseline construction updated to match new spatial activity estimates, baseline construction with baseline spatial distribution but scaled to match fuel based emission totals, new construction estimates including total emissions and relative spatial adjustment.

	NO_x[a]	O_3[a]	$PM_{2.5}$[b]	EC[b]
Bias[c]	ppb / %	ppb / %	($\mu g\ m^{-3}$) / %	($\mu g\ m^{-3}$) / %
Baseline	-6 / -3	10 / 3	10.70 / 44	1.00 / 102
Spatially Revised	-9 / -8	11 / 5	10.27 / 42	0.67 / 75
Tot. Activity Rev.	-11 / -15	11 / 6	9.84 / 40	0.60 / 73
Combined Rev.	-11 / -16	11 / 6	9.74 / 40	0.50 / 65
Error[d]				
Baseline	24 / 59	20 / 31	10.70 / 44	1.06 / 103
Spatially Revised	23 / 55	21 / 31	10.27 / 42	0.80 / 79
Tot. Activity Rev.	24 / 54	21 / 31	9.84 / 40	0.77 / 78
Combined Rev.	24 / 54	21 / 31	9.75 / 40	0.70 / 71

[a] Reported is bias / normalized bias or error / normalized error. Gross values are in ppb. Comparisons are made to routine air monitoring sites throughout the model domain.
[b] Reported is bias / normalized bias or error / normalized error. Gross values are in $\mu g/m^3$. Comparisons are made to MATESIII measurements.
[c] Bias was calculated as the mean of the residuals. In the calculation of the normalized bias, each residual was normalized by its corresponding observation.
[d] Error was calculated as the mean of the absolute value of the residuals. In the calculation of the normalized error, each residual was normalized by its corresponding observation.

A.5: Updated PM speciation profiles[a] applied in the model.[b]

Emission Source EC, OC, NO3, SO4, Other, % Coarse	Citation
On-road gasoline vehicles 0.32, 0.45, 0.00, 0.00, 0.23, 0.10[c]	Ban-Weiss et al. (2008b)
On-road diesel 0.64, 0.32, 0.00, 0.00, 0.04, 0.08[c]	Ban-Weiss et al. (2008b)
Paved Road dust 0.02, 0.16, 0.00, 0.01, 0.81, 0.93	Chow et. al. (2004b)
Cooking 0.09, 0.88, 0.00, 0.00, 0.02, 0.21	Chow et. al. (2004b)/ Long et al. (2000)
Biomass Burning 0.16, 0.64, 0.00, 0.02, 0.17, 0.07	Chow et. al. (2004b)
Jet aircraft 0.70, 0.26, 0.00, 0.00, 0.04, 0.03[c]	SPECIATE 4.0 (EPA, 2006)
Cement production 0.03, 0.13, 0.05, 0.18, 0.62, 0.38[c]	SPECIATE 4.0 (EPA, 2006)
Residential natural gas combustion 0.00, 0.83, 0.03, 0.13, 0.01, 0.00[c]	SPECIATE 4.0 (EPA, 2006)

[a] The speciation profiles define the total split between PM/$PM_{2.5}$ and the relative abundance of elemental (EC) and organic (OC) carbon, nitrate (NO_3), and sulfate (SO_4) and unidentified (other) particle emissions (the unidentified particle mass is treated as non-reactive elements by the model) and where % coarse is ratio of coarse particles (diameter > 2.5 microns) to total PM.
[b] Other important speciation profiles were found to be accurate and left at there baseline values.
[c] The value of the "% coarse" reported here, or total percentage of PM emissions greater than PM2.5 in diameter was left unchanged from the baseline estimate, and not based on the referenced citation.

A.6: City fraction of permitting and population as a function of population growth. (Does not include Los Angeles as its large share of the total induces correlation between the different estimates that is not necessarily representative of relationships for the other smaller cities.)

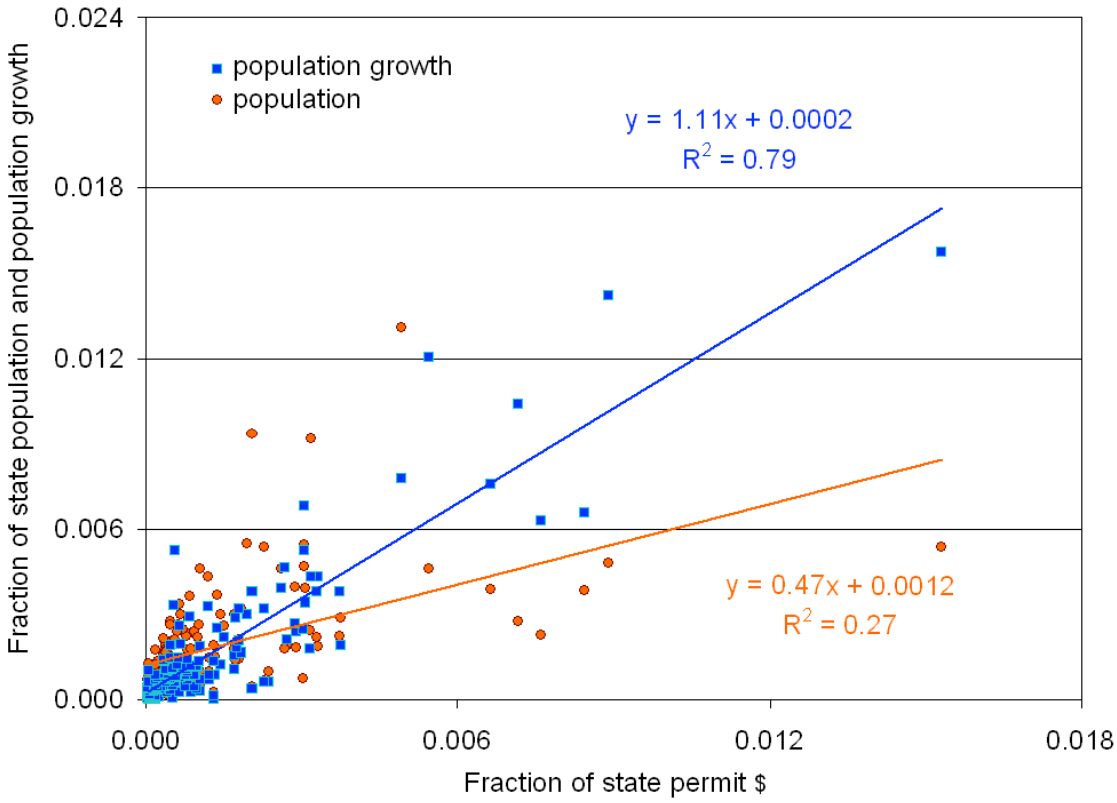

A.7: Percentage of total construction activity for both the base case (Panel A) and the scenario with construction activity based on population and permitting data (Panel B).

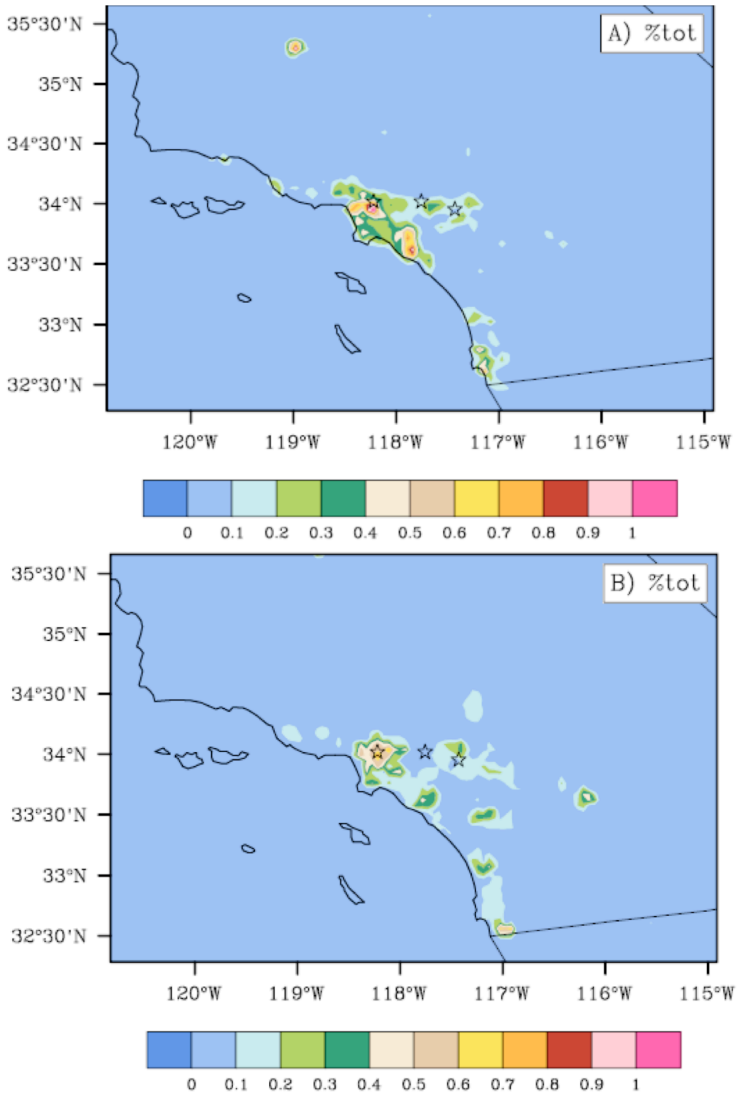

Appendix B

Appendix B contains material related to Chapter 5. Presented is modeled and observed average normalized weekday pollutant concentrations. Model and observed O_3, NO_2, NO_x and modeled PM constituents were normalized by 7-day moving average. Observed PM normalized by 19-day moving average with measurements every 3rd day.

B.1: Modeled and observed average normalized weekday EC concentrations.

	Summer			Fall		
Modeled EC	Sat	Sun	Mon	Sat	Sun	Mon
Anaheim	0.88±0.22	0.9±0.18	0.98±0.18	0.85±0.21	0.65±0.42	1.3±0.31
Burbank	0.89±0.09	0.75±0.1	1.02±0.14	0.6±0.43	0.56±0.37	1.32±0.47
Compton	0.88±0.05	0.72±0.15	0.96±0.14	0.69±0.24	0.8±0.21	1.07±0.15
Fontana	0.81±0.17	0.81±0.11	1.03±0.16	0.76±0.42	0.51±0.29	1.14±0.42
North Long Beach	0.9±0.18	0.81±0.16	0.97±0.13	0.76±0.22	0.81±0.28	1.04±0.07
Los Angeles	0.86±0.1	0.77±0.1	1.07±0.13	0.66±0.25	0.63±0.31	1.25±0.28
Pico Rivera	0.85±0.1	0.74±0.11	1.03±0.1	0.68±0.17	0.68±0.27	1.14±0.16
Rubidoux	0.86±0.1	0.8±0.09	1.03±0.08	0.7±0.22	0.5±0.27	1.21±0.25
Sun Valley	0.91±0.09	0.77±0.11	1.01±0.12	0.57±0.43	0.46±0.39	1.4±0.53
Wilmington_West Long Beach	0.88±0.12	0.75±0.14	0.99±0.15	0.68±0.18	0.79±0.18	1.05±0.13
Santa Ana	0.88±0.22	0.89±0.17	0.99±0.12	0.79±0.25	0.64±0.5	1.37±0.48
mean±S.D.	0.87±0.03	0.79±0.06	1.01±0.03	0.7±0.08	0.64±0.12	1.21±0.13
Observed EC	Sat	Sun	Mon	Sat	Sun	Mon
Anaheim	1.26±0.61	0.81±0.51	0.84±0.42	1.08±0.51	0.79±0.34	0.89±0.59
Burbank	0.93±0.42	0.59±0.19	1.02±0.36	0.96±0.45	0.76±0.33	0.89±0.5
Compton	1±0.42	0.74±0.28	0.78±0.25	0.89±0.51	0.8±0.33	0.87±0.45
Fontana	0.93±0.42	0.62±0.23	1.03±0.37	1.02±0.43	0.58±0.36	0.72±0.53
North Long Beach	0.85±0.33	0.7±0.31	0.97±0.38	0.95±0.49	0.79±0.4	0.92±0.59
Los Angeles	0.92±0.36	0.63±0.22	1.05±0.41	0.91±0.39	0.7±0.3	0.95±0.42
Pico Rivera	0.97±0.38	0.63±0.41	1.07±0.45	0.91±0.35	0.7±0.26	0.94±0.29
Rubidoux	0.94±0.49	0.67±0.24	0.97±0.39	1.13±0.59	0.67±0.44	0.71±0.51
Sun Valley	0.75±0.18	0.5±0.16	1.13±0.18	0.94±0.47	0.59±0.31	0.8±0.46
Wilmington_West Long Beach	0.91±0.51	0.63±0.25	0.95±0.41	0.88±0.4	0.65±0.38	1.14±0.79
Santa Ana	1.07±0.1	0.8±0.31	0.71±0.11	0.7±0.23	0.88±0.39	1.18±0.8
mean±S.D.	0.96±0.13	0.67±0.09	0.96±0.13	0.94±0.11	0.72±0.09	0.91±0.15

B.2: Modeled and observed average normalized weekday nitrate concentrations.

	Summer			Fall		
Modeled Nitrate	Sat	Sun	Mon	Sat	Sun	Mon
Anaheim	1.06±0.58	1.24±0.48	0.77±0.34	1.01±0.64	0.77±0.9	1.15±0.54
Burbank	1.12±0.33	1.07±0.78	0.86±0.23	0.52±0.62	0.61±0.68	1.5±0.92
Compton	1.29±0.6	1.09±0.73	0.75±0.35	0.81±0.24	1.27±0.95	1.35±0.49
Fontana	0.98±0.63	1.05±0.61	1.02±0.47	1.17±0.71	0.2±0.26	0.93±1.09
North Long Beach	0.95±0.59	1.04±0.75	0.72±0.45	0.9±0.23	1.27±1.07	1.31±0.36
Los Angeles	1.16±0.41	1.24±0.59	0.91±0.25	0.99±0.63	0.78±0.73	1.35±0.57
Pico Rivera	1.19±0.39	1.18±0.55	0.97±0.25	0.88±0.42	0.92±0.63	1.37±0.57
Rubidoux	1.11±0.16	1.11±0.27	1.03±0.22	1.02±0.82	0.38±0.68	0.8±0.74
Sun Valley	1.14±0.35	1.12±0.74	0.84±0.21	0.4±0.43	0.54±0.62	1.5±0.96
Wilmington_West Long Beach	1.09±0.63	1.05±0.77	0.73±0.4	0.85±0.17	1.34±1.09	1.34±0.39
Santa Ana	1.09±0.6	1.23±0.43	0.84±0.3	1.03±0.75	0.73±0.96	1.09±0.5
mean±S.D.	1.11±0.09	1.13±0.08	0.86±0.11	0.87±0.23	0.8±0.37	1.25±0.23

Observed Nitrate	Sat	Sun	Mon	Sat	Sun	Mon
Anaheim	1.07±0.53	0.98±0.29	0.91±0.46	1.73±1.15	1.16±1.04	0.54±0.45
Burbank	1.05±0.41	0.97±0.32	1.09±0.68	1.39±1.11	1.08±0.83	0.56±0.58
Compton	1.16±0.49	1.04±0.37	0.94±0.53	1.53±1.03	1.06±0.78	0.5±0.49
Fontana	1.01±0.51	1.02±0.41	0.85±0.61	1.6±1.09	1.08±0.8	0.43±0.52
North Long Beach	1.07±0.4	0.9±0.38	1.03±0.37	1.74±1.13	1.02±0.88	0.47±0.35
Los Angeles	1.07±0.44	0.98±0.33	1.03±0.44	1.5±1.23	1.19±0.99	0.47±0.54
Pico Rivera	1.25±0.43	0.92±0.3	1.18±0.64	1.61±1.06	1.06±0.78	0.46±0.36
Rubidoux	1.05±0.58	0.93±0.4	1.01±0.47	1.6±1.21	1.26±1.07	0.59±0.64
Sun Valley	0.76±0.43	1.23±0.63	1.28±0.42	1.53±1.12	1.04±1.01	0.78±0.8
Wilmington_West Long Beach	1.06±0.4	0.95±0.3	1±0.35	1.61±1.17	0.99±0.75	0.57±0.47
Santa Ana	1.22±0.82	1.15±0.52	0.73±0.46	1.49±1.1	1.01±1.01	0.81±0.55
mean±S.D.	1.07±0.13	1.01±0.1	1±0.15	1.58±0.1	1.09±0.08	0.56±0.13

B.3: Modeled and observed average normalized weekday $PM_{2.5}$ concentrations.

	Summer			Fall		
Modeled PM2.5	Sat	Sun	Mon	Sat	Sun	Mon
Anaheim	1±0.18	1.06±0.26	0.97±0.12	1.01±0.35	0.78±0.56	1.19±0.22
Burbank	1.04±0.15	0.96±0.33	0.97±0.1	0.7±0.57	0.65±0.45	1.28±0.58
Compton	1.02±0.16	0.88±0.26	0.87±0.08	0.84±0.28	1.02±0.44	1.06±0.42
Fontana	0.93±0.27	0.97±0.24	1.02±0.21	0.91±0.48	0.56±0.34	0.98±0.56
North Long Beach	0.98±0.19	0.91±0.23	0.94±0.09	0.91±0.24	1.04±0.54	1.01±0.25
Los Angeles	1±0.12	1.01±0.26	1±0.09	0.9±0.46	0.76±0.39	1.2±0.36
Pico Rivera	1.03±0.12	0.99±0.25	0.98±0.09	0.92±0.29	0.86±0.36	1.16±0.36
Rubidoux	1.04±0.04	1.04±0.16	1.02±0.13	0.99±0.36	0.56±0.41	1±0.42
Sun Valley	1.05±0.16	0.99±0.31	0.95±0.07	0.63±0.48	0.59±0.46	1.33±0.62
Wilmington_West Long Beach	1.01±0.18	0.88±0.22	0.93±0.08	0.81±0.25	1.07±0.46	1±0.29
Santa Ana	1.01±0.21	1.07±0.24	0.99±0.13	0.98±0.43	0.78±0.62	1.2±0.24
mean±S.D.	1.01±0.03	0.98±0.07	0.97±0.04	0.87±0.12	0.79±0.19	1.13±0.12

Observed PM2.5	Sat	Sun	Mon	Sat	Sun	Mon
Anaheim	1.02±0.27	1.02±0.31	1.05±0.37	1.42±0.68	1.05±0.55	0.64±0.24
Burbank	0.94±0.3	1.05±0.23	1.21±0.53	1.33±0.66	1.05±0.57	0.69±0.39
Compton	0.99±0.34	1.01±0.25	1.07±0.4	1.3±0.74	1.06±0.56	0.67±0.34
Fontana	0.98±0.32	0.91±0.21	1.13±0.58	1.36±0.84	1±0.6	0.64±0.46
North Long Beach	0.95±0.31	0.99±0.26	1.07±0.32	1.44±0.78	0.98±0.48	0.64±0.29
Los Angeles	0.96±0.28	0.95±0.24	1.04±0.36	1.38±0.8	1.05±0.66	0.65±0.35
Pico Rivera	1±0.26	1.01±0.16	1.31±0.5	1.4±0.61	0.92±0.43	0.67±0.23
Rubidoux	1.03±0.43	0.98±0.33	1.07±0.47	1.43±0.84	1.11±0.68	0.59±0.46
Sun Valley	0.8±0.25	1.05±0.25	1.1±0.28	1.34±0.88	1±0.77	0.86±0.52
Wilmington_West Long Beach	0.93±0.34	0.95±0.27	1±0.29	1.35±0.76	0.92±0.39	0.78±0.36
Santa Ana	1.02±0.35	1.17±0.43	0.95±0.16	1.18±0.63	1.12±0.6	0.78±0.3
mean±S.D.	0.97±0.06	1.01±0.07	1.09±0.1	1.36±0.07	1.02±0.07	0.69±0.08

B.4: Modeled and observed average normalized weekday O_3 and NO_2 concentrations.

	Summer			Fall		
Modeled Ozone	Sat	Sun	Mon	Sat	Sun	Mon
North Long Beach	1.17±0.19	1.21±0.23	0.84±0.15	1.17±0.61	1.53±0.44	1.01±0.29
Anaheim	1.17±0.14	1.2±0.19	0.86±0.14	0.98±0.28	1.61±0.42	0.97±0.44
Compton	1.13±0.17	1.26±0.19	0.88±0.16	1.45±0.82	1.6±0.63	0.86±0.31
Rubidoux	1.07±0.07	1.2±0.17	0.98±0.09	1.21±0.26	1.64±0.51	0.82±0.33
Los Angeles	1.19±0.18	1.33±0.23	0.81±0.12	1.28±0.59	1.55±0.56	0.86±0.48
Fontana	1.05±0.07	1.16±0.17	1.03±0.17	1.04±0.17	1.28±0.24	1.04±0.15
Burbank	1.18±0.25	1.32±0.29	0.84±0.15	1.27±0.37	1.29±0.38	0.86±0.45
mean±S.D.	1.14±0.06	1.24±0.07	0.89±0.08	1.2±0.16	1.5±0.15	0.92±0.09
Observed Ozone	Sat	Sun	Mon	Sat	Sun	Mon
North Long Beach	1.12±0.05	1.25±0.13	0.88±0.15	1.32±0.59	1.25±0.28	1.1±0.53
Anaheim	1.02±0.07	1.12±0.05	0.99±0.06	0.98±0.34	1.18±0.34	1.03±0.27
Compton	1.07±0.09	1.14±0.04	0.9±0.13	1.15±0.53	1.1±0.27	1.12±0.28
Rubidoux	1.06±0.11	1.28±0.09	1±0.09	1.11±0.35	1.57±0.5	0.84±0.34
Los Angeles	1.08±0.11	1.19±0.1	0.86±0.09	0.86±0	1.09±0	1.15±0
Fontana	1.12±0.17	1.32±0.21	0.92±0.15	1.44±0.54	1.57±0.33	0.9±0.25
Burbank	1.16±0.17	1.33±0.09	0.99±0.13	1.49±0.66	1.59±0.38	0.97±0.29
mean±S.D.	1.09±0.05	1.23±0.08	0.93±0.06	1.19±0.24	1.34±0.23	1.02±0.12
Modeled NO2	Sat	Sun	Mon	Sat	Sun	Mon
North Long Beach	0.92±0.14	0.84±0.1	0.98±0.08	0.9±0.2	0.98±0.18	1.1±0.08
Anaheim	0.84±0.23	0.83±0.14	0.99±0.13	0.93±0.17	0.75±0.31	1.15±0.11
Compton	0.96±0.07	0.82±0.11	0.95±0.1	0.87±0.17	1±0.13	1.14±0.12
Rubidoux	0.83±0.09	0.73±0.08	1.05±0.1	0.81±0.19	0.65±0.28	1.22±0.1
Los Angeles	0.92±0.09	0.84±0.1	1.01±0.12	0.85±0.23	0.83±0.25	1.18±0.08
Fontana	0.81±0.17	0.76±0.13	1.04±0.16	0.79±0.36	0.53±0.25	1.18±0.28
Burbank	0.91±0.09	0.77±0.15	1.03±0.1	0.69±0.4	0.66±0.37	1.25±0.2
mean±S.D.	0.88±0.06	0.8±0.05	1.01±0.04	0.83±0.08	0.77±0.18	1.17±0.05
Observed NO2	Sat	Sun	Mon	Sat	Sun	Mon
North Long Beach	0.74±0.16	0.69±0.09	1.09±0.09	0.92±0.28	1.01±0.18	1.08±0.16
Anaheim	0.85±0.25	0.78±0.26	1.03±0.34	0.98±0.25	0.98±0.27	1.09±0.15
Compton	0.86±0.14	0.79±0.1	1.04±0.06	0.93±0.23	1.01±0.2	1.09±0.09
Rubidoux	0.95±0.14	0.66±0.18	1.09±0.2	0.82±0.31	0.75±0.42	1.28±0.31
Los Angeles	0.82±0.14	0.61±0.09	0.98±0.12	0.75±0.31	0.92±0.25	1.19±0.21
Fontana	0.87±0.09	0.73±0.1	1.11±0.13	0.78±0.22	0.71±0.28	1.18±0.22
Burbank	0.85±0.09	0.63±0.12	0.96±0.13	0.78±0.25	0.84±0.29	1.22±0.22
mean±S.D.	0.85±0.06	0.7±0.07	1.04±0.06	0.85±0.09	0.89±0.13	1.16±0.08

B.5: Modeled and observed average normalized weekday NO_x concentrations.

	Summer			Fall		
Modeled NOx	Sat	Sun	Mon	Sat	Sun	Mon
North Long Beach	0.91±0.16	0.8±0.14	1.02±0.16	0.81±0.25	0.78±0.24	1±0.04
Anaheim	0.82±0.22	0.8±0.17	1.03±0.16	0.85±0.26	0.62±0.36	1.26±0.26
Compton	0.91±0.05	0.76±0.14	0.97±0.17	0.74±0.23	0.79±0.22	1.05±0.16
Rubidoux	0.81±0.09	0.73±0.09	1.05±0.1	0.73±0.2	0.54±0.25	1.2±0.2
Los Angeles	0.87±0.1	0.76±0.08	1.08±0.12	0.71±0.25	0.68±0.29	1.21±0.27
Fontana	0.79±0.16	0.76±0.11	1.04±0.17	0.79±0.37	0.52±0.26	1.14±0.33
Burbank	0.88±0.08	0.75±0.1	1.05±0.13	0.64±0.44	0.59±0.36	1.3±0.46
mean±S.D.	0.86±0.05	0.77±0.03	1.03±0.03	0.75±0.07	0.65±0.11	1.17±0.11
Observed NOx	Sat	Sun	Mon	Sat	Sun	Mon
North Long Beach	0.73±0.12	0.67±0.09	1.12±0.07	0.89±0.47	0.95±0.33	0.91±0.34
Anaheim	0.82±0.27	0.7±0.25	1±0.41	0.93±0.41	0.94±0.38	1.1±0.44
Compton	0.84±0.15	0.77±0.08	1.09±0.1	0.93±0.45	1.05±0.33	0.88±0.28
Rubidoux	0.9±0.16	0.59±0.2	1.02±0.24	0.82±0.54	0.71±0.58	1.29±0.48
Los Angeles	0.76±0.2	0.5±0.09	1.02±0.24	0.7±0.47	0.77±0.31	1.01±0.2
Fontana	0.87±0.1	0.63±0.1	1.03±0.15	0.73±0.32	0.63±0.39	1.22±0.28
Burbank	0.81±0.16	0.56±0.12	0.96±0.16	0.69±0.4	0.75±0.46	1.11±0.09
mean±S.D.	0.82±0.06	0.63±0.09	1.03±0.05	0.81±0.11	0.83±0.15	1.07±0.15

REFERENCES

Abolhasani, S., Frey, H. C., Kim, K., Rasdorf, W., Lewis, P., and Pang, S. H., (2008). Real-world in-use activity, fuel use, and emissions for nonroad construction vehicles: A case study for excavators. J. Air Waste Manage. Assoc., 58, 1033-1046.

Adams, K. M., Davis, L. I., Japar, S. M., and Pierson, W. R., (1989). Real-time, in situ measurements of atmospheric optical absorption in the visible via photoacoustic spectroscopy. II. Validation for atmospheric elemental carbon aerosol. Atmos. Environ., 23, 693-700.

Allen, G. A., Lawrence, J., and Koutrakis, P., (1999). Field validation of a semi-continuous method for aerosol black carbon (aethalometer) and temporal patterns of summertime hourly black carbon measurements in southwestern PA. Atmos. Environ., 33, 817-823.

Ansari, A. S., and Pandis, S. N., (1998). Response of inorganic PM to precursor concentrations. Environ. Sci. Technol., 32, 2706-2714.

Babich, P., Davey, M., Allen, G., and Koutrakis, P., (2000). Method comparisons for particulate nitrate, elemental carbon, and PM2.5 mass in seven US cities. J. Air Waste Manage. Assoc., 50, 1095-1105.

Baker, R. (2008). Characterization of the Off-Road Equipment Population, Eastern Research Group, Austin TX. Final Report to the California Air Resources Board under contract No. 04-315, January 2008.

Ban-Weiss, G. A., McLaughlin, J. P., Harley, R. A., Kean, A. J., Grosjean, E., and Grosjean, D., (2008a). Carbonyl and nitrogen dioxide emissions from gasoline- and diesel-powered motor vehicles. Environ. Sci. Technol., 42, 3944-3950.

Ban-Weiss, G. A., McLaughlin, J. P., Harley, R. A., Lunden, M. M., Kirchstetter, T. W., Kean, A. J., Strawa, A. W., Stevenson, E. D., and Kendall, G. R., (2008b). Long-term changes in emissions of nitrogen oxides and particulate matter from on-road gasoline and diesel vehicles. Atmos. Environ., 42, 220-232.

Bartolotto, B. (2009). Personal Communication. Construction Industry Research Board, Burbank, CA, January 2009.

Berner, A., Sidla, S., Galambos, Z., Kruisz, C., Hitzenberger, R., tenBrink, H. M., and Kos, G. P. A., (1996). Modal character of atmospheric black carbon size distributions. J. Geophys. Res., 101, 19559-19565.

Binkowski, F. S., and Roselle, S. J., (2003). Models-3 Community Multiscale Air Quality (CMAQ) model aerosol component. 1. Model description. J. Geophys. Res., 108(D6), doi: 10.1029/2001JD001409.

Birch, M. E., and Cary, R. A., (1996). Elemental carbon-based method for monitoring occupational exposures to particulate diesel exhaust. Aerosol Sci. Technol., 25, 221-241.

Blanchard, C. L., and Tanenbaum, S. J., (2003). Differences between weekday and weekend air pollutant levels in southern California. J. Air Waste Manage. Assoc., 53, 816-828.

Blanchard, C. L.: (2004). Spatial and Temporal Characterization of Particulate Matter, in: Particulate Matter Science for Policymakers, A NARSTO Assessment, edited by: McMurry, P. H., Shepherd, M. F., and Vickery, J. S., Cambridge University Press, Cambridge, MA, 2004.

Bond, T. C., Anderson, T. L., and Campbell, D., (1999). Calibration and intercomparison of filter-based measurements of visible light absorption by aerosols. Aerosol Sci. Technol., 30, 582-600.

Bond, T. C., Streets, D. G., Yarber, K. F., Nelson, S. M., Woo, J., and Klimont, Z., (2004). A technology-based global inventory of black and organic carbon emissions from combustion. J. Geophys. Res., 109, D14203, doi: 10.1029/2003JD003697.

Brauer, M., Koutrakis, P., Wolfson, J. M., and Spengler, J. D., (1989). Evaluation of the Gas Collection of an Annular Denuder System under Simulated Atmospheric Conditions. Atmos. Environ., 23, 1981-1986.

Brown, S. S., Ryerson, T. B., Wollny, A. G., Brock, C. A., Peltier, R., Sullivan, A. P., Weber, R. J., Dube, W. P., Trainer, M., Meagher, J. F., Fehsenfeld, F. C., and Ravishankara, A. R., (2006). Variability in nocturnal nitrogen oxide processing and its role in regional air quality. Science, 311, 67-70.

Byun, D., and Schere, K. L., (2006). Review of the governing equations, computational algorithms, and other components of the Models-3 Community Multiscale Air Quality (CMAQ) modeling system. Applied Mechanics Reviews, 59, 51-77.

Cabada, J. C., Pandis, S. N., Subramanian, R., Robinson, A. L., Polidori, A., and Turpin, B., (2004). Estimating the secondary organic aerosol contribution to PM2.5 using the EC tracer method. Aerosol Sci. Technol., 38, 140-155.

CARB (2006). Proposed Emission Reduction Plan for Ports and Goods Movement in Califonia, California Air Resource Board, Sacramento, CA, April 2006.

CARB (2007a). Recent Research Findings: Health Effects of Particulate Matter and Ozone Air Pollution, California Air Resources Board, American Lung Association of California, Sacramento, CA. Nov 2007.

CARB (2007b). User's Guide for OFFROAD2007, California Air Resources Board, Sacramento, CA, http://www.arb.ca.gov/msei/offroad/offroad.htm, November 2007.

CARB (2007c). OFFROAD 2007, version 2.0.1.2, Emission Inventory Model for off-road mobile sources, California Air Resources Board, Sacramento, CA.

CARB (2008a). Initial Statement of Reasons for Proposed Rulemaking, Adoption of the Proposed Regulation for In-Use On-Road Diesel Vehicles. California Air Resources Board, Sacramento, CA. October 2008.

CARB (2008b). Climate Change Scoping Plan, California Air Resources Board, Sacramento, CA.

CARB (2009a). Off-Road Emissions Inventory webpage, California Air Resources Board, Sacramento, CA. http://www.arb.ca.gov/msei/offroad/offroad.htm, May 2009.

CARB (2009b). Emission Inventory, Almanac Emission Projection Data, California Air Resources Board, Sacramento, CA. http://www.arb.ca.gov/ei/emissiondata.htm,.

Carslaw, D. C., (2005). Evidence of an increasing NO2/NOX emissions ratio from road traffic emissions. Atmos. Environ., 39, 4793-4802.

Carslaw, D. C., Ropkins, K., and Bell, M. C., (2006). Change-point detection of gaseous and particulate traffic-related pollutants at a roadside location. Environ. Sci. Technol., 40, 6912-6918.

Carter, W. P. L., (2000). Implementation of the SAPRC-99 Chemical Mechanism into the Models-3 Framework, College of Engineering, University of California, Riverside, CA. Report to the United States Environmental Protection Agency.

Chinkin, L. R., Coe, D. L., Funk, T. H., Hafner, H. R., Roberts, P. T., Ryan, P. A., and Lawson, D. R., (2003). Weekday versus weekend activity patterns for ozone precursor emissions in California's South Coast Air Basin. J. Air Waste Manage. Assoc., 53, 829-843.

Chow, J. C., Watson, J. G., Pritchett, L. C., Pierson, W. R., Frazier, C. A., and Purcell, R. G., (1993). The DRI Thermal Optical Reflectance Carbon Analysis System - Description, Evaluation And Applications In United-States Air-Quality Studies. Atmos. Environ., 27, 1185-1201.

Chow, J. C., Fairley, D., Watson, J. G., Demandel, R., Fujita, E. M., Lowenthal, D. H., Lu, Z. Q., Frazier, C. A., Long, G., and Cordova, J., (1995). Source Apportionment of Wintertime Pm(10) at San Jose, Calif. Journal of Environmental Engineering, 121, 378-387.

Chow, J. C., Watson, J. G., Crow, D., Lowenthal, D. H., and Merrifield, T., (2001). Comparison of IMPROVE and NIOSH carbon measurements. Aerosol Sci. Technol., 34, 23-34.

Chow, J. C., Watson, J. G., Chen, L. W. A., Arnott, W. P., and Moosmuller, H., (2004a). Equivalence of elemental carbon by thermal/optical reflectance and transmittance with different temperature protocols. Environ. Sci. Technol., 38, 4414-4422.

Chow, J. C., Watson, J. G., Kuhns, H., Etyemezian, V., Lowenthal, D. H., Crow, D., Kohl, S. D., Engelbrecht, J. P., and Green, M. C., (2004b). Source profiles for industrial, mobile, and area sources in the Big Bend Regional Aerosol Visibility and Observational study. Chemosphere, 54, 185-208.

Chow, J. C., Watson, J. G., Lowenthal, D. H., and Magliano, K. L., (2005). Loss of PM2.5 nitrate from filter samples in central California. J. Air Waste Manage. Assoc., 55, 1158-1168.

Chow, J. C., Watson, J. G., Lowenthal, D. H., Chen, L. W. A., Zielinska, B., Mazzoleni, L. R., and Magliano, K. L., (2007). Evaluation of organic markers for chemical mass balance source apportionment at the Fresno Supersite. Atmos. Chem. Phys., 7, 1741-1754.

Christoforou, C. S., Salmon, L. G., Hannigan, M. P., Solomon, P. A., and Cass, G. R., (2000). Trends in fine particle concentration and chemical composition in Southern California. J. Air Waste Manage. Assoc., 50, 43-53.

Clark, C. M., and Tilman, D., (2008). Loss of plant species after chronic low-level nitrogen deposition to prairie grasslands. Nature, 451, 712-715.

Cleveland, W. S., Graedel, T. E., Kleiner, B., and Warner, J. L., (1974). Sunday and workday variations in photochemical air pollutants in New Jersey and New York. Science, 86, 1037-1038.

CMUGDI (2008). Economic Input-Output Life Cycle Assessment (EIO-LCA), US 1997 Industry Benchmark model, Carnegie Mellon University Green Design Institute,Available from:<http://www.eiolca.net>

Coe, D. L., Gorin, C. A., Chinkin, L. R., and Reid, S. R. (2003). Observations of Weekday-Weekend Activity Patterns for Area Sources in the Los Angeles Area, Presented at the US Environmental Protection Agency 12th International Emission Inventory Conference - "Emission Inventories - Applying New Technologies", Sonoma Technology, Inc. April 2003.

Dickerson, R. R., Kondragunta, S., Stenchikov, G., Civerolo, K. L., Doddridge, B. G., and Holben, B. N., (1997). The impact of aerosols on solar ultraviolet radiation and photochemical smog. Science, 278, 827-830.

DOF (2007a). Population Projections for California and Its Counties 2000-2050, California Deptartment of Finance, Sacramento, CA, July 2007.

DOF (2007b). E-4 Historical Population Estimates for City, County and the State, 1991-2000, with 1990 and 2000 Census Counts. California Department of Finance, Sacramento, CA August 2007.

DOF (2008). E-1 Population Estimates for Cities, Counties and the State with Annual Percent Change — January 1, 2007 and 2008. California Department of Finance, Sacramento, CA, May 2008.

Dreher, D. B., and Harley, R. A., (1998). A fuel-based inventory for heavy-duty diesel truck emissions. J. Air Waste Manage. Assoc., 48, 352-358.

Durbin, T. D., Zhu, X. N., and Norbeck, J. M., (2003). The effects of diesel particulate filters and a low-aromatic, low-sulfur diesel fuel on emissions for medium-duty diesel trucks. Atmos. Environ., 37, 2105-2116.

Durbin, T. D., Cocker, D. R., Sawant, A. A., Johnson, K., Miller, J. W., Holden, B. B., Helgeson, N. L., and Jack, J. A., (2007a). Regulated emissions from biodiesel fuels from on/off-road applications. Atmos. Environ., 41, 5647-5658.

Durbin, T. D., Johnson, K., Cocker, D. R., Miller, J. W., Maldonado, H., Shah, A., Ensfield, C., Weaver, C., Akard, M., Harvey, N., Symon, J., Lanni, T., Bachalo, W. D., Payne, G., Smallwood, G., and Linke, M., (2007b). Evaluation and comparison of portable emissions measurement systems and federal reference methods for emissions from a back-up generator and a diesel truck operated on a chassis dynamometer. Environ. Sci. Technol., 41, 6199-6204.

Edgerton, E. S., Hartsell, B. E., Saylor, R. D., Jansen, J. J., Hansen, D. A., and Hidy, G. M., (2006). The Southeastern Aerosol Research and Characterization Study, part 3: Continuous measurements of fine particulate matter mass and composition. J. Air Waste Manage. Assoc., 56, 1325-1341.

EIA (2006). Fuel Oil and Kerosene Sales 2005, Energy Information Administration, U.S. Department of Energy, Washington DC. DOE/EIA-0535(05)

EPA (2004). Exhaust and Crankcase Emission Factors for Non-road Engine Modeling -- Compression-Ignition, Office of Transportation and Air Quality, United States Environmental Protection Agency, Ann Arbor, MI: EPA420-P-04-009

EPA (2005a). EPA NONROAD Emissions Model version 2005.1.0, United States Environmental Protection Agency.

EPA (2005b). User's Guide for the Final NONROAD2005 Model, Office of Transportation and Air Quality, United States Environmental Protection Agency, Ann Arbor, MI: EPA420-R-05-013

EPA (2006). Speciate 4.0 Speciation Database Development Documentation, Office of Research and Development, United States Environmental Protection Agency, Research Triangle Park, NC.

EPA, (2009). Proposed NO2 NAAQS Regulatory Impact Analysis (RIA), United States Environmental Protection Agency, Research Triangle Park, NC. July 2009.

Fenn, M. E., Baron, J. S., Allen, E. B., Rueth, H. M., Nydick, K. R., Geiser, L., Bowman, W. D., Sickman, J. O., Meixner, T., Johnson, D. W., and Neitlich, P., (2003). Ecological effects of nitrogen deposition in the western United States. Bioscience, 53, 404-420.

Fine, P. M., Jaques, P. A., Hering, S. V., and Sioutas, C., (2003). Performance evaluation and use of a continuous monitor for measuring size-fractionated PM2.5 nitrate. Aerosol Sci. Technol., 37, 342-354.

Fine, P. M., Shen, S., and Sioutas, C., (2004). Inferring the sources of fine and ultrafine particulate matter at downwind receptor sites in the Los Angeles basin using multiple continuous measurements. Aerosol Sci. Technol., 38, 182-195.

Finlayson-Pitts, B. J., and Pitts, J. N.: Chemistry of the Upper and Lower Atmosphere, Academic Press, New York, NY, 264-293, 2000.

Frey, H. C., Kim, K., Pang, S. H., Rasdorf, W. J., and Lewis, P., (2008a). Characterization of Real-World Activity, Fuel Use, and Emissions for Selected Motor Graders Fueled with Petroleum Diesel and B20 Biodiesel. J. Air Waste Manage. Assoc., 58, 1274-1287.

Frey, H. C., Rasdorf, W., Kim, K., Pang, G. H., and Lewis, P., (2008b). Comparison of Real-World Emissions of B20 Biodiesel Versus Petroleum Diesel for Selected Nonroad Vehicles and Engine Tiers. Transportation Research Record, 33-42.

Fujita, E. M., Stockwell, W. R., Campbell, D. E., Keislar, R. E., and Lawson, D. R., (2003). Evolution of the magnitude and spatial extent of the weekend ozone effect in California's South Coast Air Basin, 1981-2000. J. Air Waste Manage. Assoc., 53, 802-815.

Gent, J. F., Triche, E. W., Holford, T. R., Belanger, K., Bracken, M. B., Beckett, W. S., and Leaderer, B. P., (2003). Association of low-level ozone and fine particles with respiratory symptoms in children with asthma. Journal of the American Medical Association, 290, 1859-1867.

Gipson, G. L., (1999). Process Analysis in: Science Algorithms of the EPA Models-3 Community Multiscale Air Quality (CMAQ) Modeling System. EPA/600/R-99/030, Chapter 16. US Environmental Protection Agency, Research Triangle Park, NC.

Gorin, C. A., Collett, J. L., and Herckes, P., (2006). Wood smoke contribution to winter aerosol in Fresno, CA. J. Air Waste Manage. Assoc., 56, 1584-1590.

Hallquist, M., Wenger, J. C., Baltensperger, U., Rudich, Y., Simpson, D., Claeys, M., Dommen, J., Donahue, N. M., George, C., Goldstein, A. H., Hamilton, J. F., Herrmann, H.,

Hoffmann, T., Iinuma, Y., Jang, M., Jenkin, M. E., Jimenez, J. L., Kiendler-Scharr, A., Maenhaut, W., McFiggans, G., Mentel, T. F., Monod, A., Prevot, A. S. H., Seinfeld, J. H., Surratt, J. D., Szmigielski, R., and Wildt, J., (2009). The formation, properties and impact of secondary organic aerosol: current and emerging issues. Atmos. Chem. Phys., 9, 5155-5236.

Hansel, N. N., Breysse, P. N., McCormack, M. C., Matsui, E. C., Curtin-Brosnan, J., Williams, D. L., Moore, J. L., Cuhran, J. L., and Diette, G. B., (2008). A longitudinal study of indoor nitrogen dioxide levels and respiratory symptoms in inner-city children with asthma. Environmental Health Perspectives, 116, 1428-1432.

Hansen, A. D. A., Rosen, H., and Novakov, T., (1984). The Aethalometer - an Instrument for the Real-Time Measurement of Optical-Absorption by Aerosol-Particles. Sci. Total Environ., 36, 191-196.

Hansen, A. D. A., and McMurry, P. H., (1990). An Intercomparison of Measurements of Aerosol Elemental Carbon During the 1986 Carbonaceous Species Method Comparison Study. J. Air Waste Manage. Assoc., 40, 894-895.

Harley, R. A., Marr, L. C., Lehner, J. K., and Giddings, S. N., (2005). Changes in motor vehicle emissions on diurnal to decadal time scales and effects on atmospheric composition. Environ. Sci. Technol., 39, 5356-5362.

Harley, R. A., Hooper, D. S., Kean, A. J., Kirchstetter, T. W., Hesson, J. M., Balberan, N. T., Stevenson, E. D., and Kendall, G. R., (2006). Effects of reformulated gasoline and motor vehicle fleet turnover on emissions and ambient concentrations of benzene. Environ. Sci. Technol., 40, 5084-5088.

Hering, S., Eldering, A., and Seinfeld, J. H., (1997). Bimodal character of accumulation mode aerosol mass distributions in Southern California. Atmos. Environ., 31, 1-11.

Hering, S., and Cass, G., (1999). The magnitude of bias in the measurement of PM2.5 arising from volatilization of particulate nitrate from teflon filters. J. Air Waste Manage. Assoc., 49, 725-733.

Hering, S. V., and Friedlander, S. K., (1982). Origins Of Aerosol Sulfur Size Distributions In The Los-Angeles Basin. Atmos. Environ., 16, 2647-2656.

Herner, J. D., Hu, S. H., Robertson, W. H., Huai, T., Collins, J. F., Dwyer, H., and Ayala, A., (2009). Effect of Advanced Aftertreatment for PM and NOx Control on Heavy-Duty Diesel Truck Emissions. Environ. Sci. Technol., 43, 5928-5933.

Hies, T., Treffeisen, R., Sebald, L., and Reimer, E., (2000). Spectral analysis of air pollutants. Part 1: Elemental carbon time series. Atmos. Environ., 34, 3495-3502.

Huai, T., Shah, S. D., Durbin, T. D., and Norbeck, J. M., (2005). Measurement of operational activity for nonroad diesel construction equipment. International Journal of Automotive Technology, 6, 333-340.

Ito, K., De Leon, S. F., and Lippmann, M., (2005). Associations between ozone and daily mortality - Analysis and meta-analysis. Epidemiology, 16, 446-457.

Jackson, B. (2007). Planning and Technical Support Division, California Air Resources Board, Sacramento, CA, personal communication, Dec 2007.

Jaw, K., Yoon, S., Zhou, L., Krishnamurthy, M., Malchow, M., and Sax, T. (2009). California Statewide Truck and Bus Rule Emissions Analysis, Presented at 19th Annual CRC On-Road Vehicle Emissions Workshop, San Diego, California, March 2009.

Jayne, J. T., Leard, D. C., Zhang, X. F., Davidovits, P., Smith, K. A., Kolb, C. E., and Worsnop, D. R., (2000). Development of an aerosol mass spectrometer for size and composition analysis of submicron particles. Aerosol Sci. Technol., 33, 49-70.

Jenkin, M. E., Utembe, S. R., and Derwent, R. G., (2008). Modelling the impact of elevated primary NO2 and HONO emissions on regional scale oxidant formation in the UK. Atmos. Environ., 42, 323-336.

Jeong, S., Lee, S., and Kim, W., (2008). Numerical study on the optimum injection of urea-water solution for SCR deNOx system of a heavy-duty diesel engine to improve deNOx performance and reduce NH3 slip. Environmental Engineering Science, 25, 1017-1036.

Jerrett, M., Burnett, R. T., Pope, C. A., Ito, K., Thurston, G., Krewski, D., Shi, Y. L., Calle, E., and Thun, M., (2009). Long-Term Ozone Exposure and Mortality. New England Journal of Medicine, 360, 1085-1095.

John, W., Wall, S. M., Ondo, J. L., and Winklmayr, W., (1990). Modes in the size distributions of atmospheric inorganic aerosol. Atmos. Environ., 24, 2349-2359.

Johnson, D. R., Bedick, C. R., Clark, N. N., and McKain, D. L., (2009). Design and Testing of an Independently Controlled Urea SCR Retrofit System for the Reduction of NOx Emissions from Marine Diesels. Environ. Sci. Technol., 43, 3959-3963.

Johnson, T. V., (2004). Diesel Emission Control Technology – 2003 in Review. SAE Technical Paper series, no. 2004-01-0070.

Johnson, T. V., (2006). Diesel Emission Control in Review. SAE Technical Paper series, no. 2006-01-0030.

Kean, A. J., Sawyer, R. F., and Harley, R. A., (2000). A fuel-based assessment of off-road diesel engine emissions. J. Air Waste Manage. Assoc., 50, 1929-1939.

Kean, A. J., Sawyer, R. F., Harley, R. A., and Kendall, G. R., (2002). Trends in exhaust emissions from in-use California light-duty vehicles, 1994-2001. SAE Technical Paper Series, paper no. 2002-01-1713

Kean, A. J., Littlejohn, D., Ban-Weiss, G. A., Harley, R. A., Kirchstetter, T. W., and Lunden, M. M., (2009). Trends in on-road vehicle emissions of ammonia. Atmos. Environ., 43, 1565-1570.

Kim, D. Y., and Ramanathan, V., (2008). Solar radiation budget and radiative forcing due to aerosols and clouds. J. Geophys. Res., 113, D02203, doi:10.1029/2007JD008434.

Kim, S. W., Heckel, A., McKeen, S. A., Frost, G. J., Hsie, E. Y., Trainer, M. K., Richter, A., Burrows, J. P., Peckham, S. E., and Grell, G. A., (2006). Satellite-observed US power plant NOx emission reductions and their impact on air quality. Geophys. Res. Lett., 33, L22812, doi:10.1029/2006GL027749.

Kirchstetter, T. W., Harley, R. A., Kreisberg, N. M., Stolzenburg, M. R., and Hering, S. V., (1999). On-road measurement of fine particle and nitrogen oxide emissions from light- and heavy-duty motor vehicles. Atmos. Environ., 33, 2955-2968.

Kirchstetter, T. W., Agular, J., Tonse, S., Fairley, D., and Novakov, T., (2008). Black carbon concentrations and diesel vehicle emission factors derived from coefficient of haze measurements in California: 1967-2003. Atmos. Environ., 42, 480-491.

Lee, J. H., Hopke, P. K., and Turner, J. R., (2006). Source identification of airborne PM2.5 at the St. Louis-Midwest Supersite. J. Geophys. Res., 111, D10S10; doi: 10.1029/2005JD006329.

Lewis, P., Rasdorf, W., Frey, H. C., Pang, S. H., and Kim, K., (2009). Requirements and Incentives for Reducing Construction Vehicle Emissions and Comparison of Nonroad Diesel Engine Emissions Data Sources. J. Constr. Eng. Manage.-ASCE, 135, 341-351.

Lim, H. J., and Turpin, B. J., (2002). Origins of primary and secondary organic aerosol in Atlanta: Results of time-resolved measurements during the Atlanta supersite experiment. Environ. Sci. Technol., 36, 4489-4496.

Lloyd, A. C., and Cackette, T. A., (2001). Diesel engines: environmental impact and control. J. Air Waste Manage. Assoc., 51, 809-847.

Long, C. M., Suh, H. H., and Koutrakis, P., (2000). Characterization of indoor particle sources using continuous mass and size monitors. J. Air Waste Manage. Assoc., 50, 1236-1250.

Marr, L. C., and Harley, R. A., (2002a). Spectral analysis of weekday-weekend differences in ambient ozone, nitrogen oxide, and non-methane hydrocarbon time series in California. Atmos. Environ., 36, 2327-2335.

Marr, L. C., and Harley, R. A., (2002b). Modeling the effect of weekday-weekend differences in motor vehicle emissions on photochemical air pollution in central California. Environ. Sci. Technol., 36, 4099-4106.

Marshall, J. D., Granvold, P. W., Hoats, A. S., McKone, T. E., Deakin, E., and Nazaroff, W. W., (2006). Inhalation intake of ambient air pollution in California's South Coast Air Basin. Atmos. Environ., 40, 4381-4392.

Marshall, J. D., (2008). Environmental inequality: Air pollution exposures in California's South Coast Air Basin. Atmos. Environ., 42, 5499-5503.

Millstein, D. E., Harley, R. A., and Hering, S. V., (2008). Weekly cycles in fine particulate nitrate. Atmos. Environ., 42, 632-641.

Millstein, D. E., and Harley, R. A., (2009a). Revised Estimates of Construction Activity and Emissions: Effects on Ozone and Elemental Carbon Concentrations in Southern California. Atmos. Environ., 43, 6328-6335

Millstein, D. E., and Harley, R. A., (2009b). Impact of climate change on photochemical air pollution in Southern California. Atmos. Chem. Phys., 9, 3745-3754.

Millstein, J., Gilliland, F., Berhane, K., Gauderman, W. J., McConnell, R., Avol, E., Rappaport, E. B., and Peters, J. M., (2004). Effects of ambient air pollutants on asthma medication use and wheezing among fourth-grade school children from 12 southern California communities enrolled in the children's health study. Archives of Environmental Health, 59, 505-514.

Motallebi, N., Tran, H., Croes, B. E., and Larsen, L. C., (2003). Day-of-week patterns of particulate matter and its chemical components at selected sites in California. J. Air Waste Manage. Assoc., 53, 876-888.

Mulawa, P. A., Cadle, S. H., Knapp, K., Zweidinger, R., Snow, R., Lucas, R., and Goldbach, J., (1997). Effect of ambient temperature and E-10 fuel on primary exhaust particulate matter emissions from light duty vehicles. Environ. Sci. Technol., 31, 1302-1307.

Muleski, G. E., Cowherd, C., and Kinsey, J. S., (2005). Particulate emissions from construction activities. J. Air Waste Manage. Assoc., 55, 772-783.

Murphy, D. M., Capps, S. L., Daniel, J. S., Frost, G. J., and White, W. H., (2008). Weekly patterns of aerosol in the United States. Atmos. Chem. Phys., 8, 2729-2739.

Murphy, J. G., Day, D. A., Cleary, P. A., Wooldridge, P. J., Millet, D. B., Goldstein, A. H., and Cohen, R. C., (2007). The weekend effect within and downwind of Sacramento - Part 1:

Observations of ozone, nitrogen oxides, and VOC reactivity. Atmos. Chem. Phys., 7, 5327-5339.

Novakov, T., Ramanathan, V., Hansen, J. E., Kirchstetter, T. W., Sato, M., Sinton, J. E., and Sathaye, J. A., (2003). Large historical changes of fossil-fuel black carbon aerosols. Geophys. Res. Lett., 30, 1324, doi: 10.1029/2002GL016345.

Parrish, D. D., Trainer, M., Hereid, D., Williams, E. J., Olszyna, K. J., Harley, R. A., Meagher, J. F., and Fehsenfeld, F. C., (2002). Decadal change in carbon monoxide to nitrogen oxide ratio in US vehicular emissions. J. Geophys. Res., 107, doi: 10.1029/2001JD000720.

Peters, J. M., Avol, E., Navidi, W., London, S. J., Gauderman, W. J., Lurmann, F., Linn, W. S., Margolis, H., Rappaport, E., Gong, H., and Thomas, D. C., (1999). A study of twelve southern California communities with differing levels and types of air pollution - I. Prevalence of respiratory morbidity. American Journal of Respiratory and Critical Care Medicine, 159, 760-767.

Pope, C. A., and Dockery, D. W., (2006). Health effects of fine particulate air pollution: Lines that connect. J. Air Waste Manage. Assoc., 56, 709-742.

Reff, A., Bhave, P. V., Simon, H., Pace, T. G., Pouliot, G. A., Mobley, J. D., and Houyoux, M., (2009). Emissions Inventory of PM2.5 Trace Elements across the United States. Environ. Sci. Technol., 43, 5790-5796.

Reid, C. S., Turner, J. R., and Hering, S. V.: Fine Particulate Matter Nitrate Measurements by Flash Volatilization: Results from the St. Louis - Midwest Supersite, Symposium on Air Quality Measurement Methods and Technology, Air & Waste Management Association, San Francisco, CA, 2005,

Samaras, Z., and Zierock, K. H., (1995). Off-Road Vehicles - a Comparison of Emissions with Those from Road Transport. Sci. Total Environ., 169, 249-255.

Sandherr, S. (2007). California's Descision will Cost Contractors Billions, ACG of America's CEO Message, Associated General Contractors of California, Arlington, VA. September 2007.

Sawyer, R. F., Harley, R. A., Cadle, S. H., Norbeck, J. M., Slott, R., and Bravo, H. A., (2000). Mobile sources critical review. Atmos. Environ., 34, 2161-2181.

SCAQMD (2007a). Air Quality Management Plan for the South Coast Air Basin, Appendix V, Modeling and Attainment Demonstration. South Coast Air Quality Management District, Diamond Bar, CA, June 2007.

SCAQMD (2007b). Air Quality Management Plan for the South Coast Air Basin, Appendix III, Base and Future Year Emissions Inventories. South Coast Air Quality Management District, Diamond Bar, CA, June 2007.

SCAQMD (2008). Multiple Air Toxics Exposure Study III in the South Coast Air Basin Final Report, South Coast Air Quality Management District, Diamond Bar, CA, September 2008.

Schauer, J. J., and Cass, G. R., (2000). Source apportionment of wintertime gas-phase and particle-phase air pollutants using organic compounds as tracers. Environ. Sci. Technol., 34, 1821-1832.

Scott, K. (2009). Planning and Technical Support Division, California Air Resources Board, Sacramento, CA, personal communication, July 2009.

Scott, K. I., and Benjamin, M. T., (2003). Development of a biogenic volatile organic compounds emission inventory for the SCOS97-NARSTO domain. Atmos. Environ., 37, S39-S49.

Seinfeld, J. H., and Pandis, S. N.: Atmospheric Chemistry and Physics: From Air Pollution to Climate Change, Wiley-Interscience, New York, NY, 531-543, 1998.

Sioutas, C., Pandis, S. N., Allen, D. T., and Solomon, P. A., (2004). Special issue of Atmospheric Environment on findings from EPA's Particulate Matter Supersites Program - Preface. Atmos. Environ., 38, 3101-3106.

Slanina, J., ten Brink, H. M., Otjes, R. P., Even, A., Jongejan, P., Khlystov, A., Waijers-Ijpelaan, A., and Hu, M., (2001). The continuous analysis of nitrate and ammonium in aerosols by the steam jet aerosol collector (SJAC): extension and validation of the methodology. Atmos. Environ., 35, 2319-2330.

Steiner, A. L., Tonse, S., Cohen, R. C., Goldstein, A. H., and Harley, R. A., (2006). Influence of future climate and emissions on regional air quality in California. J. Geophys. Res., 111, D18303, doi:10.1029/2005JD006935.

Stolzenburg, M. R., and Hering, S. V., (2000). Method for the automated measurement of fine particle nitrate in the atmosphere. Environ. Sci. Technol., 34, 907-914.

Stolzenburg, M. R., Dutcher, D. D., Kirby, B. W., and Hering, S. V., (2003). Automated measurement of the size and concentration of airborne particulate nitrate. Aerosol Sci. Technol., 37, 537-546.

Streets, D. G., Gupta, S., Waldhoff, S. T., Wang, M. Q., Bond, T. C., and Bo, Y. Y., (2001). Black carbon emissions in China. Atmos. Environ., 35, 4281-4296.

Sverdrup, G. M., Spicer, C. W., and Ward, G. F., (1987). Investigation of the Gas-Phase Reaction of Dinitrogen Pentoxide with Water-Vapor. International Journal of Chemical Kinetics, 19, 191-205.

SWRCB (2009). Construction Program Databases, California State Water Resources Control Board, CA, http://www.swrcb.ca.gov/water_issues/programs/stormwater/databases.shtml.

Szidat, S., Jenk, T. M., Synal, H.-A., Kalberer, M., Wacker, L., Hajdas, I., Kasper-Giebl, A., and Baltensperger, U., (2006). Contributions of fossil fuel, biomass-burning, and biogenic emissions to carbonaceous aerosols in Zurich as traced by ^{14}C. J. Geophys. Res., 111, D07206, doi:10.1029/2005JD006590.

Takahama, S., Wittig, A. E., Vayenas, D. V., Davidson, C. I., and Pandis, S. N., (2004). Modeling the diurnal variation of nitrate during the Pittsburgh Air Quality Study. J. Geophys. Res., 109, D16S06; doi:10.1029/2003JD004149.

Tonse, S. R., Brown, N. J., Harley, R. A., and Jinc, L., (2008). A process-analysis based study of the ozone weekend effect. Atmos. Environ., 42, 7728-7736.

Turpin, B. J., Cary, R. A., and Huntzicker, J. J., (1990). An in situ, time-resolved analyzer for aerosol organic and elemental carbon. Aerosol Sci. Technol., 12, 161-171.

Ullah, S. M. R., Takeuchi, M., and Dasgupta, P. K., (2006). Versatile gas/particle ion chromatograph. Environ. Sci. Technol., 40, 962-968.

UNC (2008). SMOKE v2.5 User's Manual, The Institute for the Environment, University of North Carolina, Chapel Hill, NC, September 2008.

Venkataraman, C., and Friedlander, S. K., (1994). Size Distributions Of Polycyclic Aromatic-Hydrocarbons And Elemental Carbon. 2. Ambient Measurements And Effects Of Atmospheric Processes. Environ. Sci. Technol., 28, 563-572.

Venkataraman, C., Lyons, J. M., and Friedlander, S. K., (1994). Size Distributions Of Polycyclic Aromatic-Hydrocarbons And Elemental Carbon. 1. Sampling, Measurement Methods, And Source Characterization. Environ. Sci. Technol., 28, 555-562.

Watson, J. G., Chow, J. C., Bowen, J. L., Lowenthal, D. H., Hering, S., Ouchida, P., and Oslund, W., (2000). Air quality measurements from the Fresno supersite. J. Air Waste Manage. Assoc., 50, 1321-1334.

Watson, J. G., and Chow, J. C., (2002a). Comparison and evaluation of in situ and filter carbon measurements at the Fresno supersite. J. Geophys. Res., 107, doi:10.1029/2001JD000573.

Watson, J. G., and Chow, J. C., (2002b). A wintertime PM2.5 episode at the Fresno, CA, supersite. Atmos. Environ., 36, 465-475.

Weber, R. J., Orsini, D., Daun, Y., Lee, Y. N., Klotz, P. J., and Brechtel, F., (2001). A particle-into-liquid collector for rapid measurement of aerosol bulk chemical composition. Aerosol Sci. Technol., 35, 718-727.

Weingartner, E., Saathoff, H., Schnaiter, M., Streit, N., Bitnar, B., and Baltensperger, U., (2003). Absorption of light by soot particles: determination of the absorption coefficient by means of aethalometers. Journal of Aerosol Science, 34, 1445-1463.

Wittig, A. E., Anderson, N., Khlystov, A. Y., Pandis, S. N., Davidson, C., and Robinson, A. L., (2004a). Pittsburgh air quality study overview. Atmos. Environ., 38, 3107-3125.

Wittig, A. E., Takahama, S., Khlystov, A. Y., Pandis, S. N., Hering, S., Kirby, B., and Davidson, C., (2004b). Semi-continuous PM2.5 inorganic composition measurements during the Pittsburgh air quality study. Atmos. Environ., 38, 3201-3213.

Yanowitz, J., McCormick, R. L., and Graboski, M. S., (2000a). In-use emissions from heavy-duty diesel vehicles. Environ. Sci. Technol., 34, 729-740.

Yanowitz, J., McCormick, R. L., and Graboski, M. S., (2000b). In-use emissions from heavy-duty diesel vehicles. Environ. Sci. Technol., 34, 729-740.

Yarwood, G., Stoeckenius, T. E., Heiken, J. G., and Dunker, A. M., (2003). Modeling weekday/weekend Los Angeles region for 1997. J. Air Waste Manage. Assoc., 53, 864-875.

Yarwood, G., Grant, J., Koo, B., and Dunker, A. M., (2008). Modeling weekday to weekend changes in emissions and ozone in the Los Angeles basin for 1997 and 2010. Atmos. Environ., 42, 3765-3779.

Ying, Q., Lu, J., and Kleeman, M., (2009). Modeling air quality during the California Regional PM10/PM2.5 Air Quality Study (CPRAQS) using the UCD/CIT source-oriented air quality model - Part III. Regional source apportionment of secondary and total airborne particulate matter. Atmos. Environ., 43, 419-430.

Zhang, Q., Jimenez, J. L., Canagaratna, M. R., Allan, J. D., Coe, H., Ulbrich, I., Alfarra, M. R., Takami, A., Middlebrook, A. M., Sun, Y. L., Dzepina, K., Dunlea, E., Docherty, K., DeCarlo, P. F., Salcedo, D., Onasch, T., Jayne, J. T., Miyoshi, T., Shimono, A., Hatakeyama, S., Takegawa, N., Kondo, Y., Schneider, J., Drewnick, F., Borrmann, S., Weimer, S., Demerjian, K., Williams, P., Bower, K., Bahreini, R., Cottrell, L., Griffin, R. J., Rautiainen, J., Sun, J. Y., Zhang, Y. M., and Worsnop, D. R., (2007). Ubiquity and dominance of oxygenated species in organic aerosols in anthropogenically-influenced Northern Hemisphere midlatitudes. Geophys. Res. Lett., 34, doi: 10.1029/2007GL029979